

Electronic Thesis and Dissertation Repository

4-14-2011 12:00 AM

A Model System for Rapid Identification and Functional Testing of Genes Involved in Early Breast Cancer Progression

Lesley H. Souter, *The University of Western Ontario*

Supervisor: Dr. Ann Chambers, *The University of Western Ontario*

Joint Supervisor: Dr. Alan Tuck, *The University of Western Ontario*

A thesis submitted in partial fulfillment of the requirements for the Doctor of Philosophy degree in Pathology

© Lesley H. Souter 2011

Follow this and additional works at: <https://ir.lib.uwo.ca/etd>



Part of the [Neoplasms Commons](#)

Recommended Citation

Souter, Lesley H., "A Model System for Rapid Identification and Functional Testing of Genes Involved in Early Breast Cancer Progression" (2011). *Electronic Thesis and Dissertation Repository*. 122.
<https://ir.lib.uwo.ca/etd/122>

This Dissertation/Thesis is brought to you for free and open access by Scholarship@Western. It has been accepted for inclusion in Electronic Thesis and Dissertation Repository by an authorized administrator of Scholarship@Western. For more information, please contact wlsadmin@uwo.ca.

**A MODEL SYSTEM FOR RAPID IDENTIFICATION AND
FUNCTIONAL TESTING OF GENES INVOLVED IN EARLY
BREAST CANCER PROGRESSION**

(Spine title: A Model System of Breast Cancer Progression)

(Thesis format: Integrated-Article)

By

Lesley H. Souter

Graduate Program
in Pathology

A thesis submitted in partial fulfillment
of the requirements for the degree of
Doctor of Philosophy

The School of Graduate and Postdoctoral Studies
The University of Western Ontario
London, Ontario, Canada

© Lesley H. Souter 2011

THE UNIVERSITY OF WESTERN ONTARIO
THE SCHOOL OF GRADUATE AND POSTDOCTORAL STUDIES

CERTIFICATE OF EXAMINATION

Joint-Supervisor

Dr. Ann Chambers

Joint-Supervisor

Dr. Alan Tuck

Supervisory Committee

Dr. David Rodenhiser

Dr. Joe Mymryk

Examiners

Dr. Joan Knoll

Dr. Chandan Chakraborty

Dr. John DiGuglielmo

Dr. Brenda Coomber

The thesis by
Lesley Hope Souter

entitled:

**A Model System for Rapid Identification and Functional Testing of
Genes Involved in Early Breast Cancer Progression**

is accepted in partial fulfillment of the
requirements for the degree of
Doctor of Philosophy

Date: _____

Chair of the Thesis Examination Board

ABSTRACT

Early breast cancer progression involves advancement through specific morphologic stages including atypical ductal hyperplasia (ADH), ductal carcinoma in situ (DCIS) and invasive mammary carcinoma (IMC), although not always in a linear fashion. Histological studies have examined differences in breast tissues representing these stages of progression, but model systems which allow for experimental testing of factors influencing transition through these stages are scarce. The purpose of these studies was to develop a 3D *in vitro* model of early breast cancer progression that reflected the *in vivo* sequence of events, and to use this system to identify and functionally test genes important in controlling the processes. The 21T series cell lines, originally derived from the same patient with metastatic breast cancer, were shown to mimic specific stages of human breast cancer progression (21PT, ADH; 21NT, DCIS; 21MT-1, IMC) when grown in the mammary fat pad of nude mice. When grown in 3D Matrigel, the cell lines showed characteristic morphologies in which aspects of the stage-specific *in vivo* behaviours were recapitulated.

Gene expression profiling of the 21T cells revealed characteristic patterns for each, with differential expression of certain key genes in common with clinical specimens. Subsequent studies focused on functionally characterizing the roles of VANGL1, S100A2 and TBX3 in breast cancer progression. Genes were up- or down-regulated to determine if alterations could affect transitioning between stages of progression. VANGL1 was differentially expressed in the ADH (21PT) to DCIS (21NT) transition (higher in DCIS) and was found functionally to promote

the transition from ADH to a malignant phenotype (DCIS and even IMC). S100A2 and TBX3 were both differentially expressed in the DCIS to IMC (21MT-1) transition (S100A2 lower in IMC, TBX3 higher in IMC). S100A2 was found to functionally inhibit the transition from DCIS to IMC, while TBX3 promoted progression to invasion.

These studies demonstrate that the 21T series cell lines provide a model of early breast cancer progression when grown in 3D. In addition, the model provides a means of testing the functional effects of genes on transitions between stages of pre-malignant to malignant growth, which may elucidate potential therapeutic targets.

KEYWORDS: Breast Cancer Progression, Atypical Ductal Hyperplasia, Ductal Carcinoma in situ, Invasive Mammary Carcinoma, Matrigel, VANGL1, S100A2, TBX3

CO-AUTHORSHIP

Chapter 2 of the following thesis was previously published as “Human 21T breast epithelial cell lines mimic breast cancer progression *in vivo* and *in vitro* and show stage-specific gene expression patterns” by L.H. Souter, J.D. Andrews, G. Zhang, A.C. Cook, C.O. Postenka, W. Al-Katib, H.S. Leong, D.I. Rodenhiser, A.F. Chambers, A.B. Tuck, in *Laboratory Investigation*, vol. 90: pp. 1247-1258, 2010. Copyright permission for thesis reproduction is not required by *Laboratory Investigation*, see Appendix A.

The *in vivo* experiment was conducted prior to the start of this thesis project by A.B. Tuck, with technical assistance from Charu Hota. The animal protocol approval can be found in Appendix A. W. Al-Katib was consulted when analyzing the pathology of the *in vivo* study. G. Zhang and A.C. Cook performed preliminary 3D *in vitro* colony formation assays. I repeated these 3D *in vitro* colony formation assays with Matrigel cell plugs of my own and also created the Matrigel cell plugs for immunohistochemistry. C.O. Postenka performed the H&E and immunohistochemical staining on the Matrigel plugs, which I then analyzed. I designed the microarray study and prepared the RNA. J.D. Andrews aided in the microarray study design and performed preliminary data analysis. In addition, J.D. Andrews created the clinically relevant database from the literature, which I then used to choose my genes of interest. H.S. Leong provided image analysis expertise when analyzing the time lapse invasion assays that I conducted. I

wrote the manuscript under the supervision of A.F. Chambers, D.I. Rodenhiser and A.B. Tuck.

In Chapter 3, I created expression vectors for VANGL1 and TBX3. H.S. Leong aided in planning the cloning experiments, as well as being available for consultation during their creation. In addition, H.S. Leong performed the confocal microscopy experiments using TBX3 overexpressing cells I prepared. Finally, H.S. Leong conducted the ZsGreen western blot using cell lysates that I prepared. As with Chapter 2, C.O. Postenka once again performed the H&E and immunohistochemical staining on Matrigel plugs, which I prepared and then analyzed. I performed the remainder of the experiments.

DEDICATION

I would like to dedicate this thesis to my wonderful husband, Christopher, without whom this thesis would never have happened.

ACKNOWLEDGMENTS

I would first like to thank my supervisors, Dr. Ann Chambers and Dr. Alan Tuck for their support and encouragement throughout my degree. I have learned so much more under their guidance than just how to design and conduct experiments. Ann is a wonderful role model for any female scientist and her dedication is inspiring. Without Alan's support and patience, I wouldn't have made it this far. I would also like to thank my advisory committee members, Dr. David Rodenhiser and Dr. Joe Mymryk for their valuable feedback and direction, which helped shape my work.

Next, I need to acknowledge the many members of the Chambers' lab. I have witnessed many members come and go in the 4.5 years that I have been a part of the laboratory. All have been helpful at some time or in some way; however, there are a few that require extra gratitude. First, David Dales is a wonderful head technician and deserves thanks for answering my many questions. Next Carl Postenka needs to be thanked for putting up with my pestering for slides and for diverting me with BlackBerry discussions. Joe Andrews was paramount in my ever making enough high quality RNA for the microarray study. Thank you Joe for the encouragement during those frustrating weeks and for teaching me wonderful sayings, like "Fill your boots". I will never eat sushi again without remembering David, Carl and Joe. Mike Lizardo has been a great friend, especially during the writing process, which we experienced together. The many text messages and phone calls shared between us the past few months have helped to maintain my sanity. We will make our shirts yet Mike!

Jen Mutrie also needs to be thanked. Jen is a wonderful person and her positivity and optimism was a great pick-me-up on difficult days. On the not difficult days, just having her in the cubicle beside me, made the day more enjoyable. Finally, I need to express my sincere gratitude to Hon Leong. Hon is one of the most supportive and encouraging people I have ever met. Thank you Hon. Your friendship has made a huge difference in my life.

Members of my family also require many thanks. My parents are wonderful people that have always supported me. Although not understanding exactly what I do on a day-to-day basis, their constant encouragement and motivation was greatly appreciated. Next, Chris Coady, my husband, who is only a little miffed that I have not taken his name, has been my rock throughout my degree. He has supported me when I needed someone to lean on, picked me up when I was down and pushed me to be the person that I had lost. Finally, and strangely to anyone that does not know me well, I need to acknowledge Chloe. Chloe is my anti-stress therapy. After a stressful day, Chloe's blind admiration and simple desire to remove my socks always erased my bad mood and gave me the strength to start again.

Lastly, although not directly helping in my thesis project or in thesis writing, I need to thank the amazing breast cancer survivors I met through Journeys in Sharing and the generous women I met through SOWCC. All of these remarkable women altered how I viewed my research and the motivation for conducting it.

GRANT SUPPORT

The work described in this thesis has been supported in part by Grant no. 42511 from the Canadian Institutes for Health Research and Grant no. 016506 from the Canadian Breast Cancer Research Alliance with special funding support from the Canadian Breast Cancer Foundation and the Cancer Research Society.

L.H. Souter was the recipient of a Studentship from the Pamela Greenaway Kohlmeier Translational Breast Cancer Unit from the London Regional Cancer Program with funding from the Southwestern Ontario Women's Charity Cashspiel Fundraiser for the duration of this thesis project.

TABLE OF CONTENTS

CERTIFICATE OF EXAMINATION	ii
ABSTRACT	iii
CO-AUTHORSHIP	v
DEDICATION	vii
ACKNOWLEDGMENTS	viii
GRANT SUPPORT	x
TABLE OF CONTENTS	xi
LIST OF TABLES	xv
LIST OF FIGURES	xvi
LIST OF APPENDICES	xix
LIST OF ABBREVIATIONS	xx
<u>CHAPTER 1. INTRODUCTION</u>	
1.1. EARLY BREAST CANCER PROGRESSION	1
1.1.1. Breast Cancer	1
1.1.2. Morphology of Early Breast Cancer Progression	2
1.1.3. Relative Risk of Progression to IMC	4
1.1.4. Identification of Molecular Targets in Breast Cancer Progression	5
1.1.5. Models of Breast Cancer Progression	5
1.2. THE 21T SERIES HUMAN BREAST CANCER CELL LINES	7
1.2.1. Establishment of the 21T Series Cell Lines	7
1.2.2. Characteristics of the 21T Series Cells	8
1.3. <i>IN VIVO</i> VS 3D <i>IN VITRO</i> CULTURE	9
1.3.1. Xenograft Mouse Model Limitations	9
1.3.2. Matrigel and 3D <i>In Vitro</i> Culture	10

1.4. THESIS BACKGROUND STUDIES AND HYPOTHESES	11
1.4.1. 21T Series Cell Lines Mimic Stages of Breast Cancer Progression <i>In Vivo</i>	11
1.4.2. Thesis Hypotheses	12
1.5. EXPERIMENTAL OBJECTIVES	12
1.6. REFERENCES	13

CHAPTER 2. 21T SERIES CELL LINES MIMIC SPECIFIC STAGES OF BREAST CANCER PROGRESSION IN 3D CULTURE AND SHOW STAGE-SPECIFIC GENE EXPRESSION PATTERNS

2.1. INTRODUCTION	19
2.2. MATERIALS AND METHODS	22
2.2.1. Cell Lines and Culture	22
2.2.2. <i>In Vivo</i> Studies	23
2.2.3. 3D <i>In Vitro</i> Cultures	24
2.2.4. Morphologic Characterization of 3D <i>In Vitro</i> Cultures	24
2.2.5. Proliferation and Apoptosis in 3D Culture	25
2.2.6. Matrigel Invasion Assay	25
2.2.7. Gene Expression Profiling in 3D Culture	26
2.2.8. Quantitative Real Time-PCR (qRT-PCR) Validation	28
2.2.9. Statistical Analysis	29
2.3. RESULTS	29
2.3.1. <i>In Vivo</i> Cultures of 21T Series Cell Lines Model Stages of Early Progression	29
2.3.2. 3D <i>In Vitro</i> Cultures of 21T Series Cells Display Features of Specific Stages of Early Progression	33
2.3.3. Differential Proliferation, Apoptosis and Invasiveness of 21T Series Cells	35
2.3.4. Profiling Elucidates Differential Gene Expression between the Three 21T Series Cell Lines Grown in 3D	37
2.4. DISCUSSION	46
2.5. REFERENCES	52

CHAPTER 3. THE ROLES OF VANGL1, S100A2 AND TBX3 IN THE TRANSITIONS BETWEEN STAGES OF EARLY BREAST CANCER PROGRESSION

3.1. INTRODUCTION	59
3.1.1. Van Gogh-like 1 (VANGL1)	62
3.1.2. S100A2	65
3.1.3. T-box 3 (TBX3)	68
3.2. MATERIALS AND METHODS	71
3.2.1. Cell Lines and Culture	71
3.2.2. VANGL1 Expression Vector	72
3.2.3. TBX3 Expression Vector	76
3.2.4. shRNA against S100A2	80
3.2.5. Transient and Stable Transfections	82
3.2.6. 3D <i>In Vitro</i> Cultures	83
3.2.7. Collection and Quantification of RNA and Protein from 3D Cultures	83
3.2.8. Quantitative Real Time-PCR (qRT-PCR) Validation	84
3.2.9. Western Blotting	85
3.2.10. Morphologic Characterization of 3D In Vitro Cultures	87
3.2.11. Proliferation and Apoptosis in 3D Cultures	88
3.2.12. Transwell Invasion Assay	89
3.2.13. Matrigel Invasion Assay	90
3.2.14. Confocal Microscopy	91
3.2.15. Statistical Analysis	93
3.3. RESULTS	93
3.3.1. VANGL1	93
3.3.1.1. VANGL1 mRNA Expression Levels are Altered in 21NT Compared to 21PT Cells	93
3.3.1.2. VANGL1-Transfected 21PT Cells Show mRNA and Protein Levels Similar to 21NT Cells	94
3.3.1.3. 3D <i>In Vitro</i> Cultures of 21PT+VANGL1 Cells Display Features of More Advanced Progression than 21PT+EV Cells	97
3.3.1.4. Altered Proliferation, Apoptosis and Invasive Ability of 21PT+VANGL1 Cells Indicate Conversion to a Later Stage of Progression	100
3.3.2. S100A2	103
3.3.2.1. S100A2 mRNA Expression Levels are Altered in 21MT-1 Compared to 21NT Cells	103
3.3.2.2. 21NT+shS100A2 Cells Show mRNA and Protein Levels Similar to 21MT-1 Cells	105
3.3.2.3. 3D <i>In Vitro</i> Cultures of 21NT+shS100A2 Cells Display Features of a Later Stage of Progression	105

3.3.2.4.	21NT+shS100A2 Cells Exhibit Characteristics of a More Aggressive Phenotype Including Alterations in Proliferation, Apoptosis and Invasion	108
3.3.3.	TBX3	113
3.3.3.1.	TBX3 mRNA Expression Levels are Altered in 21MT-1 Compared to 21NT Cells	113
3.3.3.2.	21NT+TBX3 Iso1 and 21NT+TBX3 Iso2 Cells Show mRNA and Protein Levels Increased Over 21NT+EV Cells	115
3.3.3.3.	3D <i>In Vitro</i> Cultures of 21NT+TBX3 Cells Display Features of a More Advanced Stage of Progression	121
3.3.3.4.	Altered Proliferation, Apoptosis and Invasive Ability Indicate 21NT+TBX3 Cells Exhibit Characteristics of a More Invasive Phenotype	123
3.3.3.5.	21NT+TBX3 Cells Show Vimentin and E-Cadherin Alterations Consistent with EMT	125
3.4.	DISCUSSION	127
3.4.1.	VANGL1 Promotes the Transition from ADH to Invasive Malignancy	130
3.4.2.	S100A2 Inhibits the Transition to an Invasive Phenotype	133
3.4.3.	TBX3 Promotes the Transition to an Invasive Phenotype	135
3.4.4.	Genes Identified by the 21T Series Model System are Involved in Controlling the Transitions Between Stages of Progression	139
3.5.	REFERENCES	141
<u>CHAPTER 4. GENERAL DISCUSSION</u>		
4.1.	THESIS SUMMARY	148
4.2.	DISCUSSION	152
4.3.	FUTURE DIRECTIONS	156
4.4.	REFERENCES	160
APPENDICES		165
CURRICULUM VITAE		185

LIST OF TABLES

Table 2.1.	Histopathology of 21T series cell lines in vivo on year after orthotopic mammary fat pad injection into 6-8 week old nude mice.	30
Table 2.2.	Genes that are concurrently: (1) significantly different among the 21T series cell lines, (2) present on clinically relevant databases from the literature and (3) found within the top 10 functional and canonical pathways represented according to Ingenuity Pathways Analysis.	40
Table 2.3.	qRT-PCR validated genes of interest showing significant difference between 21T series cell lines that are of potential clinical relevance and are of the top 10 functional and canonical pathways represented (IPA).	44
Table 3.1.	Primer sequences for VANGL1 cloning, TBX3 cloning and TBX3 qRT-PCR.	74

LIST OF FIGURES

Figure 1.1.	Morphology of early breast cancer progression.	3
Figure 2.1.	Histopathology of 21T series cells <i>in vivo</i> , 1 year after injection of 1×10^7 cells into the mammary fat pad of 6-8 week old female nude mice.	32
Figure 2.2.	<i>In vitro</i> characteristics of 21PTci, 21NTci and 21MT-1 cells after 15 days growth in 3D Matrigel.	34
Figure 2.3.	Proliferative and apoptotic activity of 21PTci, 21NTci and 21MT-1 cells after 9 and 15 days growth in 3D Matrigel.	36
Figure 2.4.	21T series cell invasion through Matrigel matrix.	38
Figure 3.1.	Genes identified as altered between 21T series cell lines and breast cancer progression stages.	61
Figure 3.2.	VANGL1 cell signalling.	63
Figure 3.3.	Nuclear effects of S100A2.	66
Figure 3.4.	Effects and signalling of TBX3.	69
Figure 3.5.	Plasmid map for VANGL1 expression vector.	75
Figure 3.6.	Cloning primer design and plasmid map for TBX3 expression vector.	78
Figure 3.7.	Plasmid map for S100A2 shRNA vector.	81
Figure 3.8.	mRNA expression levels of VANGL1 in 21PTci and 21NTci cells grown in 2D and 3D culture.	95
Figure 3.9.	mRNA expression levels of VANGL1 in 21PTci, 21NTci, 21PT and 21PTci cells grown in 3D culture.	96
Figure 3.10.	mRNA and protein levels of VANGL1 after transfection into 21PT cells.	98
Figure 3.11.	Characteristics of 21T and VANGL1 overexpressing cells after 15 days growth in 3D Matrigel.	99

Figure 3.12.	Proliferative and apoptotic activity of 21T and VANGL1 overexpressing cell lines after 15 days growth in 3D Matrigel.	101
Figure 3.13.	Invasion of VANGL1 overexpressing cells using a transwell system.	102
Figure 3.14.	mRNA expression levels of S100A2 in 21NTci and 21MT-1 cells grown in 2D and 3D culture.	104
Figure 3.15.	mRNA expression levels of S100A2 in 21NTci and 21NT cells compared to 21MT-1 cells.	106
Figure 3.16.	mRNA and protein levels of S100A2 after shRNA transfection into 21NT cells.	107
Figure 3.17.	Characteristics of 21T and S100A2 knockdown cells after 15 days growth in 3D Matrigel.	109
Figure 3.18.	Proliferative and apoptotic activity of 21T and S100A2 knockdown cell lines after 15 days growth in 3D Matrigel.	110
Figure 3.19.	Cell invasion through Matrigel matrix for 21T and S100A2 knockdown cells.	112
Figure 3.20.	mRNA expression levels of TBX3 in 21NTci and 21MT-1 cells grown in 2D and 3D culture.	114
Figure 3.21.	mRNA expression levels of TBX3 in 21NTci and 21NT cells compared to 21MT-1 cells.	116
Figure 3.22.	mRNA and protein levels of endogenous TBX3 and TBX3-ZsGreen after transfection into 21NT cells.	118
Figure 3.23.	Relationship between TBX3 and ZsGreen using confocal microscopy.	120
Figure 3.24.	Characteristics of 21T and TBX3 transfected cells after 15 days growth in 3D Matrigel.	122
Figure 3.25.	Proliferative and apoptotic activity of 21T and TBX3 transfected cell lines after 15 days growth in 3D Matrigel.	124
Figure 3.26.	Cell invasion through Matrigel matrix for 21T and TBX3 transfected cells.	126

Figure 3.27.	Levels of E-cadherin in TBX3-ZsGreen transfected cells using confocal microscopy.	128
Figure 3.28.	Levels of vimentin in TBX3-ZsGreen transfected cells using confocal microscopy.	129
Figure 3.29.	The roles of VANGL1, S100A2 and TBX3 in early breast cancer progression.	140

LIST OF APPENDICES

Appendix A	Copyright agreement for previously published work and animal protocol approval	165
Appendix B	Supplementary data for Chapter 2	169
Appendix C	Supplementary data for Chapter 3	177

LIST OF ABBREVIATIONS

2D	Two dimensional
3D	Three dimensional
ADH	Atypical ductal hyperplasia
ALH	Atypical lobular hyperplasia
ANOVA	Analysis of variance
ATP	Adenosine triphosphate
BSA	Bovine serum albumin
cDNA	Complementary DNA
CIP	Calf intestinal phosphatase
Cox-2	Cyclooxygenase-2
DCIS	Ductal carcinoma in situ
DNA	Deoxyribonucleic acid
Dvl	Dishevelled
ECL	Enhanced chemiluminescence
ECM	Extracellular matrix
EGF	Epidermal growth factor
EGFR	Epidermal growth factor receptor
EMT	Epithelial to mesenchymal transition
ER	Estrogen receptor
ERK	Extracellular signal-regulated kinase
ERM	Ezrin, radixin and moesin
EV	Empty vector
FBS	Fetal bovine serum

FGF	Fibroblast growth factor
Fmi	Flamingo
Fzd	Frizzled
GCOS	GeneChip Operating Software
H&E	Hematoxylin and eosin
HEPES	4-(2-hydroxyethyl)-1-piperazineethanesulfonic acid
HER-2	Human epidermal growth factor receptor 2
HDAC	Histone deacetylase
HNSCC	Head and neck squamous cell carcinoma
Ig	Immunoglobulin
IMC	Invasive mammary carcinoma
IPA	Ingenuity Pathways Analysis
iPS	Induced pluripotent stem
KITENIN	KAI1 COOH-terminal interacting tetraspanin
LB	Luria Bertani
LCIS	Lobular carcinoma in situ
MAPK	Mitogen-activated protein kinase
MARCKS	Myristoylated alanine-rich C kinase substrate
MEM	Minimal essential medium
MMP	Matrix metalloproteinase
mRNA	Messenger RNA
NFkB2	Nuclear factor of kappa light polypeptide gene enhancer in B-cells 2
PBS	Phosphate buffered saline
PCP	Planar cell polarity

PCR	Polymerase chain reaction
PGE2	Prostaglandin E2
PKC	Protein kinase C
PR	Progesterone receptor
PVDF	Polyvinylidene fluoride
qRT-PCR	Quantitative real-time PCR
RNA	Ribonucleic acid
RUNX3	Runt-related transcription factor 3
S100A2	S100 calcium binding protein 2
SDS	Sodium dodecyl sulphate
Shh	Sonic hedgehog
shRNA	Short hairpin RNA
TBS	Tris-buffered saline
TBS-T	TBS with 0.1% Tween
TBX3	T-box 3
TDLU	Terminal duct lobular unit
TGF α	Transforming growth factor alpha
TGF β	Transforming growth factor beta
μ g	Microgram
μ L	Microlitre
μ m	Micrometer
UMS	Ulnar-mammary syndrome
UTR	Untranslated region
VANGL1	Van Gogh-like 1

CHAPTER 1. INTRODUCTION

1.1. EARLY BREAST CANCER PROGRESSION

1.1.1. Breast Cancer

Every hour of every day, 20 people in Canada are diagnosed with some form of cancer [1]. Cancer is characterized by uncontrolled growth of cells and can arise in many different organs within the body. In fact, the Canadian Cancer Society recognizes over 30 different types of cancer, based on the organ in which the tumour originates. Cancer may be characterized by uncontrolled growth, but this oversimplifies the complexity of the disease. Research has determined that cancer is a highly complex, multistep process that involves numerous alterations at the molecular level and confers upon cells a growth advantage that facilitates the conversion of normal cells to malignant cells. Even with this knowledge, our understanding of the molecular changes and how they drive progression of cancer is still greatly limited.

Breast cancer is the most common cancer in women [2-4] and is the leading cause of death in women aged 40 to 59 and the second leading cause, after lung cancer, for women aged 60-79 [3]. Breast cancers generally arise in the terminal ductules of the lobular units of the breast [5]. When caught at an early stage, survivability is very high, as the disease has not spread and local excision may be curative. However, once the cancer is able to spread to life-supporting organs, chance of survival is greatly reduced [3]. If the factors responsible for promoting progression of breast cancer can be discovered, it will

be possible to develop new therapeutic interventions directed at inhibiting this process. In order to find these factors, we need to study the mechanisms of early breast cancer progression and identify the genes that control the transitions between the stages of progression. The gene targets may then be used to develop therapeutics for treatment.

1.1.2. Morphology of Early Breast Cancer Progression

Invasive ductal carcinoma (of “no specific type”), one of the most common types of breast cancer, accounts for 20-30% of all newly diagnosed breast cancers [6]. It has been documented that stem cells from the terminal duct lobular units (TDLUs) can give rise to atypical ductal hyperplasia (ADH) [5, 7-10]. At the stage of ADH, the breast duct is partially filled with two epithelial cell populations (Figure 1.1). One population includes atypical cells, which may be neoplastic, while the second population includes more normal-appearing cells [5, 8, 9]. Ductal carcinoma *in situ* (DCIS) may arise from ADH and is characterized by a breast duct filled with neoplastic cells [5, 7, 11-13] (Figure 1.1). If left untreated at the DCIS stage, the carcinoma may become invasive (invasive mammary carcinoma, IMC) and lead to metastases at distant sites [5, 7, 11, 12, 14] (Figure 1.1). These three stages of progression may not always occur in a linear fashion however, and the histologic patterns are most likely phenotypic indicators of the underlying molecular events which are driving the stages of progression [15]. Identification of these molecular events may elucidate both the timing and likelihood of a lesion’s progression to malignancy. In addition, an

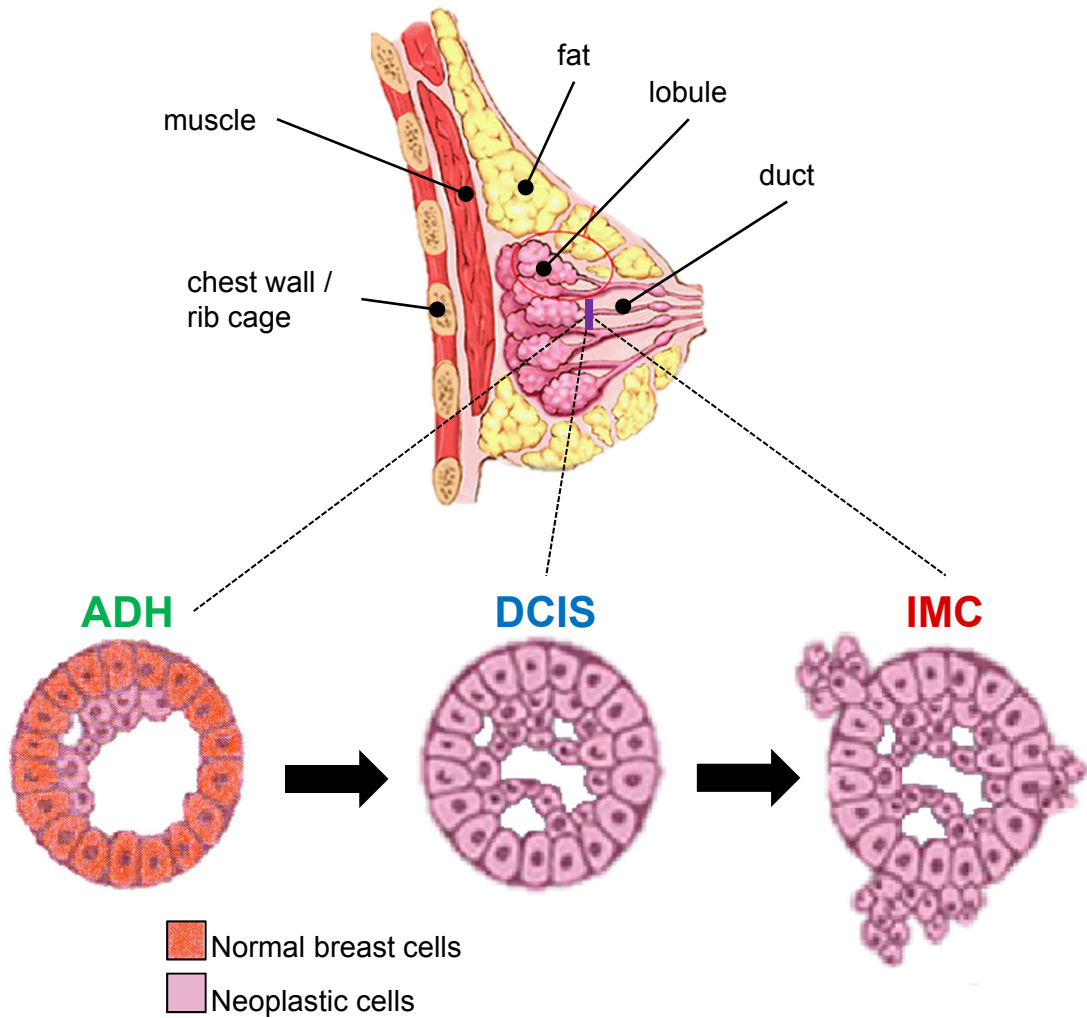


Figure 1.1. Morphology of early breast cancer progression. Stem cells from the lobular unit give rise to atypical ductal hyperplasia (ADH). During ADH, two epithelial populations are present within the duct. One population includes atypical cells, presumed to be neoplastic, while the other population is more normal-appearing. ADH can progress to ductal carcinoma in situ (DCIS), which is characterized by a breast duct filled with neoplastic cells. Finally, DCIS can progress to invasive mammary carcinoma (IMC), in which cells are able to invade through the basement membrane and move to distant sites. This image was adapted from <http://www.breastcancer.org/symptoms/types/dcis/diagnosis.jsp>.

understanding of the molecular events may aid us in determining ways to halt progression at the early stages.

1.1.3. Relative Risk of Progression to IMC

Formation of metastases in vital organs, as a result of IMC is life threatening. It has already been noted that breast cancer progression may not always follow a linear pathway from ADH through DCIS to IMC; however, histological examination of human specimens have demonstrated that ADH and DCIS are markers for higher risk of IMC occurrence [7, 9, 14, 16]. Atypical hyperplasias, including ADH and atypical lobular hyperplasia (ALH), are non-obligate precursors of IMC and in fact a diagnosis of ADH or ALH correlates with an increased risk to develop IMC in either breast [9, 14, 16]. Compared to the general public, women who have had a biopsy positive for ADH or ALH have a 4-5 times increased risk of developing IMC [9]. In contrast, DCIS is commonly regarded as an obligate precursor lesion for IMC and results in an 8-10 times increased risk for developing invasive disease [9]. DCIS is considered an obligate precursor due to the common discovery of invasion at the original site of DCIS diagnosis [16]. Even if progression does not always occur in a linear fashion, both non-obligate and obligate precursors commonly share histologic continuity with IMC [14, 15] and analyzing progression from a linear perspective serves as an appropriate framework for studies into the molecular mechanisms which drive tumour progression [9, 14, 16].

1.1.4. Identification of Molecular Targets in Breast Cancer Progression

The molecular events within a cell are driven by the cell's genotypic signature. Both microarray technology, which looks at the gene expression profile within a cell and proteomics, which looks at the proteins expressed within a cell, have identified candidate genes and their protein products potentially involved in breast cancer progression. These candidates are thought to be involved in cancer characteristics, such as proliferation, apoptosis, migration, invasion and adhesion [17-22]. However, although changes have been associated in the literature with specific stages of progression, there is little information on what alterations are functionally involved in driving the transitions between the stages. In essence, we are seeing a static picture of what is actually a very complex and dynamic process. In order to address which alterations have significant functional effect, model systems to study progression are needed.

1.1.5. Models of Breast Cancer Progression

Using different approaches, several model systems of early breast cancer progression have been developed. Some models have used human breast epithelial cell lines modified with activated oncogenes to drive production of premalignant lesions in immune deficient mouse hosts [23, 24, 24-27]). Two of these models are the HMT-3522 series (reviewed in [23, 27]) and the MCF10AT series (reviewed in [24, 26, 28]). The HMT-3522 series was derived from a woman with fibrocystic change and consists of three cell lines [23, 27]. The HMT-3522/S1 cell line, produced after *in vitro* culture of the explant, is nontumorigenic in nude mice [27]. The HMT-3522/S2 cell line was created by

EGF-independent growth selection *in vitro* and is able to form tumours in nude mice. However the tumours are slow growing and tumour take is low [27]. Finally, the HMT-3522/T4-2 cell line was created from a HMT-3522/S2 tumour and these cells are highly tumourigenic [27]. The MCF10AT series was also derived from a woman with fibrocystic change and represents a wide range of breast cancer pathologies [24, 26, 28]. The MCF10A cells are normal immortalized breast epithelial cells [28]. These cells were transfected with T-24 ras and renamed MCF10AneoT [24]. The MCF10AneoT cells are able to form tumours and in fact the MCF10AT cell line is a derivative of a MCF10AneoT lesion [24]. The MCF10AT cell line is able to form lesions with various premalignant histologies, including hyperplasia, ADH and DCIS with a quarter of the lesions able to progress to invasion [24, 28]. The most advanced cell line in the series are the MCF10CA cells, which are fully malignant and also form lesions with histological variation ranging from undifferentiated carcinomas to well differentiated adenocarcinomas [26, 28]. Both the HMT-3522 and MCF10AT series systems have proven useful; however, both series suffer from disadvantages. Both HMT-3522 and MCF10AT series show mixed phenotypes and lack of stability of the phenotypes after culture. Additionally, the HMT-3522 series lack a pre-DCIS or early stage of progression, while the MCF10AT series is dependent on a ras transformation, which is an alteration that is uncommon in spontaneous human breast cancers. Other breast cancer progression model systems have made use of murine models that have been genetically engineered to develop mammary epithelial preneoplasia or neoplasia (reviewed in [29]). Alternately, other murine models of progression have viral, chemical or hormonal

agent induced premalignant lesions (reviewed in [30]). It is worth noting however that in both types of murine models, the pre-malignant lesions being studied are mouse-derived and these lesions, while being similar to human lesions in some respects, are still different in other respects due to their mouse origins [29]. Additionally, the morphological progression continuum that has been described in human breasts cancer has not been described in genetically engineered murine mammary glands [29]. In order to study the molecular events underlying early breast cancer progression most efficiently, a human model system that represents all stages of progression is needed.

1.2. THE 21T SERIES HUMAN BREAST CANCER CELL LINES

1.2.1. Establishment of the 21T Series Cell Lines

The 21T human cell lines have been proposed to represent a progression series of early breast cancer. The series consists of three cell lines, which were derived from a single patient and are representative of different stages of progression [31]. The 36 year old patient originally presented with estrogen- and progesterone-receptor negative DCIS plus infiltrating ductal carcinoma (no special type) [31]. The 21PT and 21NT cell lines were derived from the mastectomy specimen and have been found to be stably non-tumourigenic and tumourigenic but non-metastatic, respectively, in nude mice [31]. One year post-mastectomy, the patient developed lung metastases with pleural effusion [31]. The third cell line, 21MT-1 cells, was derived from this pleural effusion and has been found to be both tumourigenic and metastatic [31].

In order to isolate the 21PT and 21NT cell lines from the mastectomy specimen, breast tissue was dissociated and cultured [31]. Fibroblasts from this mixed population were removed from the epithelial population by selective trypsinization [31]. The resulting pure epithelial population in 2D culture was composed of both normal-appearing epithelial cells and cells which looked to be more tumour-like [31]. The tumour-like cells were selectively expanded by both clonal isolation and serum selection and are what constitutes the 21PT and 21NT cells [31]. The 21MT-1 cells, which were isolated from the pleural effusion, were first pelleted down and then cultured in dishes [32]. After cells were attached, several washes were used to remove red blood cells and debris [32]. Loosely adhered mesothelial cells were also removed by repeated washing [32]. Percoll gradient fractionation was finally used to enhance the epithelial population [32]. The few mesothelial cells that remained after fractionation senesced after prolonged culture [32]. These cells were named 21MT cells. However, after approximately 100 population doublings two cell populations predominated [31]. One population was easily released from the culture plastic and this population was dubbed the 21MT-1 cells [31]. All three cell lines (21PT, 21NT, 21MT-1) were in continuous culture for over 2 years before publication [31].

1.2.2. Characteristics of the 21T Series Cells

As mentioned above, the 21PT cells are non-tumourigenic, while the 21NT cells are tumourigenic, but not metastatic and the 21MT-1 cells are tumourigenic and metastatic [31]. Karyotype were originally explored by Band *et al.* [31] and further refined by our laboratory [33]. Additional characterization of the cell series

has determined that the 21T cells all express cytokeratins 8, 18 and 19 [31, 34], as well as HMFG-2 [31], identifying them as epithelial cells of mammary origin. Although all three cell lines were initially thought to be ER and PR negative, as was the original tumour, subsequent work showed the 21PT cell line to express a variant ER-receptor, which is not well detected by conventional anti-ER antibodies [35, 36]. Mutations in the p53 gene were also investigated in the cell series since mutations in this gene are very common in breast cancer. It was found that all the 21T series cells have a frame-shift mutation in the p53 gene, which results in the loss of p53 expression and p53-mediated effects [37]. Finally, the 21T series cell lines all contain lower mRNA levels of epidermal growth factor receptor (EGFR) than normal breast epithelial cells, while mRNA levels of transforming growth factor alpha (TGF α), a ligand for EGFR, are reduced in 21MT-1 cells, but consistent with normal cells in 21PT and 21NT cells [31]. The HER-2 gene (neu, ERBB2; Human epidermal growth factor receptor 2), a marker for aggressive breast cancer, is overexpressed at both the mRNA and protein levels in all 21T series cells, with 21MT-1 cells producing higher levels than the other 21T series cells [31].

1.3. IN VIVO VS 3D IN VITRO CULTURE

1.3.1. Xenograft Mouse Model Limitations

Xenograft mouse models are extremely useful when studying human disease due to the fact that they share organ systems and an immense degree of genetic similarity to humans [38]. In fact, in the modern era, nearly every

successful cancer therapy has undergone xenograft testing [39]. Additionally, murine xenograft models have enabled the identification of early diagnostic markers and novel therapeutic targets, and an understanding of the *in vivo* biology and genetics of human tumour initiation, promotion, progression and metastasis [38]. However, xenograft mouse models are not perfect. Growth of human cells in mice requires that the mouse host be immunodeficient. The immunodeficiency of the mice means that the mouse host does not possess all the proper immune response that would be present in a human host [39]. Additionally the fact that human cells are injected into a mouse background can often result in an inability of the human cells to adapt and can lead to low tumour take [39]. Other issues arise in the variability that can arise between mice. In fact, mice purchased from different vendors may reproduce different experimental results due to genetic differences in the mouse strain between colonies [40]. Finally, mouse models are often slow, making it difficult to produce high throughput studies and rendering the study of the effects of individual genes on tumour cells more cumbersome than an *in vitro* system. The ease of manipulation of an *in vitro* system is also an advantage over an *in vivo* one. Due to the shorter time frame and ease of manipulation, there is increasing interest in the use of 3D *in vitro* model systems.

1.3.2. Matrigel and 3D In Vitro Culture

In vitro systems are very useful for high throughput studies. However, it has been shown that when grown in 2-dimensional (2D) *in vitro* culture, cell lines have distinctly different morphology and genetic profiles than when grown *in vivo*

[41-47]. Moreover, important signals released by the extracellular matrix, which govern normal homeostasis and tissue phenotypes are lost when cells are cultured on 2D plastic [41]. Alternatively, if cells are grown in laminin-rich extracellular matrix 3D cultures, many of these signals remain present [41]. Growing cells in 3D with extracellular matrix signals intact, allows for study of cell proliferation, apoptosis, cell morphogenesis and invasiveness in a closed system. In fact, there have been several studies using 3D systems to look at the molecular control of morphogenesis in breast epithelial cells [43, 48-57]. However, use of a 3D system to directly model aspects of early breast cancer progression has been limited. Growing the 21T series cell lines in a 3D *in vitro* model system, which will mimic the characteristics of their behaviour *in vivo*, should produce a more predictive model of the molecular/cellular events governing early tumour progression compared to a 2D *in vitro* system.

1.4. THESIS BACKGROUND STUDIES AND HYPOTHESES

1.4.1. 21T Series Cell Lines Mimic Stages of Breast Cancer Progression In Vivo

Prior to my own work, experiments in our laboratory were performed in order to verify the *in vivo* growth characteristics of the 21T series cell lines. The three 21T series cell lines were injected into the mammary fat pads of female nude mice, left for up to a year to develop lesions, and histology was performed on mammary fat pad and other organs on necropsy. Through the course of this work, it was discovered that the lesions formed in each case were of

characteristic morphology on hematoxylin and eosin (H&E) sectioning of the mammary fat pad (21PTci – ADH; 21NTci – DCIS; 21MT-1 – IMC). The results of this work have been included in our recent publication [58] and contribute to the work discussed in Chapter 2 of this thesis. The *in vivo* data included in Chapter 2 of this thesis was thus, completed before the beginning of the thesis work and was the basis for formation of the thesis hypothesis.

1.4.2. Thesis Hypotheses

I hypothesize first that the 21T series cells grown in a 3D culture system can be used to identify genes involved in the transitions between early stages of breast cancer. Secondly, I also hypothesize that this 3D system can then be used to determine the functional role of the identified genes in early breast cancer progression.

1.5. EXPERIMENTAL OBJECTIVES

1. To determine the growth characteristics of the 21T series cell lines in 3D *in vitro* culture.
2. To identify genes involved in the transition from ADH to DCIS and genes involved in the transition from DCIS to IMC.
3. To functionally characterize validated genes in the 3D system to determine their role in induction of tumour progression inhibition.

These experimental objectives are described in detail in Chapters 2 and 3. Both objectives 1 and 2 are addressed in Chapter 2, which proposes that the 21T

series cell lines are an appropriate model of early breast cancer progression when grown in 3D culture. Furthermore, Chapter 2 identified genes that are specifically altered in the transitions from ADH to DCIS and DCIS to IMC. Three of these genes, VANGL1, S100A2 and TBX3 were the focus of further study and are the subject of Chapter 3. It was found that VANGL1 plays a role in the transition from ADH to DCIS, while both S100A2 and TBX3 are involved in controlling the transition from DCIS to an invasive phenotype (IMC).

Together these two chapters demonstrate the ability of the 21T series cell lines to elucidate and test genes involved in controlling the transitions between stages of early breast cancer progression. Furthermore, genes identified and validated with this system may prove to be potential therapeutic targets in the future.

1.6. REFERENCES

1. "Canadian Cancer Society's Steering Committee": **Canadian Cancer Statistics 2010**. *Canadian Cancer Society* 2010, :.
2. Boyle P, Ferlay J: **Mortality and survival in breast and colorectal cancer**. *Nat Clin Pract Oncol* 2005, **2**(9):424-425.
3. Jemal A, Siegel R, Ward E, Hao Y, Xu J, Murray T, Thun MJ: **Cancer statistics, 2008**. *CA Cancer J Clin* 2008, **58**(2):71-96.
4. Jemal A, Siegel R, Xu J, Ward E: **Cancer statistics, 2010**. *CA Cancer J Clin* 2010, **60**(5):277-300.
5. Arpino G, Laucirica R, Elledge RM: **Premalignant and in situ breast disease: biology and clinical implications**. *Ann Intern Med* 2005, **143**(6):446-457.
6. Tang P, Hajdu SI, Lyman GH: **Ductal carcinoma in situ: a review of recent advances**. *Curr Opin Obstet Gynecol* 2007, **19**(1):63-67.

7. Allred DC, Wu Y, Mao S, Nagtegaal ID, Lee S, Perou CM, Mohsin SK, O'Connell P, Tsimelzon A, Medina D: **Ductal carcinoma in situ and the emergence of diversity during breast cancer evolution.** Clin Cancer Res 2008, **14**(2):370-378.
8. Page DL, Dupont WD, Rogers LW, Rados MS: **Atypical hyperplastic lesions of the female breast. A long-term follow-up study.** Cancer 1985, **55**(11):2698-2708.
9. Page DL, Dupont WD: **Anatomic indicators (histologic and cytologic) of increased breast cancer risk.** Breast Cancer Res Treat 1993, **28**(2):157-166.
10. Wellings SR, Jensen HM: **On the origin and progression of ductal carcinoma in the human breast.** J Natl Cancer Inst 1973, **50**(5):1111-1118.
11. Bodian CA, Perzin KH, Lattes R, Hoffmann P: **Reproducibility and validity of pathologic classifications of benign breast disease and implications for clinical applications.** Cancer 1993, **71**(12):3908-3913.
12. Carter CL, Corle DK, Micozzi MS, Schatzkin A, Taylor PR: **A prospective study of the development of breast cancer in 16,692 women with benign breast disease.** Am J Epidemiol 1988, **128**(3):467-477.
13. Dupont WD, Parl FF, Hartmann WH, Brinton LA, Winfield AC, Worrell JA, Schuyler PA, Plummer WD: **Breast cancer risk associated with proliferative breast disease and atypical hyperplasia.** Cancer 1993, **71**(4):1258-1265.
14. Allred DC, Mohsin SK, Fuqua SA: **Histological and biological evolution of human premalignant breast disease.** Endocr Relat Cancer 2001, **8**(1):47-61.
15. Polyak K: **Is breast tumor progression really linear?** Clin Cancer Res 2008, **14**(2):339-341.
16. Page DL, Dupont WD: **Anatomic markers of human premalignancy and risk of breast cancer.** Cancer 1990, **66**(6 Suppl):1326-1335.
17. Sgroi DC, Teng S, Robinson G, LeVangie R, Hudson JR, Jr, Elkahloun AG: **In vivo gene expression profile analysis of human breast cancer progression.** Cancer Res 1999, **59**(22):5656-5661.

18. Worsham MJ, Pals G, Raju U, Wolman SR: **Establishing a molecular continuum in breast cancer DNA microarrays and benign breast disease.** *Cytometry* 2002, **47**(1):56-59.
19. Li Z, Tsimelzon A, Immaneni A, Mohsin SK, Hilsenbeck SG, Clark GC, Fuqua SAW, Osborne CK, O'Connell P, Allred DC: **A cDNA microarray study comparing noninvasive and invasive human breast cancer.** *Proc Am Assoc Cancer Res* 2002, **43**:901-902.
20. Ma XJ, Salunga R, Tuggle JT, Gaudet J, Enright E, McQuary P, Payette T, Pistone M, Stecker K, Zhang BM, Zhou YX, Varnholt H, Smith B, Gadd M, Chatfield E, Kessler J, Baer TM, Erlander MG, Sgroi DC: **Gene expression profiles of human breast cancer progression.** *Proc Natl Acad Sci U S A* 2003, **100**(10):5974-5979.
21. Abba MC, Drake JA, Hawkins KA, Hu Y, Sun H, Notcovich C, Gaddis S, Sahin A, Baggerly K, Aldaz CM: **Transcriptomic changes in human breast cancer progression as determined by serial analysis of gene expression.** *Breast Cancer Res* 2004, **6**(5):R499-513.
22. Schuetz CS, Bonin M, Clare SE, Nieselt K, Sotlar K, Walter M, Fehm T, Solomayer E, Riess O, Wallwiener D, Kurek R, Neubauer HJ: **Progression-specific genes identified by expression profiling of matched ductal carcinomas in situ and invasive breast tumors, combining laser capture microdissection and oligonucleotide microarray analysis.** *Cancer Res* 2006, **66**(10):5278-5286.
23. Weaver VM, Howlett AR, Langton-Webster B, Petersen OW, Bissell MJ: **The development of a functionally relevant cell culture model of progressive human breast cancer.** *Semin Cancer Biol* 1995, **6**(3):175-184.
24. Miller FR: **Xenograft models of premalignant breast disease.** *J Mammary Gland Biol Neoplasia* 2000, **5**(4):379-391.
25. Stampfer MR, Yaswen P: **Culture models of human mammary epithelial cell transformation.** *J Mammary Gland Biol Neoplasia* 2000, **5**(4):365-378.
26. Santner SJ, Dawson PJ, Tait L, Soule HD, Eliason J, Mohamed AN, Wolman SR, Heppner GH, Miller FR: **Malignant MCF10CA1 cell lines derived from premalignant human breast epithelial MCF10AT cells.** *Breast Cancer Res Treat* 2001, **65**(2):101-110.
27. Briand P, Lykkesfeldt AE: **An in vitro model of human breast carcinogenesis: epigenetic aspects.** *Breast Cancer Res Treat* 2001, **65**(2):179-187.

28. Miller FR, Santner SJ, Tait L, Dawson PJ: **MCF10DCIS.com xenograft model of human comedo ductal carcinoma in situ.** J Natl Cancer Inst 2000, **92**(14):1185-1186.
29. Cardiff RD, Moghanaki D, Jensen RA: **Genetically engineered mouse models of mammary intraepithelial neoplasia.** J Mammary Gland Biol Neoplasia 2000, **5**(4):421-437.
30. Medina D: **The preneoplastic phenotype in murine mammary tumorigenesis.** J Mammary Gland Biol Neoplasia 2000, **5**(4):393-407.
31. Band V, Zajchowski D, Swisshelm K, Trask D, Kulesa V, Cohen C, Connolly J, Sager R: **Tumor progression in four mammary epithelial cell lines derived from the same patient.** Cancer Res 1990, **50**(22):7351-7357.
32. Band V, Zajchowski D, Stenman G, Morton CC, Kulesa V, Connolly J, Sager R: **A newly established metastatic breast tumor cell line with integrated amplified copies of ERBB2 and double minute chromosomes.** Genes Chromosomes Cancer 1989, **1**(1):48-58.
33. Xu J, Souter LH, Chambers AF, Rodenhiser DI, Tuck AB: **Distinct karyotypes in three breast cancer cell lines --21PTCi, 21NTCi, and 21MT-1 --derived from the same patient and representing different stages of tumor progression.** Cancer Genet Cytogenet 2008, **186**(1):33-40.
34. Trask DK, Band V, Zajchowski DA, Yaswen P, Suh T, Sager R: **Keratins as markers that distinguish normal and tumor-derived mammary epithelial cells.** Proc Natl Acad Sci U S A 1990, **87**(6):2319-2323.
35. Biswas DK, Cruz A, Pettit N, Mutter GL, Pardee AB: **A therapeutic target for hormone-independent estrogen receptor-positive breast cancers.** Mol Med 2001, **7**(1):59-67.
36. Biswas DK, Averboukh L, Sheng S, Martin K, Ewaniuk DS, Jawde TF, Wang F, Pardee AB: **Classification of breast cancer cells on the basis of a functional assay for estrogen receptor.** Mol Med 1998, **4**(7):454-467.
37. Liu XL, Band H, Gao Q, Wazer DE, Chu Q, Band V: **Tumor cell-specific loss of p53 protein in a unique in vitro model of human breast tumor progression.** Carcinogenesis 1994, **15**(9):1969-1973.
38. Hann B, Balmain A: **Building 'validated' mouse models of human cancer.** Curr Opin Cell Biol 2001, **13**(6):778-784.

39. Sharpless NE, Depinho RA: **The mighty mouse: genetically engineered mouse models in cancer drug development.** Nat Rev Drug Discov 2006, **5**(9):741-754.
40. Welch DR: **Technical considerations for studying cancer metastasis in vivo.** Clin Exp Metastasis 1997, **15**(3):272-306.
41. Lee GY, Kenny PA, Lee EH, Bissell MJ: **Three-dimensional culture models of normal and malignant breast epithelial cells.** Nat Methods 2007, **4**(4):359-365.
42. Fournier MV, Martin KJ: **Transcriptome profiling in clinical breast cancer: from 3D culture models to prognostic signatures.** J Cell Physiol 2006, **209**(3):625-630.
43. Hebner C, Weaver VM, Debnath J: **Modeling morphogenesis and oncogenesis in three-dimensional breast epithelial cultures.** Annu Rev Pathol 2008, **3**:313-339.
44. Shaw KR, Wrobel CN, Brugge JS: **Use of three-dimensional basement membrane cultures to model oncogene-induced changes in mammary epithelial morphogenesis.** J Mammary Gland Biol Neoplasia 2004, **9**(4):297-310.
45. Kenny PA, Lee GY, Myers CA, Neve RM, Semeiks JR, Spellman PT, Lorenz K, Lee EH, Barcellos-Hoff MH, Petersen OW, Gray JW, Bissell MJ: **The morphologies of breast cancer cell lines in three-dimensional assays correlate with their profiles of gene expression.** Mol Oncol 2007, **1**(1):84-96.
46. Martin KJ, Patrick DR, Bissell MJ, Fournier MV: **Prognostic breast cancer signature identified from 3D culture model accurately predicts clinical outcome across independent datasets.** PLoS One 2008, **3**(8):e2994.
47. Schmeichel KL, Bissell MJ: **Modeling tissue-specific signaling and organ function in three dimensions.** J Cell Sci 2003, **116**(Pt 12):2377-2388.
48. Fauquette W, Dong-Le Bourhis X, Delannoy-Courdent A, Boilly B, Desbiens X: **Characterization of morphogenetic and invasive abilities of human mammary epithelial cells: correlation with variations of urokinase-type plasminogen activator activity and type-1 plasminogen activator inhibitor level.** Biol Cell 1997, **89**(7):453-465.
49. Weaver VM, Petersen OW, Wang F, Larabell CA, Briand P, Damsky C, Bissell MJ: **Reversion of the malignant phenotype of human breast cells in three-dimensional culture and in vivo by integrin blocking antibodies.** J Cell Biol 1997, **137**(1):231-245.

50. Wang F, Weaver VM, Petersen OW, Larabell CA, Dedhar S, Briand P, Lupu R, Bissell MJ: **Reciprocal interactions between beta1-integrin and epidermal growth factor receptor in three-dimensional basement membrane breast cultures: a different perspective in epithelial biology.** Proc Natl Acad Sci U S A 1998, **95**(25):14821-14826.
51. Hirai Y, Lochter A, Galosy S, Koshida S, Niwa S, Bissell MJ: **Epimorphin functions as a key morphoregulator for mammary epithelial cells.** J Cell Biol 1998, **140**(1):159-169.
52. Soriano JV, Pepper MS, Orci L, Montesano R: **Roles of hepatocyte growth factor/scatter factor and transforming growth factor-beta1 in mammary gland ductal morphogenesis.** J Mammary Gland Biol Neoplasia 1998, **3**(2):133-150.
53. Simian M, Hirai Y, Navre M, Werb Z, Lochter A, Bissell MJ: **The interplay of matrix metalloproteinases, morphogens and growth factors is necessary for branching of mammary epithelial cells.** Development 2001, **128**(16):3117-3131.
54. Niemann C, Brinkmann V, Birchmeier W: **Hepatocyte growth factor and neuregulin in mammary gland cell morphogenesis.** Adv Exp Med Biol 2000, **480**:9-18.
55. Ball EM, Risbridger GP: **Activins as regulators of branching morphogenesis.** Dev Biol 2001, **238**(1):1-12.
56. Debnath J, Brugge JS: **Modelling glandular epithelial cancers in three-dimensional cultures.** Nat Rev Cancer 2005, **5**(9):675-688.
57. Debnath J, Mills KR, Collins NL, Reginato MJ, Muthuswamy SK, Brugge JS: **The role of apoptosis in creating and maintaining luminal space within normal and oncogene-expressing mammary acini.** Cell 2002, **111**(1):29-40.
58. Souter LH, Andrews JD, Zhang G, Cook AC, Postenka CO, Al-Katib W, Leong HS, Rodenhiser DI, Chambers AF, Tuck AB: **Human 21T breast epithelial cell lines mimic breast cancer progression in vivo and in vitro and show stage-specific gene expression patterns.** Lab Invest 2010, **90**(8):1247-1258.

CHAPTER 2. 21T SERIES CELL LINES MIMIC SPECIFIC STAGES OF BREAST CANCER PROGRESSION IN 3D CULTURE AND SHOW STAGE-SPECIFIC GENE EXPRESSION PATTERNS

The contents of this chapter has been adapted from a paper entitled “Human 21T breast epithelial cell lines mimic breast cancer progression *in vivo* and *in vitro* and show stage specific gene expression patterns”, published in Laboratory Investigation, vol 90: pp. 1247-1258 (2010), by Lesley H. Souter, Joseph D. Andrews, Guihua Zhang, Amy C. Cook, Carl O. Postenka, Waleed Al-Katib, Hon S. Leong, David I. Rodenhiser, Ann F. Chambers and Alan B. Tuck. The *in vivo* experiment was conducted prior to this thesis project.

2.1. INTRODUCTION

Pathologic and epidemiologic evidence has led to a histologic model of breast cancer evolution in which stem cells from the terminal duct lobular unit (TDLU) give rise to atypical ductal hyperplasia (ADH) or atypical lobular hyperplasia (ALH), which can then progress to ductal carcinoma *in situ* (DCIS) or lobular carcinoma *in situ* (LCIS) respectively, and eventually to invasive mammary carcinomas (IMC) [1-6]. These histologic patterns are, however, most likely only rough phenotypic indications of underlying cellular and molecular events determining progression [7], and may not necessarily occur in a linear fashion. There is currently much interest in identifying the nature of the cellular and molecular events involved, not only for use in determining at which point a

lesion is most likely to progress to malignancy, but also in hopes of finding a way to halt progression at these early stages.

Microarray technology and proteomics have identified candidate genes with potential involvement in cell proliferation, cell death, cell adhesion, migration, invasion, etc., at different stages of breast cancer progression [8-13]. Although providing important information concerning gene expression between samples at any given stage of progression, this is only a static representation of what is presumed to be a dynamic process. Model systems are thus needed, in addition to histological analysis of human breast specimens, to directly evaluate the effects of expression of specific genes, in order to determine the functional roles of these genes at different stages of tumour progression.

There have been a number of different approaches to modeling early breast cancer progression. Some have made use of murine models whereby premalignant lesions are induced by viral, chemical, or hormonal agents (reviewed in [14]), or whereby genetically engineered mice are generated which are susceptible to developing mammary epithelial neoplasia or preneoplasia (reviewed in [15]). In these instances, it is mouse-derived pre-malignant lesions that are being generated and studied, which show both similarities and differences with their human counterparts. Other models have used human breast epithelial cell lines that have been spontaneously transformed, transduced with oncogenic viruses, or transfected with activated oncogenes to derive altered cells that mimic premalignant lesions when tested in immune deficient rodent hosts (egs. HMT-3522 and MCF10AT series, reviews in [16, 17, 17-20]). These systems are useful, but suffer the disadvantages of lack of representation of

earlier (pre-DCIS) stages of progression (HMT-3522 series), the presence of mixed phenotypes, lack of stability of the phenotypes after culture (both series), or the dependence on *ras* transformation (MCF10AT series).

For ease of experimental manipulation, there has been much interest in comparing cells of premalignant and malignant status in 3D *in vitro* cultures [21-27]. By allowing cells to grow in 3D conformation in extracellular matrix certain characteristics of cell morphogenesis, proliferation, apoptosis and invasiveness may be studied in a controlled system. Using such 3D culture systems, much information has been generated on the molecular controls of morphogenesis in breast epithelial cells of different origins [21-23, 28-35]. To this point however, only limited use has been made of such 3D *in vitro* systems to directly model aspects of early breast cancer progression.

The 21T series cell lines, which were derived from a single patient with metastatic breast cancer, have been proposed to represent a human breast cancer progression series [36]. The 21PT and 21NT cell lines were established from the mastectomy specimen and have been found to be stably non-tumourigenic, and tumourigenic but non-metastatic, respectively, in nude mice [36]. The third cell line, 21MT-1, was derived from a malignant pleural effusion and has been found to be both tumourigenic and metastatic [36]. 21T series cells all express cytokeratins 8, 18 and 19, as well as HMFG-2 [36], identifying them as epithelial cells of mammary origin. Although all three cell lines were initially thought to be ER and PR negative, subsequent work showed the 21PT cell line to express a variant ER-receptor, which is not well detected by conventional anti-ER antibodies [37, 38].

To further explore the potential of the 21T series human breast cell lines as a functional model of early breast cancer progression, we have investigated their behaviour both histologically *in vivo* and in 3D *in vitro* cultures. Characterization of these cells at the molecular level, using gene expression profiling of cells grown in 3D culture, revealed stage-specific differences in genes involved in certain signalling pathways and functional categories reflective of progression to a more aggressive phenotype. Comparison with published microarray data from clinical human specimens has generated a “genes of interest” short list, consisting of genes which have potential clinical relevance and are thus prime candidates for further functional testing and development as stage-specific targets to block breast cancer progression.

2.2. MATERIALS AND METHODS

2.2.1. Cell Lines and Culture

The 21T series cell lines (21PT, 21NT, 21MT-1) were obtained as a kind gift of Dr Vimla Band (Dana Farber Cancer Institute) [36]. These cells were maintained in culture in α -MEM supplemented with 10% fetal bovine serum (FBS), 2 mM L-glutamine (both from Gibco Life Technologies, Grand Island, NY), insulin (1 μ g/mL), epidermal growth factor (12.5 ng/mL), hydrocortisone (2.8 mM), 10mM 4-(2-hydroxyethyl)-1-piperazineethanesulfonic acid (HEPES), 1mM sodium pyruvate, 0.1 mM nonessential amino acids and 50 mg/mL gentamycin reagent (all from Sigma Chemical, St. Louis, MO), as previously described [39]. After addition of all reagents, this growth medium was referred to as α HE. The

21PT and 21NT-derived cell lines used in this work, designated 21PTci and 21NTci, are a pooled population of vector-only (pcDNA3) transfected cells and have been used as control cells for previous work in our laboratory [40]. Culture medium for these cell lines is the same as for the parental cell lines, with the addition of 0.2 mg/mL G418 as a selection marker (Gibco Life Technologies).

2.2.2. *In Vivo Studies*

Female athymic NCr nude mice (*nu/nu*) were housed and cared for in accordance with the recommendations of the Canadian Council on Animal Care, under a protocol approved by the University of Western Ontario Council on Animal Care. Cell lines were grown in 150 mm tissue culture dishes to ~ 80% confluency (log phase of growth). The cells were gently trypsinized, washed twice with sterile PBS, and resuspended in serum-free α HE media at a concentration of 1×10^7 cells per 100 μ l. Cells were injected into the second thoracic mammary fat pad of 8-9 week old female nude mice, as described elsewhere [41]. Animals were routinely monitored for health and primary tumours, when palpable, were measured every 7-14 days. Animals were euthanized early if the tumour burden became too great, or at the end point of the experiment (1 year post-injection). Animals were sacrificed and necropsies performed, examining the injected mammary fat pad, locoregional lymph nodes, and all major viscera, whether or not a palpable lesion was present. Tissues were formalin-fixed, paraffin embedded, sectioned (4 μ m thick) and examined histologically by hematoxylin and eosin (H&E) staining.

2.2.3. 3D In Vitro Cultures

For all 3D cultures, cells were grown in Matrigel Basement Membrane Matrix (BD Biosciences, Mississauga, ON) for 9 or 15 days. Cultures were created in 48-well plates (Nunc Brand Products, Rochester, NY) with three distinct layers. The bottom layer consisted of undiluted Matrigel for a solid base. The middle layer contained a 1:1 mix of Matrigel and 2×10^5 cells in media supplemented with 0.1% bovine serum albumin (BSA), instead of FBS. These two layers were topped with growth media supplemented with 0.1% BSA (without FBS). After growth in Matrigel, 10% neutral buffered formalin was added to the dishes for 48 hours and the cultures were removed as intact Matrigel plugs. The formalin-fixed plugs were then processed, paraffin-embedded and sectioned for H&E staining and immunohistochemistry.

2.2.4. Morphologic Characterization of 3D In Vitro Cultures

Histomorphology was determined by examination of 4 μm , H&E stained sections of the Matrigel plugs. Characterization of behaviour included assessment of extracellular lumen formation, number of groups with polarized cells, spherical (vs. non-spherical) colony formation and proportion of single cells. Each of these parameters was assessed in terms of a percentage of total “events” counted. Appendix B Figure 1 illustrates each of the cell colony morphologies. For each cell line, 10 high power (400X) fields of view from three replicate Matrigel plugs were examined. This yielded between 200 and 275 events per 10 high power fields.

2.2.5. Proliferation and Apoptosis in 3D Culture

The 21T series cell lines were grown in Matrigel for 9 or 15 days. Matrigel plugs were immunostained for the proliferation marker, Ki67, and for the apoptotic marker, caspase 3. For caspase 3 immunohistochemistry, deparaffinized sections were pretreated in a microwave oven for epitope retrieval. Caspase 3 antibody, which recognized cleaved caspase 3 (Cell Signaling Technologies, Danvers, MA) was applied (1/300 dilution) for 15 min at room temperature. Ki67 staining was performed following a previously published protocol [42] with Ki67 antibody (Dako, Mississauga, ON) applied (1/150 dilution) overnight at 4°C. For both caspase 3 and Ki67, detection was performed with the UltraVision LP Detection System HRP Polymer (Thermo Scientific, Waltham, MA) kit, following the manufacturer's protocol. Slides were counterstained with Harris's Hematoxylin. Positive and negative controls were included. For each cell line, the Ki67 and caspase 3 indices, defined as the number of cells positive for Ki67 or caspase 3 staining divided by the total cells counted, were calculated from examination of 10 high power (400X) fields of view from three replicate Matrigel plugs per cell line, yielding between 200 and 350 cells. In order to determine the balance of dividing cells vs. apoptosing cells, the ratio of proliferation over apoptosis was calculated for each cell line.

2.2.6. Matrigel Invasion Assay

21T series cell lines were grown in Matrigel for 9 days in 8-well chamber slides (Nunc Brand Products). Matrigel cultures were formed as above, with adjustment made in volumes of the three layers for the smaller 8-well chamber

slide. 1.5×10^4 cells were used in the middle layer. Slides were then moved to an incubated stage platform of a Zeiss Axiovert 200M microscope for time lapse photography. Z-stack microscopy images at 5 positions were taken for each cell line every 12 hours until day 15 of growth. All cells found within the 5 positions per cell line (around 100 cells total) were then followed using AxioVision 4.5 software (Carl Zeiss Imaging Solutions) to determine the percentage of cells that invaded through the Matrigel matrix and the distance the cells traveled. A cell was defined as moving if any part of the cell was in a different location compared to the image taken 12 hours previously. The minimum distance a cell could travel to be designated as moving was 5 μm . The distance a moving cell travelled was measured using the AxioVision 4.5 software.

2.2.7. Gene Expression Profiling in 3D Culture

For expression profiling in 3D culture, cells were grown in Matrigel for 9 days in 24-well plates (Nunc Brand Products). Matrigel cultures were formed as above with an adjustment made in volumes of the three layers for the larger 24-well plate volume. Three wells per cell line, representing 3 biological replicates, were grown. Total RNA from each biological replicate was isolated using Cell Recovery Solution (BD Biosciences) to non-enzymatically dissociate the Matrigel, followed by TRIzol (Invitrogen International, Mississauga, ON), as per the manufacturer's instructions. RNA (10 μg) was then sent to the London Regional Genomics Centre (www.lrgc.ca, London, ON) and was used to produce Biotin labeled cRNA, which was hybridized to Affymetrix HGU133_Plus_2 arrays (Affymetrix, Inc., Santa Clara, CA). Washing, scanning and probe quantification

were carried out according to the manufacturer's instructions, using GeneChip Operating Software (GCOS, www.affymetrix.com), with target intensity set to 150. For each array, GCOS output was imported as .txt files into Genespring GX 7.3 software (Agilent Technologies, Santa Clara, CA), and data were normalized as follows: Values <0.01 were set to 0.01 and the median intensity of each array was normalized to the 50th percentile of all arrays. Finally, the intensity of each probe set in each of the three 21NTci or 21MT-1 arrays was divided by the normalized mean intensity of that probe set in the appropriate control arrays. The geometric mean of these 3 ratios is reported. In order to control the family-wise error rate, two separate analyses were performed: 21NTci vs. 21PTci, with 21PTci as control, and 21MT-1 vs. 21NTci, with 21NTci as control. After normalization, the data were first prefiltered. Any probe set flagged 'absent' by GCOS software in all 9 arrays was removed from further consideration. The full raw data for all 9 arrays can be found at <http://www.ncbi.nlm.nih.gov/geo/>, data series GSE18370. Next, any probe set not changing at least 1.5-fold in 21NTci relative to 21PTci or 21MT-1 relative to 21NTci was removed. Probe sets passing these criteria were analyzed using the student's t-test tool in Genespring, with the nominal p-value set at $p < 0.05$. This resulted in two lists of genes, one with genes significantly changed in 21NTci vs. 21PTci (Supplemental Table 1) and the other with genes significantly changed in 21MT-1 vs. 21NTci (Supplemental Table 2). In order to focus our search to genes relevant in a clinical setting, the "significantly altered" gene lists were then compared to gene expression profiling information on clinically relevant databases we established from the literature related to early progression, invasion/metastasis and prognosis of breast cancer [11-13, 43-51]

(Supplemental Table 3). New gene lists created from gene expression alterations in common with the clinical databases (Appendix B Table 1) were imported into Ingenuity Pathways Analysis[®] (IPA) (Ingenuity[®] Systems, www.ingenuity.com). Each gene identifier in the data sets was mapped to its corresponding gene in the Ingenuity Pathways Knowledge Base, and if present, was considered for analysis. Functional analysis identified biological functions and/or diseases that were most significant to the data set. Canonical pathway analysis identified pathways from the IPA library that were most significant to the data set.

2.2.8. Quantitative Real Time-PCR (qRT-PCR) Validation

Total RNA was extracted from 4 biological replicates of each cell line following 9 days of growth in 3D Matrigel, using the same methodology employed for gene expression profiling. cDNA was synthesized from 1 μ g total RNA using Superscript II (Invitrogen International), with random primers (Invitrogen International), as per the manufacturer's instructions. qRT-PCR was performed using a Rotor-Gene RG-3000 (Corbett Life Science, San Francisco, CA), in combination with SYBR-Green. RT2 qPCR primers for the selected targets (BAX, CCL20, CCR1, CDH1, CXCR4, DCN, MAX, MCM4, MGA, S100A2, S100A3, SERPINB5, SNAI2, TBX3, TFF2, TNFAIP3, VANGL1, WISP1, WNT5A) and RT2 SYBR-Green qPCR Master Mix were purchased from SuperArray Bioscience Corporation. 18S rRNA was used as an endogeneous control (SuperArray Biosciences Corporation). Genes were considered to be validated if

the qRT-PCR results showed statistically significant expression alterations in agreement with the microarray.

2.2.9. Statistical Analysis

The differences between experimental groups were analyzed using one-way analysis of variance (ANOVA), followed by Tukey's test for post hoc analysis. For the Matrigel invasion assay, a Kruskal-Wallis nonparametric ANOVA was used when calculating the percent of cells that moved, as the values were not normally distributed. This was also followed by a Tukey's post hoc test. For all statistics, a p-value of less than 0.05 was considered statistically significant.

2.3. RESULTS

2.3.1. *In Vivo Cultures of 21T Series Cell Lines Model Stages of Early Progression*

Mice injected in the mammary fat pad with each of the three 21T series cell lines were monitored for tumour growth for up to a year. This study confirmed the previously published findings of Band and colleagues [36] that 21PT-derived cells are non-tumourigenic and non-metastatic, 21NT-derived cells are tumourigenic but non-metastatic, and 21MT-1 cells are tumourigenic and metastatic in some mice (Table 2.1). In addition, in our study, systematic histologic examination of the mammary fat pads of all animals, whether or not tumours were palpable, was performed at end-point and provided some very

Table 2.1. Histopathology of 21T series cell lines *in vivo* one year after orthotopic mammary fat pad injection into 6-8 week old female nude mice.

	No. of mice showing ADH ¹ only	No. of mice showing DCIS ² only	No. of mice showing invasive carcinoma	No. of mice showing metastases
21PTci	2/32	0/32	0/32	0/32
21NTci	0/29	6/29	1/29	0/29
21MT-1	0/15	0/15	10/15	5/15

¹ ADH, atypical ductal hyperplasia

² DCIS, ductal carcinoma in situ

novel information. Where microscopically discernible lesions formed, each of the injected cell lines gave rise to a characteristic histomorphology. Mammary fat pads of 21PTci-injected mice showed scattered ducts with features of ADH (Table 2.1 and Figure 2.1A). In keeping with ADH [6], involved ducts of these animals showed a mixture of two epithelial cell populations, one atypical/neoplastic appearing (non-high grade), and the other normal/benign appearing (Figure 2.1A inset). None of the ducts in 21PTci-injected mice displayed a morphology that met criteria for DCIS (incomplete duct filling by atypical cell population, < 2.0 mm in greatest extent). In contrast, mammary fat pads of 21NTci-injected mice showed a pattern of DCIS (intermediate and high nuclear grade, solid and cribriform, with zonal necrosis), which in 6/7 of those mice forming lesions had no associated invasive component (Table 2.1 and Figure 2.1B). In the one 21NTci-injected animal where associated invasive carcinoma was present, the degree of invasion was minimal, and no metastases were seen (Table 2.1). In sharp contrast to both, mammary fat pads of 21MT-1 injected mice showed a pattern of IMC in all instances where a histologically discernable lesion formed, and half of these were also associated with pulmonary metastases (Table 2.1 and Figure 2.1C). The *in vivo* growth characteristics of these three 21T series cell lines thus reproducibly model distinct histologic stages of early breast progression, from ADH (21PTci) to DCIS (21NTci) to IMC (21MT-1), up to one year after mammary fat pad injection in mice.

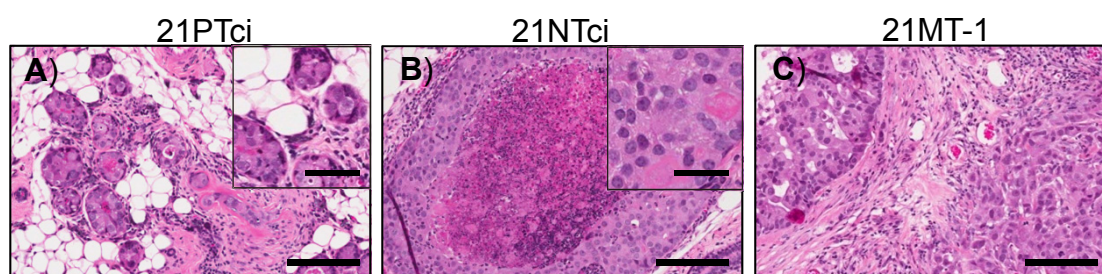


Figure 2.1. Histopathology of 21T series cells *in vivo*, 1 year after injection of 1×10^7 cells into the mammary fat pad of 6-8 week old female nude mice. Histology was analyzed for mammary fat pads of all mice injected. A) 21PTci cells mimicked aspects of ADH, with both atypical (non-high grade) and normal-appearing populations visible in a given involved duct/ductule and with the atypical cell population represented over an area of < 2.0 mm (i.e. not meeting pathologic criteria for DCIS). B) 21NTci cell morphology mimicked DCIS, with the neoplastic cells filling an entire mammary fat pad duct, often with accompanying central zonal necrosis. This pattern was seen in multiple duct cross-sections (over an area > 2.0 mm). C) 21MT-1 cells displayed a histology of IMC (no special type, SBR Grade III/III), associated with a background DCIS. All sections are H&E stained. Scale bars represent $200\mu\text{m}$, except for the inset of a) and b), which represents $100\mu\text{m}$. All images are 24-bit resolution TIFFs (1.8 MP) captured with an Aperio Scanscope, scanning with the 400x objective.

2.3.2. 3D *In Vitro* Cultures of 21T Series Cells Display Features of Specific Stages of Early Progression

In order to develop a more rapid, readily manipulatable *in vitro* system for assessing the biologic differences between these cells, we made use of a 3D Matrigel model. Cells were grown in 3D Matrigel plugs for 9 or 15 days, and characterized using a number of morphologic and functional parameters, including colony profile (spherical vs. irregular), lumen formation, cell polarization, proportion of single cells, Ki67 proliferation index, caspase 3 apoptosis index and cell invasion (by time lapse microscopy). By day 15, 21PTci cells were found to form many spherical colonies, which had a high proportion of polarized cells and extracellular lumen formation (Figure 2.2A, D, G). Interestingly, many of the 21PTci cell colonies had an admixture of cells with nuclei that appeared either normal or atypical in morphology. In contrast, 21NTci cells showed fewer spherical colony profiles, and a lesser degree of cell polarization and lumen formation than the 21PTci cells (Figure 2.2B, E, G). Most of the 21NTci cell groups showed significant nuclear atypia. Finally, 21MT-1 cells showed a much lower proportion of spherical colonies (more were of irregular profile) and a high proportion of single cells than either of the other lines. Additionally, 21MT-1 cell groups show even less polarization and extracellular lumen formation than 21NTci cells (Figure 2.2C, F, G).

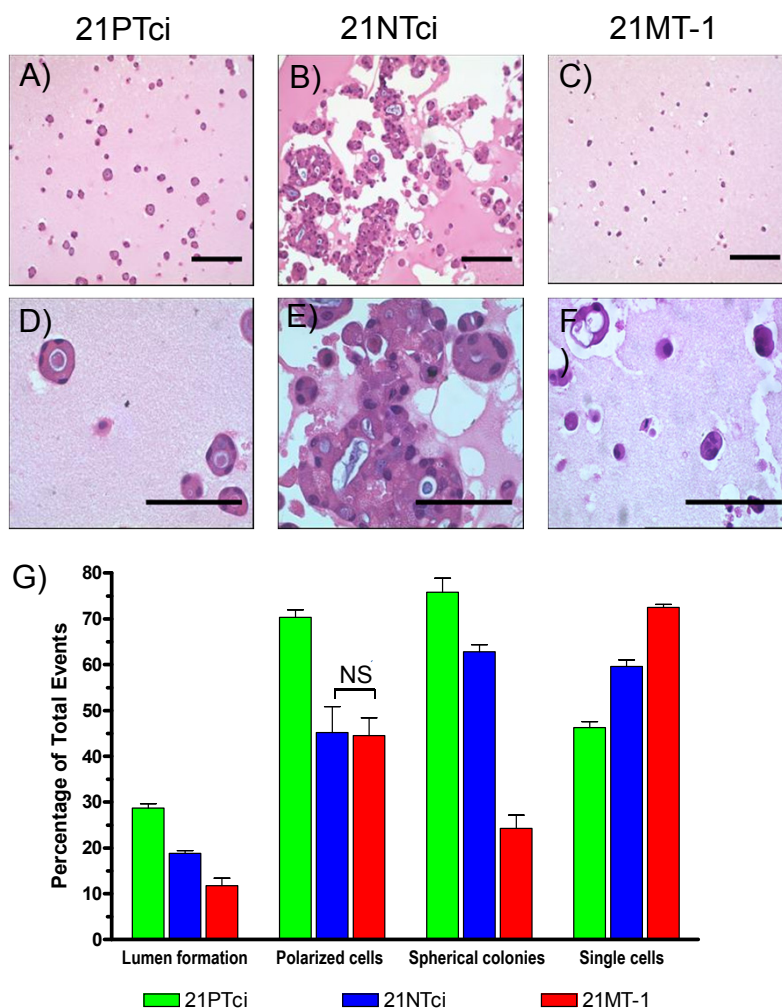


Figure 2.2. *In vitro* characteristics of 21PTci, 21NTci and 21MT-1 cells after 15 days growth in 3D Matrigel. 21PTci cells (A,D,G) formed more polarized cell groups than 21NTci ($p < 0.05$) or 21MT-1 ($p < 0.05$) cells, with higher frequency of extracellular lumen formation (~10%, $p < 0.01$ and ~17%, $p < 0.001$ respectively) and more crisply-defined spherical colonies than 21NTci ($p < 0.05$) or 21MT-1 ($p < 0.001$) cells. 21NTci cells (B,E,G) formed large numbers of cohesive spherical colonies (~38% compared to 21MT-1 cells, $p < 0.001$), but have less tendency towards cell polarization. 21MT-1 cells (C,F,G) were present more as single cells (~26% more than 21PTci cells, $p < 0.001$ and ~13% more than 21NTci cells, $p < 0.001$) and small groups, which were non-spherical and less polarized (than 21PTci), in an invasive pattern of distribution. All sections are H&E stained. Images were chosen to demonstrate structures of 3D cell colonies and not typical cell density within a Matrigel plug. In (G) for 'single cells', an "event" is either a single cell or a cell group/colony, while for the 'spherical colonies', 'lumen formation' and 'polarized cells' comparisons, an "event" was defined as a cell group/colony. Also for (G) all bars within each group are significantly different from each other at a p -value of at least < 0.05 , except when indicated by NS (non significant). Scale bars for (A,B,C) represent 100 μm, while scale bars for (D,E,F) represent 50 μm.

2.3.3. Differential Proliferation, Apoptosis and Invasiveness of 21T Series Cells

Assessment of proliferative rates by Ki67 immunohistochemistry showed that at day 9, 21NTci cells showed significantly more proliferative events than 21PTci or 21MT-1 cells ($p < 0.01$) (Figure 2.3A). However, the proliferative rate of both 21NTci and 21PTci had dropped off by 15 days of growth in Matrigel, whereas that of 21MT-1 cells was highest at day 15 (3x that of 21PTci, $p < 0.01$) (Figure 2.3A). Apoptotic rates by caspase 3 immunohistochemistry showed that there were no significant differences between cell lines at day 9, however by day 15, apoptotic rates drop slightly and not significantly for 21PTci cells and slightly and significantly ($p < 0.01$) for 21MT-1 cells (Figure 2.3B). The ratios of proliferation/apoptosis were calculated for the 21T series cell lines grown in Matrigel, using Ki67 (proliferation) vs. caspase 3 (apoptosis) index. Results indicate that at day 9, 21NTci cells had the highest ratio of proliferation/apoptosis, compared to 21PTci cells ($p < 0.05$) or 21MT-1 cells ($p < 0.05$) (Figure 2.3C). However, by day 15, 21MT-1 cells showed an increased proliferation/apoptosis ratio, which was higher than either of the other 2 cell lines ($p < 0.01$ compared to 21PTci and 21NTci) (Figure 2.3C). The 21NTci cells, which showed a high rate of growth at day 9, had a significantly decreased ($p < 0.05$) ratio on day 15 (Figure 2.3C). The 21PTci cells showed a trend towards a decrease in proliferation/apoptosis at day 15 compared to day 9, but this was not significant. Interestingly, by day 15 (vs. day 9), a higher proportion of 21PTci and 21NTci cells were present as polarized groups showing extracellular lumen formation, suggesting that the decrease in ratio of cell proliferation/apoptosis may be related

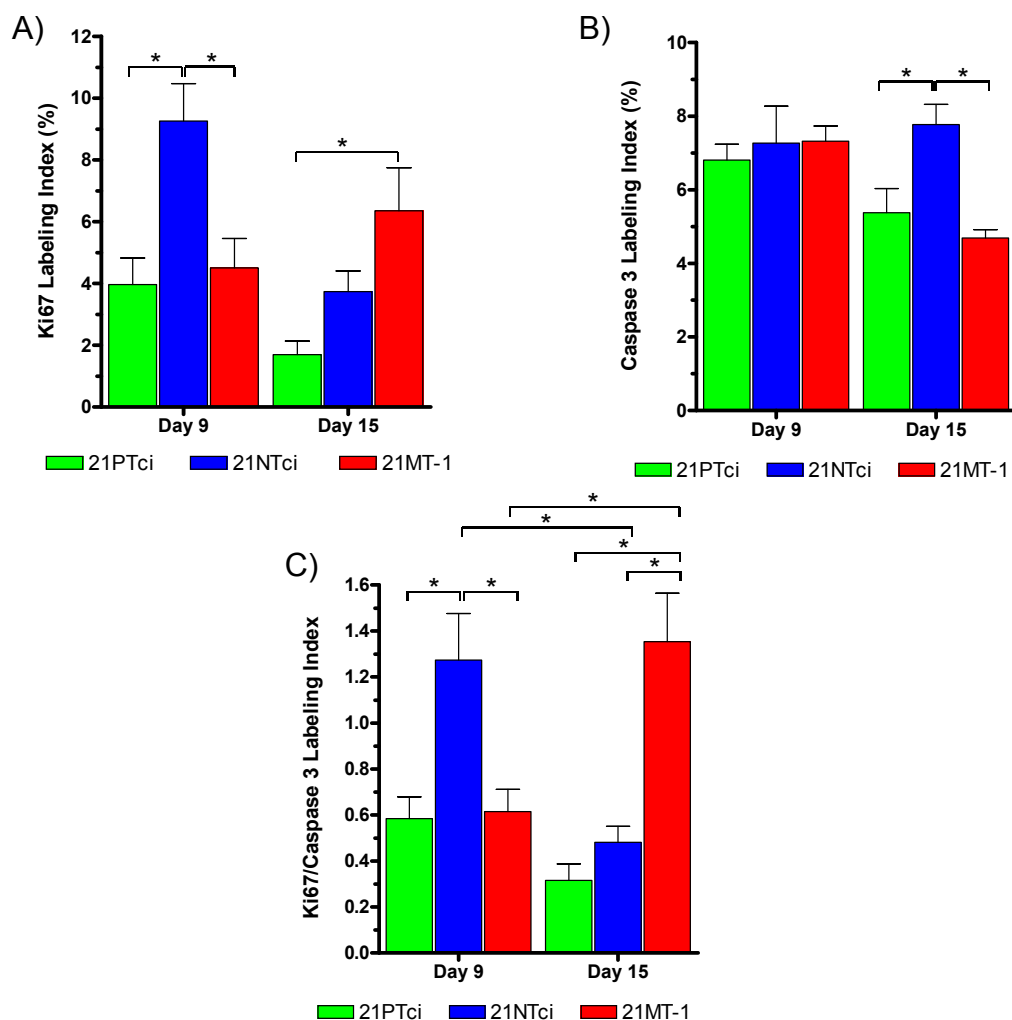


Figure 2.3. Proliferative and apoptotic activity of 21PTci, 21NTci and 21MT-1 cells after 9 and 15 days growth in 3D Matrigel. A) Proliferation was quantified by Ki67 immunohistochemical staining of Matrigel plugs. 21PTci cells showed a modest proliferative activity at day 9, which trailed off by day 15. 21NTci cells showed an initial burst of proliferative activity at day 9, which decreased significantly ($p < 0.01$) by day 15. 21MT-1 cells showed a modest proliferative activity that was higher by day 15. B) Apoptosis was quantified by caspase 3 immunohistochemical staining of Matrigel plugs. At day 9, there were no significant differences in apoptotic rates among cell lines. At day 15, apoptotic rates of both 21PTci and 21MT-1 cells decreased slightly (non significantly and significantly ($p < 0.05$), respectively). C) When the ratio of proliferation/apoptosis was calculated, 21PTci cells showed a modest cell division over cell death ratio at day 9, which trended towards a decreased ratio at day 15, at which time there was evidence of differentiation in terms of extracellular lumen formation and polarized groups (c.f. Figure 2.2). 21NTci cells showed an initial burst of proliferative activity over apoptosis at day 9, which decreased significantly ($p < 0.05$) by day 15. 21MT-1 cells showed a modest proliferation/apoptosis ratio at day 9, which significantly increased ($p < 0.05$) at day 15. * indicates significance at a level of $p < 0.05$.

to increased differentiation (data not shown), while the 21MT-1 showed very little polarization/extracellular lumen formation and instead exhibited increased growth between day 9 and day 15 (cf. Figure 2.2, Figure 2.3).

Finally, to assess invasive ability, cells were grown in Matrigel for 9 days and then followed with time lapse microscopy until day 15. It was found that 100% of 21MT-1 cells were able to travel through the Matrigel in both horizontal and vertical directions, compared to only 25% of 21PTci and 30% of 21NTci cells (Figure 2.4A). In addition 21MT-1 cells traveled 219 μ m on average over the seven days, which was significantly ($p < 0.01$) farther than that for 21PTci (22 μ m) and 21NTci (18 μ m) cells (Figure 2.4B). Whereas the majority of 21MT-1 cells that moved showed individual translational cell movement, 21PTci and 21NTci cell movement predominantly involved localized arrangement into cell groups within a confined area.

2.3.4. Profiling Elucidates Differential Gene Expression between the Three 21T Series Cell Lines Grown in 3D

In order to determine differential gene profiles between the 21T series cell lines, 3D *in vitro* microarray expression arrays were performed, which identified stage-specific gene alterations. For the 21PTci to 21NTci comparison, 366 probe sets were at least 1.5-fold altered ($p < 0.05$) (Supplemental Table 1), whereas for the 21NTci to 21MT-1 comparison, 3067 probe sets were at least 1.5-fold up- or down-regulated ($p < 0.05$) (Supplemental Table 2). In order to assess whether these alterations would potentially apply to breast cancer progression in a clinical situation (i.e. to establish potential clinical relevance), we compared our list of

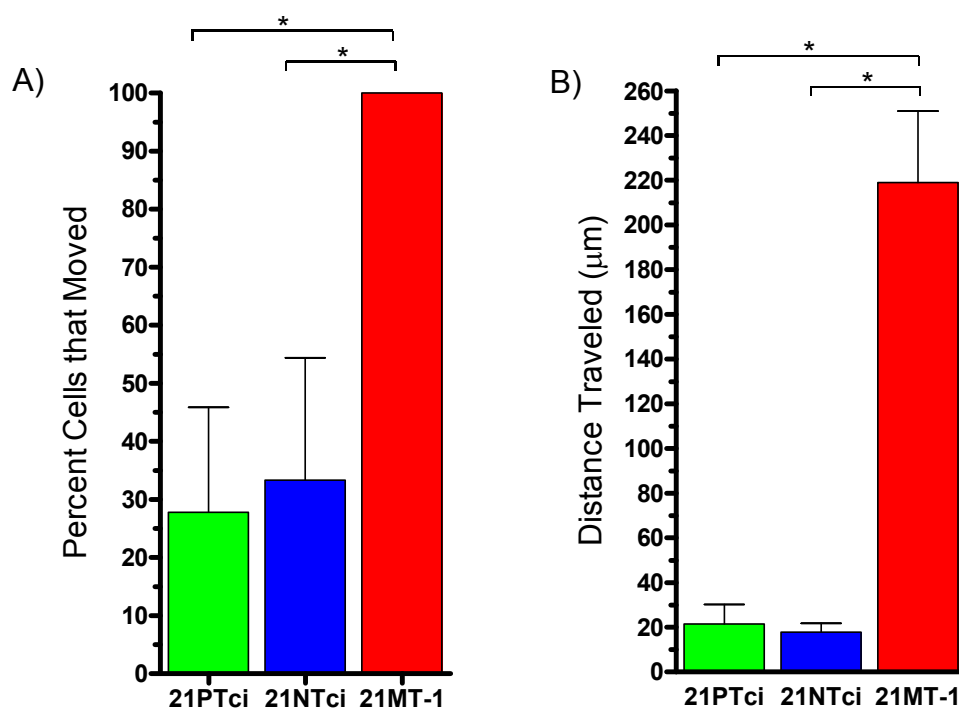


Figure 2.4. 21T series cell invasion through Matrigel matrix. Cells were grown in Matrigel for 9 days and then transferred to the incubator stage platform of a time lapse microscope until day 15. Z-stack images were taken every 12 hours. All individual cells imaged were followed for the full 6 day interval. A) Percentage of total cells that moved (invaded) through the Matrigel matrix. A cell was defined as moving if any part of the cell was in a different location compared to the image taken 12 hours previously. 100% of 21MT-1 cells showed translational movement, compared to only 27% of 21PTci and 33% 21NTci cells. B) Distance (μm) moving cells traveled through Matrigel matrix. 21MT-1 cells moved significantly further than 21PTci ($p < 0.01$) or 21NTci ($p < 0.01$) cells, which each showed minimal translational movement/invasive ability, consistent with the invasive (21MT-1) vs. non-invasive (21PTci, 21NTci) morphologies of these cells when grown *in vivo*. *indicates significance at a level of $p < 0.05$.

differentially expressed genes with a database we generated from established literature on gene expression profiling of clinical cancer specimens, including papers related to progression [11-13, 49-51], metastasis [45, 46, 48, 49] and prognosis [43, 44, 47, 50, 51] of breast cancer (Supplemental Table 3). Overlaps between our initial gene lists (Supplemental Table 1 and 2) and the clinically-relevant databases (Supplemental Table 3) were used to make two more focused gene lists of statistically altered and potentially clinically-relevant genes (21PTci to 21NTci: 23 probe IDs; 21NTci to 21MT-1: 208 probe IDs) (Appendix B, Table 1). These gene lists were then uploaded into Ingenuity Pathways Analysis (IPA) for further analysis, which identified representation of several major functional and canonical categories. Gene lists were then pared down to all genes found within the top 10 functional categories and canonical pathways (21PTci to 21NTci: 20 genes; 21NTci to 21MT-1: 66 genes) and the gene function as described by GeneCards (www.gencards.org) was recorded (Table 2.2). Based on gene function as described by GeneCards, 19 representative genes between the two transitions were chosen for 3D qRT-PCR validation, with 2 genes (DCN, WNT5A) represented in both transitions (Table 2.3). If a gene was significantly different ($p < 0.05$) between the 2 cell lines of interest and in the same direction as the microarray, the gene was considered validated. Of the 19 genes, all genes except BAX and MCM4 were validated by qRT-PCR (Table 2.3). For the 21PTci to 21NTci comparison, differential expression of BAX, DCN, MAX, MCM4, MGA, VANGL1, WISP1 and WNT5A were analyzed by real-time PCR. CCL20, CCR1, CDH1, CXCR4, DCN, S100A2, S100A3, SERPINB5, SNAI2, TBX3, TFF2, TNFAIP3 and WNT5A were validated in the 21NTci to 21MT-1 comparison. It is

Table 2.2. Genes that are concurrently: (1) significantly different among the 21T series cell lines¹, (2) present on clinically relevant databases from the literature² and (3) found within the top 10 functional and canonical pathways represented according to Ingenuity Pathways Analysis.

Common Name	Gene Name	GeneCard Function	Microarray Fold Change
21PTci to 21NTci			
ATRX	Alpha thalassemia/mental retardation syndrome X-linked	Transcription regulator	1.97
BAX	BCL-2 associated X protein	Accelerates programmed cell death	-1.75
DCN	Decorin	Affects rate of fibrils formation	7.52
ECGF1	Endothelial cell growth factor 1	Role in maintaining integrity of blood vessels	1.6
JMJD2C	Jumonji domain containing 2C	Histone demethylase	1.66
HIST1H4H	Histone cluster 1, H4h	Core component of nucleosome	1.56
MAX	MYC associated factor X	Transcription regulator	-1.54
MCM4	Minichromosome maintenance complex 4	Involved in control of DNA replication	-1.56
MGA	MAX gene associated	Transcription regulator	3.23
MMP1	Matrix metalloproteinase 1	Cleaves collagen	-4.17
NEFL	Neurofilament, light polypeptide	involved in maintenance of neuronal caliber	-3.23
PCM1	Pericentriolar material 1	Required for centrosome assembly and function	-1.54
PIK3R1	Phosphoinositide-3-kinase, regulatory subunit	Binds to activated protein-Tyr kinase	1.75
PIP	Prolactin-induced protein	Binding factor that plays a role in host defense against infections	3.95
SFRP4	Secreted frizzled-related protein 4	Modulator of Wnt signalling	-1.53
SLIT2	Slit homolog 2	Acts as a molecular guidance cue in cellular migration	-1.92
UPLC1	Development and differentiation enhancing factor-like 1	Promotes cell proliferation	9.31
VANGL1	Vang-like 1	Planar cell polarity signalling molecule	2.19
WISP1	WNT1 inducible signal pathway protein 1	Downstream regulator in the Wnt/Frizzled signalling pathway	2.18
WNT5A	Wingless-type MMTV integration site family, member 5A	Ligand for members of frizzled family	-1.89

21NTci to 21MT-1			
AIM2	Absent in melanoma 2	Tumour suppressor	7.16
ALDH3A1	Aldehyde dehydrogenase 3 family, member A1	Involved in detoxification of alcohol-derived acetaldehyde	-93.46
ANGPTL4	Angiopoietin-like 4	Regulator of angiogenesis	-3.58
BCL3	B-cell CLL/lymphoma 3	Transcriptional activating factor	1.84
BLNK	B-cell linker	Central linker protein that bridges kinases associated with B-cell receptor with multiple signalling pathways	26.67
CASP1	Caspase 1, apoptosis-related cysteine peptidase	Thiol protease that cleaves IL-1 beta	3.62
CCL20	Chemokine (C-C motif) ligand 20	Chemotactic factor	19.98
CCR1	Chemokine receptor 1	Receptor for C-C type chemokine	7.85
CDH1	Cadherin 1, type 1, E-cadherin	Promotes non-amyloidogenic degradation	-59.88
CDH11	Cadherin 11, type 2, OB-cadherin	Calcium dependent cell adhesion protein	-4.13
CDK2	Cyclin-dependent kinase 2	Involved in the control of cell cycle	-3.77
CHI3L1	Chitinase 3-like 1	Carbohydrate-binding lectin with a preference for chitin	-7.47
CLDN4	Claudin 4	Plays a major role in tight junction-specific obliteration of intercellular space	-45.87
CLU	Clusterin	May play a role in resistance to chemotherapy	3.43
COL4A3	Collagen, type IV, alpha 3	Tumstatin, a cleavage fragment	1.64
CST7	Cystatin F	Inhibits papain and cathepsin L	18.14
CX3CL1	Chemokine (C-X3-C motif)	Soluble form is chemotactic for T-cells and monocytes,	2.04
CXCL2	Chemokine (C-X-C motif) ligand 2	Produced by activated monocytes and neutrophils and expressed at sites of inflammation	-23.81
CXCR4	Chemokine (C-X-C motif) receptor 4	Receptor for the C-X-C chemokine CXCL12/SDF-1	-3.81
CYP1B1	Cytochrome P450, family 1, subfamily B, polypeptide 1	Participates in metabolism of an unknown biologically active molecule	1.48
DCN	Decorin	Affects rate of fibrils formation	33.94
DGKA	Diacylglycerol kinase, alpha	Upon cell stimulation converts the second messenger diacylglycerol into phosphatidate	-4.37
EFEMP1	EGF-containing fibulin-like extracellular matrix protein 1	An antagonist of angiogenesis {{146 Sadr-Nabavi,A. 2009; }}	-13.69
EMP1	Epithelial membrane protein 1	Involved in the drug-resistance mechanism of tumours	-1.81
ETV1	ETS variant 1	Transcriptional activator	2.05

IL13RA2	Interleukin 13 receptor, alpha 2	Binds as a monomer with high affinity to interleukin 13	13.55
IL15	Interleukin 15	Cytokine that stimulates the proliferation of T-lymphocytes	6.56
IL18	Interleukin 18	Augments natural killer cell activity	-16.5
ITGB4	Integrin, beta 4	Integrin alpha-6/beta-4 is a receptor for laminin	-23.69
KRT7	Keratin 7	Blocks interferon-dependent interphase and stimulates DNA synthesis	-9.44
LAMB1	Laminin, beta 1	Mediates attachment, migration and organization of cells into tissues during embryonic development	1.84
LTBP1	Latent transforming growth factor beta binding protein 1	May be involved in the assembly, secretion and targeting of TGFB1	15.51
LY75	Lymphocyte antigen 75	Acts as an endocytic receptor to direct captures antigens from the extracellular space to a specialized antigen-processing compartment	-6.34
MAPRE2	Microtubule-associated protein, RP/EB family, member 2	May be involved in microtubule polymerization and spindle function	-10.73
MCAM	Melanoma cell adhesion molecule	Plays a role in cell adhesion and in cohesion of the endothelial monolayer at intercellular junctions in vascular tissue	3.28
MME	Membrane metallo-endopeptidase	Biologically important in the destruction of opioid peptides	2.16
MMP2	Matrix metallopeptidase 2	Cleaves gelatin, collagens and KiSS1	-2.09
MMP3	Matrix metallopeptidase 3	Can degrade fibronectin, laminin, gelatins, collagens and cartilage proteoglycans	7.41
MMP7	Matrix metallopeptidase 7	Degrades casein, gelatins and fibronectin	-4.2
NDP	Norrie disease	Activates the canonical Wnt signalling pathway through FZD4 and LRP coreceptor	-1.61
NNMT	Nicotinamide N-methyltransferase	Catalyzed the N-methylation of nicotinamide and other pyridines to form pyridinium ions	5.23
NOX4	NADPH oxidase 4	Constitutive NADPH oxidase	1.91
ORM1	Orosomuroid 1	Modulates activity of the immune system during acute-phase reaction	46.41
PCOLCE	Procollagen C-endopeptidase enhancer	May have metalloproteinase inhibitory activity	3.31
PDGFC	Platelet derived growth factor C	Potent mitogen and chemoattractant for cells of mesenchymal origin	-14.29
PDGFRL	Platelet derived growth factor receptor-like	May function as a tumour suppressor	7.3
PLAU	Plasminogen activator, urokinase	Cleaves the zymogen plasminogen to form active enzyme plasmin	-1.82

PSCDBP	Cytohesin 1 interacting protein	Modifies activation of ARFs	18.29
PTPN12	Protein tyrosine phosphatase, non-receptor type 12	May have a regulatory role in controlling cell shape and mobility	1.67
S100A2	S100 calcium binding protein 2	Plays a role in suppressing tumour cell growth	-1.59
S100A3	S100 calcium binding protein 3	Involved in calcium-dependent cuticle cell differentiation	3.67
SDC1	Syndecan 1	Cell surface proteoglycan	-4.34
SERPINB5	Maspin	Tumour suppressor, blocks growth, invasion and metastatic properties of mammary tumours	-31.33
SLC2A3	Solute carrier family 2	Facilitative glucose transporter	4.06
SNAI2	Snail homolog 2, Slug	Transcriptional repressor	2.93
SOCS3	Suppressor of cytokine signalling 3	Involved in negative regulation of cytokines	7.01
TBX3	T-box 3	Transcription repressor involved in developmental processes	2.84
TFF2	Trefoil factor 2	Inhibits gastrointestinal motility	9.71
TNFAIP3	Tumour necrosis factor, alpha-induced protein 3	Inhibitor of programmed cell death	3.94
TNFSF10	Tumour necrosis factor (ligand) superfamily, member 10	Induces apoptosis	-14.93
TP53	Tumour protein p53	Acts as a tumour suppressor; induces growth arrest or apoptosis	1.62
TSLP	Thymic stromal lymphopoietin	Cytokine that induces release of T cell-attracting chemokines	3.88
TUSC3	Tumour suppressor candidate 3	May be involved in N-glycosylation	-1.99
TXNIP	Thioredoxin interacting protein	May act as an oxidative stress mediator	-3.21
WNT5A	Wingless-type MMTV integration site family, member 5A	Ligand for members of frizzled family	9.3
ZNF185	Zinc finger protein 185	May be involved in the regulation of cellular proliferation and/or differentiation	-2.7

¹ Supplemental Table 1 and 2

² Supplemental Table 3

Table 2.3. qRT-PCR validated genes of interest showing significant difference between 21T series cell lines that are of potential clinical relevance¹ and are of the top 10 functional and canonical pathways represented (IPA).

Common Name	Gene Name	GeneCard Function	Microarray Fold Change	qRT-PCR Fold Change ²
<u>21PTci to 21Ntci</u>				
BAX	BCL2-associated X protein	Accelerates programmed cell death	-1.75	1.03
DCN	Decorin	Affects rate of fibrils formation	7.52	6.38
MAX	MYC associated factor X	Transcription regulator	-1.54	-1.38
MCM4	Minichromosome maintenance complex 4	Involved in control of DNA replication	-1.56	1.14
MGA	MAX gene associated	Transcription regulator	3.23	2.75
VANGL1	Vang-like 1	Planar cell polarity signalling molecule	2.19	1.60
WISP1	WNT1 inducible signal pathway protein 1	Downstream regulator in the Wnt/Frizzled signalling pathway	2.18	2.15
WNT5A	Wingless-type MMTV integration site family, member 5A	Ligand for members of frizzled family	-1.89	-1.61
<u>21NTci to 21MT-1</u>				
CCL20	Chemokine (C-C motif) ligand 20	Chemotactic factor	19.98	10.90
CCR1	Chemokine receptor 1	Receptor for C-C type chemokine	7.85	4.10
CDH1	Cadherin 1, type 1, E-cadherin	Promotes non-amyloidogenic degradation	-59.88	-2.31
CXCR4	Chemokine (C-X-C motif) receptor 4	Receptor for the C-X-C chemokine CXCL12/SDF-1	-3.81	-33.33
DCN	Decorin	Affects rate of fibrils formation	33.94	72.51
S100A2	S100 calcium binding protein 2	Plays a role in suppressing tumour cell growth	-1.59	-3.02
S100A3	S100 calcium binding protein 3	Involved in calcium-dependent cuticle cell differentiation	3.67	6.44
SERPIN B5	Maspin	Tumour suppressor, blocks growth, invasion and metastatic properties of mammary tumours	-31.33	-47.20
SNAI2	Snail homolog 2, Slug	Transcriptional repressor	2.93	33.58

TBX3	T-box 3	Transcription repressor involved in developmental processes	2.84	2.70
TFF2	Trefoil factor 2	Inhibits gastrointestinal motility	9.71	6.80
TNFAIP3	Tumour necrosis factor, alpha-induced protein 3	Inhibitor of programmed cell death	3.94	2.31
WNT5A	Wingless-type MMTV integration site family, member 5A	Ligand for members of frizzled family	9.30	9.34

¹ Genes found on clinical databases created from the literature [11-13, 43-51] (Supplemental Table 3)

² Seventeen genes (not BAX and MCM4) validating the microarray data

apparent from this analysis that genes associated with the Wnt pathway (e.g. WNT5A, VANGL1, WISP1), and control of cell proliferation vs cell death (eg. MAX, MGA), were particularly associated with the 21PTci to 21NTci (ADH vs DCIS) comparison, whereas in the 21NTci to 21MT-1 (DCIS vs IMC) comparison, loss of tumour suppressors (e.g. SERPINB5, S100A2), alterations in transcriptional regulators (eg. TBX3, TNFAIP3, SNAI2), chemokines and their receptors (e.g. CCL20, CCR1), and genes associated with motility/invasiveness (e.g. TFF2, SERPINB5, S100A2) were identified.

2.4. DISCUSSION

With the institution of mammographic screening programs and advances in breast imaging in recent years, breast cancer is being detected at earlier stages [52]. The liberal use of core biopsies to assess abnormalities detected on imaging has reduced the number of patients inappropriately going to open biopsy when these lesions are benign [53], but has also increased the number of patients for which potential precursor lesions (such as ADH or DCIS) are detected [54]. When ADH or DCIS are identified on core biopsy, the mainstay of management is surgical excision (with radiotherapy in most cases of DCIS). However, there is little information on the natural biology and progression of these lesions [55]. When there is a chance of residual disease following treatment, options are limited as to further management when the lesions are difficult to detect (eg. lack associated calcifications) or are widespread. Further, in patients who are genetically predisposed to developing these lesions (such as BRCA1/BRCA2 carriers), management options (short of prophylactic

mastectomies) are limited [56, 57]. Although there are a few molecularly based systemic options for the management of DCIS either existing or under investigation, (e.g. tamoxifen for ER positive DCIS, trastuzumab for HER2-positive DCIS), a better understanding of the molecular basis of progression is needed to develop further targeted therapy for these early lesions [58].

Information from clinical studies examining pre-invasive lesions vs. invasive mammary carcinoma has yielded abundant gene expression profile differences between stages of progression (ADH vs. DCIS vs. IMC) (eg. [11-13, 49, 50]). What is lacking is the understanding of which of these differentially expressed genes may be key players regulating transition through the stages of breast progression, not only to predict which of the lesions are more likely to progress, but to provide potential novel targets for preventative therapies. Unfortunately, few *in vivo* and *in vitro* model systems exist that would allow individual candidate genes to be tested for their influence on human breast cancer progression, or to allow for efficient screening of the many candidate genes of interest. One such system, the HMT-3522 human breast epithelial cell series, has been described and utilized to identify specific matrix metalloproteinases required for the invasive phenotype [59]. A major advantage of such a system, wherein all of the representative cell lines are derived from the same patient, is that variability related to the individual's genetic background is eliminated (a common problem in comparing across cell lines of differing patient origin). The system we describe here has all the same advantages, and has the further advantage of representation of an even earlier stage, pre-DCIS (ADH-like) phenotype (as we described for the 21PTci cells).

We found the 21PT-derived cell line 21PTci to be consistently non-tumourigenic and non-metastatic after injection into the mammary fat pads of nude mice, confirming previous work [36]. However, upon histologic examination of the mammary fat pad of these mice, we found occasional lesions mimicking that of atypical ductal hyperplasia (ADH). Features consistent with ADH were the mixture of two epithelial cell populations within a given duct, one normal-appearing, the other atypical (and non-high grade), with the atypical cell population represented over an area of < 2.0 mm [2-4, 6]. Interestingly, when these cells were grown in 3D Matrigel, they were capable of forming large numbers of well-defined tubular/acinar structures, with maintenance of cell polarity in the vast majority of the groups. Furthermore, many of these groups showed a mixture of cells with normal-appearing and more atypical nuclei. Proliferative and apoptosis rates were low and cell movement was largely restricted to collective organization within these groups.

In contrast, we found the 21NT-derived cells to be tumourigenic and non-metastatic in those mice that did form lesions (tumour take in about 20%), as described by Band *et al.* [36]. Although these cells were tumourigenic, we found that the majority of mice in which lesions formed showed a histology representative of DCIS, with no associated invasion. The involved ducts showed a uniform neoplastic cell population, with intermediate and high grade nuclei, solid and cribriform architectural patterns, with zonal necrosis. Only 1/7 of the injected animals that formed lesions showed an associated invasive component, which was localized to the fat pad, with no evidence of locoregional lymph node involvement or distant metastases. This cell line thus represents a good model of

DCIS, in that although in most injected animals it maintains morphology of DCIS only, it does show the potential for a low rate of spontaneous progression to invasive ability. The phenotype is similar to that described for MCF10DCIS cells [60], although in contrast to MCF10DCIS, 21NT cells are not ras-transformed (a rare event in spontaneous human breast cancer), and show a more stable (less “leaky”) DCIS phenotype than MCF10DCIS cells, which have a higher propensity for invasion with time *in vivo* [17]. When 21NTci cells are grown in 3D Matrigel, features consistent with DCIS-like behaviour, including the tendency of cells to arrange into groups, but with poor polarization of the constituent cells, nuclear atypia in all the constituent cells, the spherical, non-infiltrative nature of colonies that formed, and a lack of translational invasive behaviour when followed by time lapse microscopy, were observed.

The 21MT-1 cells, as described by Band *et al.* [36], were found to be tumourigenic (in the majority of orthotopically-injected mice), and metastatic in half the mice that formed primary tumours. Upon histologic examination, we found that all of the mice that formed tumours showed invasive mammary carcinoma (no special type, SBR grade III/III), most with admixed DCIS of intermediate and high nuclear grade in the background. Consistent with this *in vivo* phenotype, when the cells were grown in 3D Matrigel, they formed more disorganized, non-spherical colonies, less polarization or lumen formation of cell groups, more single cells, and a much greater ability to show translational movement through Matrigel upon time-lapse microscopy, when compared to the other two cell lines.

We have identified unique differential gene expression profiles for each of the 21T series cell lines, grown in Matrigel. Interestingly, of those genes with

evidence for clinical relevance, Wnt pathway alterations (eg. WNT5A, VANGL1, WISP1) are particularly predominant in the comparison between 21PTci and 21NTci (representing the ADH to DCIS transition). This is consistent with recent studies implicating both the canonical and noncanonical Wnt signalling pathways in initiation and maintenance of breast tumourigenesis (reviewed in [61]), as well as in cancer stem cell self renewal and the initiation of the epithelial to mesenchymal transition [62]. In particular, the planar cell polarity (PCP) pathway (a non-canonical Wnt pathway), involving ligand WNT5A, has been said to have either inhibitory or promoting roles in various cancers, depending on the context (reviewed in [63]). It has been suggested that early in progression, the PCP pathway functions mainly in an inhibitory role, by down-regulating canonical Wnt signalling (through β -catenin), and promoting differentiation, whereas later in progression, the PCP pathway may promote progression, by stimulating cell migration and invasion [64]. In the 21T series cell lines, WNT5A is down-regulated between 21PTci and 21NTci (ADH to DCIS), and is upregulated between 21NTci and 21MT-1 (DCIS to IMC), in keeping with an early suppressive role and a later promoting role on progression.

Also prominent amongst genes differentially expressed between 21PTci and 21NTci were genes associated with signalling processes potentially involved with control of cell growth vs. apoptosis (eg. MAX, MGA). Such changes, resulting in a net increase in cell growth (vs. apoptosis), would be consistent with the morphologic transition from ADH to DCIS, where the neoplastic cell population is seen to expand from partially, to completely filling duct cross-sections. In the comparison between 21NTci (DCIS-like) and 21MT-1 (IMC-like),

which focuses on progression to an invasive and metastatic phenotype, differentially expressed genes of potential clinical relevance included the loss of tumour suppressors (eg. SERPINB5, S100A2), alterations in transcriptional regulators believed to be involved in regulating cell senescence/apoptosis (eg. TBX3, TNFAIP3) and promoting invasiveness and epithelial to mesenchymal transition (EMT) (eg. SNAI2), certain chemokines and their receptors (eg. CCL20, CCR1), and genes more directly associated with motility/invasiveness (eg. TFF2, SERPINB5, S100A2). Collectively, these alterations would be expected to increase the malignancy of breast cancer cells, allowing for invasive and metastatic phenotypes to emerge in the DCIS to IMC transition.

The advantages of the approach we have taken in these 21T cell comparisons are two-fold. Firstly, by using a filter for genes showing altered expression in published clinical literature on early breast cancer progression, invasion/metastasis and prognosis, we have narrowed our initial search to genes with potential relevance in a clinical setting. This is not to say that genes showing altered expression that did not “make” this list are irrelevant, but simply allows us to focus our search to those with some existing support for clinical import. Second, the use of the 21T model provides us with a manipulatable *in vitro* and *in vivo* system for future studies to test the relative functional impact of specific genes on transitions between these early stages of breast cancer progression (ADH to DCIS to IMC). We expect that use of this system will provide an important tool to unlocking some of the intricacies of the molecular influences on early breast progression. The information gathered will be critical to our ability to

target and prevent this process and effectively stop breast cancer not just “in its tracks”, but “before it makes tracks”.

2.5. REFERENCES

1. Lakhani SR, Collins N, Stratton MR, Sloane JP: **Atypical ductal hyperplasia of the breast: clonal proliferation with loss of heterozygosity on chromosomes 16q and 17p.** J Clin Pathol 1995, **48**(7):611-615.
2. Page DL, Dupont WD, Rogers LW, Rados MS: **Atypical hyperplastic lesions of the female breast. A long-term follow-up study.** Cancer 1985, **55**(11):2698-2708.
3. Page DL, Dupont WD: **Anatomic indicators (histologic and cytologic) of increased breast cancer risk.** Breast Cancer Res Treat 1993, **28**(2):157-166.
4. Allred DC, Mohsin SK, Fuqua SA: **Histological and biological evolution of human premalignant breast disease.** Endocr Relat Cancer 2001, **8**(1):47-61.
5. Allred DC, Wu Y, Mao S, Nagtegaal ID, Lee S, Perou CM, Mohsin SK, O'Connell P, Tsimelzon A, Medina D: **Ductal carcinoma in situ and the emergence of diversity during breast cancer evolution.** Clin Cancer Res 2008, **14**(2):370-378.
6. Arpino G, Laucirica R, Elledge RM: **Premalignant and in situ breast disease: biology and clinical implications.** Ann Intern Med 2005, **143**(6):446-457.
7. Polyak K: **Is breast tumor progression really linear?** Clin Cancer Res 2008, **14**(2):339-341.
8. Sgroi DC, Teng S, Robinson G, LeVangie R, Hudson JR, Jr, Elkahloun AG: **In vivo gene expression profile analysis of human breast cancer progression.** Cancer Res 1999, **59**(22):5656-5661.
9. Worsham MJ, Pals G, Raju U, Wolman SR: **Establishing a molecular continuum in breast cancer DNA microarrays and benign breast disease.** Cytometry 2002, **47**(1):56-59.
10. Li Z, Tsimelzon A, Immaneni A, Mohsin SK, Hilsenbeck SG, Clark GC, Fuqua SAW, Osborne CK, O'Connell P, Allred DC: **A cDNA microarray study**

- comparing noninvasive and invasive human breast cancer.** Proc Am Assoc Cancer Res 2002, **43**:901-902.
11. Ma XJ, Salunga R, Tuggle JT, Gaudet J, Enright E, McQuary P, Payette T, Pistone M, Stecker K, Zhang BM, Zhou YX, Varnholt H, Smith B, Gadd M, Chatfield E, Kessler J, Baer TM, Erlander MG, Sgroi DC: **Gene expression profiles of human breast cancer progression.** Proc Natl Acad Sci U S A 2003, **100**(10):5974-5979.
 12. Abba MC, Drake JA, Hawkins KA, Hu Y, Sun H, Notcovich C, Gaddis S, Sahin A, Baggerly K, Aldaz CM: **Transcriptomic changes in human breast cancer progression as determined by serial analysis of gene expression.** Breast Cancer Res 2004, **6**(5):R499-513.
 13. Schuetz CS, Bonin M, Clare SE, Nieselt K, Sotlar K, Walter M, Fehm T, Solomayer E, Riess O, Wallwiener D, Kurek R, Neubauer HJ: **Progression-specific genes identified by expression profiling of matched ductal carcinomas in situ and invasive breast tumors, combining laser capture microdissection and oligonucleotide microarray analysis.** Cancer Res 2006, **66**(10):5278-5286.
 14. Medina D: **The preneoplastic phenotype in murine mammary tumorigenesis.** J Mammary Gland Biol Neoplasia 2000, **5**(4):393-407.
 15. Cardiff RD, Moghanaki D, Jensen RA: **Genetically engineered mouse models of mammary intraepithelial neoplasia.** J Mammary Gland Biol Neoplasia 2000, **5**(4):421-437.
 16. Weaver VM, Howlett AR, Langton-Webster B, Petersen OW, Bissell MJ: **The development of a functionally relevant cell culture model of progressive human breast cancer.** Semin Cancer Biol 1995, **6**(3):175-184.
 17. Miller FR: **Xenograft models of premalignant breast disease.** J Mammary Gland Biol Neoplasia 2000, **5**(4):379-391.
 18. Stampfer MR, Yaswen P: **Culture models of human mammary epithelial cell transformation.** J Mammary Gland Biol Neoplasia 2000, **5**(4):365-378.
 19. Santner SJ, Dawson PJ, Tait L, Soule HD, Eliason J, Mohamed AN, Wolman SR, Heppner GH, Miller FR: **Malignant MCF10CA1 cell lines derived from premalignant human breast epithelial MCF10AT cells.** Breast Cancer Res Treat 2001, **65**(2):101-110.
 20. Briand P, Lykkesfeldt AE: **An in vitro model of human breast carcinogenesis: epigenetic aspects.** Breast Cancer Res Treat 2001, **65**(2):179-187.

21. Fauquette W, Dong-Le Bourhis X, Delannoy-Courdent A, Boilly B, Desbiens X: **Characterization of morphogenetic and invasive abilities of human mammary epithelial cells: correlation with variations of urokinase-type plasminogen activator activity and type-1 plasminogen activator inhibitor level.** Biol Cell 1997, **89**(7):453-465.
22. Weaver VM, Petersen OW, Wang F, Larabell CA, Briand P, Damsky C, Bissell MJ: **Reversion of the malignant phenotype of human breast cells in three-dimensional culture and in vivo by integrin blocking antibodies.** J Cell Biol 1997, **137**(1):231-245.
23. Wang F, Weaver VM, Petersen OW, Larabell CA, Dedhar S, Briand P, Lupu R, Bissell MJ: **Reciprocal interactions between beta1-integrin and epidermal growth factor receptor in three-dimensional basement membrane breast cultures: a different perspective in epithelial biology.** Proc Natl Acad Sci U S A 1998, **95**(25):14821-14826.
24. Meiners S, Brinkmann V, Naundorf H, Birchmeier W: **Role of morphogenetic factors in metastasis of mammary carcinoma cells.** Oncogene 1998, **16**(1):9-20.
25. Benton G, Crooke E, George J: **Laminin-1 induces E-cadherin expression in 3-dimensional cultured breast cancer cells by inhibiting DNA methyltransferase 1 and reversing promoter methylation status.** FASEB J 2009.
26. Wang X, Zhang X, Sun L, Subramanian B, Maffini MV, Soto AM, Sonnenschein C, Kaplan DL: **Preadipocytes stimulate ductal morphogenesis and functional differentiation of human mammary epithelial cells in 3D silk scaffolds.** Tissue Eng Part A 2009.
27. Shaw KR, Wrobel CN, Brugge JS: **Use of three-dimensional basement membrane cultures to model oncogene-induced changes in mammary epithelial morphogenesis.** J Mammary Gland Biol Neoplasia 2004, **9**(4):297-310.
28. Hirai Y, Lochter A, Galosy S, Koshida S, Niwa S, Bissell MJ: **Epimorphin functions as a key morphoregulator for mammary epithelial cells.** J Cell Biol 1998, **140**(1):159-169.
29. Soriano JV, Pepper MS, Orci L, Montesano R: **Roles of hepatocyte growth factor/scatter factor and transforming growth factor-beta1 in mammary gland ductal morphogenesis.** J Mammary Gland Biol Neoplasia 1998, **3**(2):133-150.
30. Simian M, Hirai Y, Navre M, Werb Z, Lochter A, Bissell MJ: **The interplay of matrix metalloproteinases, morphogens and growth factors is necessary**

- for branching of mammary epithelial cells.** Development 2001, **128**(16):3117-3131.
31. Niemann C, Brinkmann V, Birchmeier W: **Hepatocyte growth factor and neuregulin in mammary gland cell morphogenesis.** Adv Exp Med Biol 2000, **480**:9-18.
 32. Ball EM, Risbridger GP: **Activins as regulators of branching morphogenesis.** Dev Biol 2001, **238**(1):1-12.
 33. Debnath J, Brugge JS: **Modelling glandular epithelial cancers in three-dimensional cultures.** Nat Rev Cancer 2005, **5**(9):675-688.
 34. Debnath J, Mills KR, Collins NL, Reginato MJ, Muthuswamy SK, Brugge JS: **The role of apoptosis in creating and maintaining luminal space within normal and oncogene-expressing mammary acini.** Cell 2002, **111**(1):29-40.
 35. Hebner C, Weaver VM, Debnath J: **Modeling morphogenesis and oncogenesis in three-dimensional breast epithelial cultures.** Annu Rev Pathol 2008, **3**:313-339.
 36. Band V, Zajchowski D, Swisshelm K, Trask D, Kulesa V, Cohen C, Connolly J, Sager R: **Tumor progression in four mammary epithelial cell lines derived from the same patient.** Cancer Res 1990, **50**(22):7351-7357.
 37. Biswas DK, Cruz A, Pettit N, Mutter GL, Pardee AB: **A therapeutic target for hormone-independent estrogen receptor-positive breast cancers.** Mol Med 2001, **7**(1):59-67.
 38. Biswas DK, Averboukh L, Sheng S, Martin K, Ewaniuk DS, Jawde TF, Wang F, Pardee AB: **Classification of breast cancer cells on the basis of a functional assay for estrogen receptor.** Mol Med 1998, **4**(7):454-467.
 39. Cook AC, Tuck AB, McCarthy S, Turner JG, Irby RB, Bloom GC, Yeatman TJ, Chambers AF: **Osteopontin induces multiple changes in gene expression that reflect the six "hallmarks of cancer" in a model of breast cancer progression.** Mol Carcinog 2005, **43**(4):225-236.
 40. Tuck AB, Arsenault DM, O'Malley FP, Hota C, Ling MC, Wilson SM, Chambers AF: **Osteopontin induces increased invasiveness and plasminogen activator expression of human mammary epithelial cells.** Oncogene 1999, **18**(29):4237-4246.
 41. Furger KA, Allan AL, Wilson SM, Hota C, Vantyghem SA, Postenka CO, Al-Katib W, Chambers AF, Tuck AB: **Beta(3) integrin expression increases**

- breast carcinoma cell responsiveness to the malignancy-enhancing effects of osteopontin.** *Mol Cancer Res* 2003, **1**(11):810-819.
42. Luzzi KJ, MacDonald IC, Schmidt EE, Kerkvliet N, Morris VL, Chambers AF, Groom AC: **Multistep nature of metastatic inefficiency: dormancy of solitary cells after successful extravasation and limited survival of early micrometastases.** *Am J Pathol* 1998, **153**(3):865-873.
43. Asaka S, Fujimoto T, Akaishi J, Ogawa K, Onda M: **Genetic prognostic index influences patient outcome for node-positive breast cancer.** *Surg Today* 2006, **36**(9):793-801.
44. O'Brien N, O'Donovan N, Foley D, Hill AD, McDermott E, O'Higgins N, Duffy MJ: **Use of a Panel of Novel Genes for Differentiating Breast Cancer from Non-Breast Tissues.** *Tumour Biol* 2008, **28**(6):312-317.
45. Minn AJ, Kang Y, Serganova I, Gupta GP, Giri DD, Doubrovin M, Ponomarev V, Gerald WL, Blasberg R, Massague J: **Distinct organ-specific metastatic potential of individual breast cancer cells and primary tumors.** *J Clin Invest* 2005, **115**(1):44-55.
46. Kang Y, Siegel PM, Shu W, Drobnjak M, Kakonen SM, Cordon-Cardo C, Guise TA, Massague J: **A multigenic program mediating breast cancer metastasis to bone.** *Cancer Cell* 2003, **3**(6):537-549.
47. Shen R, Ghosh D, Chinnaiyan AM: **Prognostic meta-signature of breast cancer developed by two-stage mixture modeling of microarray data.** *BMC Genomics* 2004, **5**(1):94.
48. Wang Y, Klijn JG, Zhang Y, Sieuwerts AM, Look MP, Yang F, Talantov D, Timmermans M, Meijer-van Gelder ME, Yu J, Jatkoe T, Berns EM, Atkins D, Foekens JA: **Gene-expression profiles to predict distant metastasis of lymph-node-negative primary breast cancer.** *Lancet* 2005, **365**(9460):671-679.
49. Nishidate T, Katagiri T, Lin ML, Mano Y, Miki Y, Kasumi F, Yoshimoto M, Tsunoda T, Hirata K, Nakamura Y: **Genome-wide gene-expression profiles of breast-cancer cells purified with laser microbeam microdissection: identification of genes associated with progression and metastasis.** *Int J Oncol* 2004, **25**(4):797-819.
50. Milovanovic T, Planutis K, Nguyen A, Marsh JL, Lin F, Hope C, Holcombe RF: **Expression of Wnt genes and frizzled 1 and 2 receptors in normal breast epithelium and infiltrating breast carcinoma.** *Int J Oncol* 2004, **25**(5):1337-1342.

51. van 't Veer LJ, Dai H, van de Vijver MJ, He YD, Hart AA, Mao M, Peterse HL, van der Kooy K, Marton MJ, Witteveen AT, Schreiber GJ, Kerkhoven RM, Roberts C, Linsley PS, Bernards R, Friend SH: **Gene expression profiling predicts clinical outcome of breast cancer.** Nature 2002, **415**(6871):530-536.
52. Duffy SW, Agbaje O, Tabar L, Vitak B, Bjurstam N, Bjorneld L, Myles JP, Warwick J: **Overdiagnosis and overtreatment of breast cancer: estimates of overdiagnosis from two trials of mammographic screening for breast cancer.** Breast Cancer Res 2005, **7**(6):258-265.
53. El-Sayed ME, Rakha EA, Reed J, Lee AH, Evans AJ, Ellis IO: **Predictive value of needle core biopsy diagnoses of lesions of uncertain malignant potential (B3) in abnormalities detected by mammographic screening.** Histopathology 2008, **53**(6):650-657.
54. Provenzano E, Pinder SE: **Pre-operative diagnosis of breast cancer in screening: problems and pitfalls.** Pathology 2009, **41**(1):3-17.
55. Simpson JF: **Update on atypical epithelial hyperplasia and ductal carcinoma in situ.** Pathology 2009, **41**(1):36-39.
56. Kauff ND, Brogi E, Scheuer L, Pathak DR, Borgen PI, Hudis CA, Offit K, Robson ME: **Epithelial lesions in prophylactic mastectomy specimens from women with BRCA mutations.** Cancer 2003, **97**(7):1601-1608.
57. Isern AE, Loman N, Malina J, Olsson H, Ringberg A: **Histopathological findings and follow-up after prophylactic mastectomy and immediate breast reconstruction in 100 women from families with hereditary breast cancer.** Eur J Surg Oncol 2008, **34**(10):1148-1154.
58. Boughey JC, Gonzalez RJ, Bonner E, Kuerer HM: **Current treatment and clinical trial developments for ductal carcinoma in situ of the breast.** Oncologist 2007, **12**(11):1276-1287.
59. Rizki A, Weaver VM, Lee SY, Rozenberg GI, Chin K, Myers CA, Bascom JL, Mott JD, Semeiks JR, Grate LR, Mian IS, Borowsky AD, Jensen RA, Idowu MO, Chen F, Chen DJ, Petersen OW, Gray JW, Bissell MJ: **A human breast cell model of preinvasive to invasive transition.** Cancer Res 2008, **68**(5):1378-1387.
60. Dawson PJ, Wolman SR, Tait L, Heppner GH, Miller FR: **MCF10AT: a model for the evolution of cancer from proliferative breast disease.** Am J Pathol 1996, **148**(1):313-319.
61. Mohinta S, Wu H, Chaurasia P, Watabe K: **Wnt pathway and breast cancer.** Front Biosci 2007, **12**:4020-4033.

62. DiMeo TA, Anderson K, Phadke P, Feng C, Perou CM, Naber S, Kuperwasser C: **A novel lung metastasis signature links Wnt signaling with cancer cell self-renewal and epithelial-mesenchymal transition in basal-like breast cancer.** *Cancer Res* 2009, **69**(13):5364-5373.
63. Kikuchi A, Yamamoto H: **Tumor formation due to abnormalities in the beta-catenin-independent pathway of Wnt signaling.** *Cancer Sci* 2008, **99**(2):202-208.
64. Wang Y: **Wnt/Planar cell polarity signaling: a new paradigm for cancer therapy.** *Mol Cancer Ther* 2009, **8**(8):2103-2109.

CHAPTER 3. THE ROLES OF VANGL1, S100A2 AND TBX3 IN THE TRANSITIONS BETWEEN STAGES OF EARLY BREAST CANCER PROGRESSION

3.1. INTRODUCTION

Ductal carcinoma is one of the most prevalent forms of breast cancer [1]. The transition from a premalignant to a malignant, *in situ* lesion and the transition from a malignant, *in situ* lesion to one that can invade and metastasize are both important transitions in early progression. With reference to ductal neoplasia, premalignant atypical ductal hyperplasia (ADH) may give rise to ductal carcinoma *in situ* (DCIS) [2-6]. This DCIS may then acquire the molecular factors necessary to penetrate the basement membrane, escape the breast duct and become invasive (invasive mammary carcinoma, IMC), potentially leading to metastasis at distant sites [2-4, 6, 7]. The histopathology of these distinct stages is well described; however, the underlying molecular events controlling progression remain unclear. To study the molecular and cellular processes involved in controlling mammary tumour progression through these stages, predictive model systems are needed.

Chapter 2 of this thesis described the 21T human breast epithelial cell line 3D model system of early breast cancer progression [8]. The 21T series cell lines were originally derived from a single patient with metastatic breast cancer [9] and show characteristics of different stages of breast cancer progression. Specifically, histologic examination of the lesions arising in nude mice injected

with these cells, into mammary fat pads, revealed morphologic characteristics of atypical ductal hyperplasia (ADH) [21PT], ductal carcinoma *in situ* (DCIS) without invasion [21NT], and invasive mammary carcinoma (IMC) [21MT-1]. When the 21T series cell lines were grown in a 3D culture system, which mimics the tissue environment, these growth characteristics were retained. Additionally, gene expression profiling of the 21T series cells in 3D culture has revealed stage-specific patterns and has identified many key targets which may be involved in controlling the transitions between stages of early breast cancer progression [8].

The key targets identified by gene profiling were common to literature based on clinical specimens of ADH, DCIS and invasive breast cancer (IMC). The present study sought to functionally characterize the role of three of the identified targets in controlling the transitions between stages of early breast cancer progression. For the transition from ADH to DCIS, VANG1, which was expressed at higher levels in 21NT (DCIS-like) cells compared to 21PT (ADH-like) cells, was functionally characterized to determine its role in promoting conversion to malignancy (Figure 3.1). Two genes in the DCIS to IMC transition were chosen for further analysis. S100A2, which was expressed at a lower level in 21MT-1 (IMC-like) cells compared to 21NT (DCIS-like) cells, was assessed for its role in inhibiting progression to invasion (Figure 3.1). TBX3, which was expressed at higher levels in 21MT-1 (IMC-like) cells compared to 21NT (DCIS-like) cells, was characterized to determine its role in the transition to an invasive phenotype (Figure 3.1).

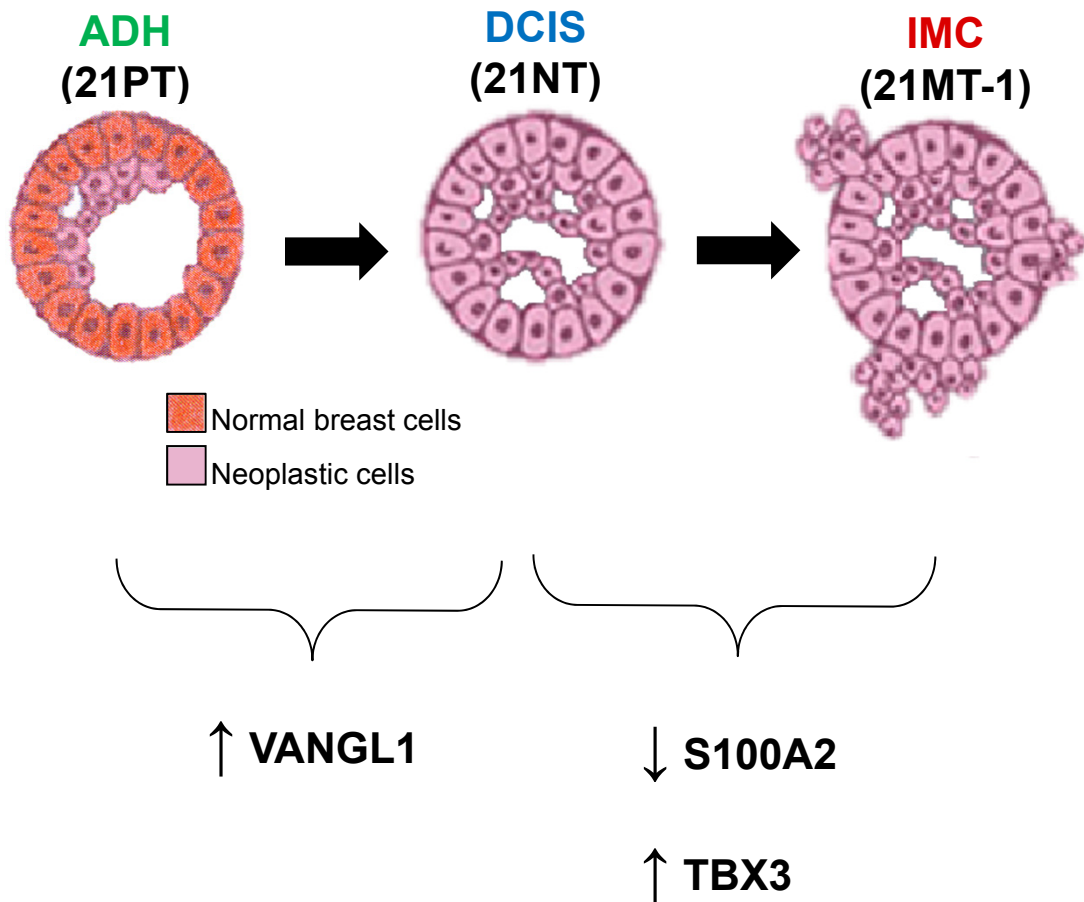


Figure 3.1. Genes identified as altered between 21T series cell lines and breast cancer progression stages. VANG1 is increased in 21NT (DCIS-like) cells compared to 21PT (ADH-like) cells. S100A2 is decreased in 21MT-1 (IMC-like) cells compared to 21NT (DCIS-like) cells. Finally, TBX3 is increased in 21MT-1 (IMC-like) cells compared to 21NT (DCIS-like) cells.

3.1.1. Van Gogh-like 1 (VANGL1)

Van Gogh-like 1 (VANGL1) is a member of the transmembrane 4 superfamily and is the human homolog of the *Drosophila* polarity gene, van gogh/strabismus. VANGL1 has been found to promote malignancy and invasion in several types of cancer, including gastric, squamous cell and laryngeal [10-12]. Additionally, loss of VANGL1 suppresses colon cancer metastasis [13]. Recently, VANGL1 was identified as a binding partner of the metastasis suppressor KAI1 (CD82) and renamed to KAI1 COOH-terminal interacting tetraspanin (KITENIN) [10]. It was theorized that VANGL1 promoted metastasis by interfering with the metastasis-suppressing ability of KAI1 either through its interaction with KAI1 or by regulating downstream signalling effectors involved in cell invasion [10] (Figure 3.2). Specifically, KAI1 interacts with integrin $\alpha3\beta1$ and the binding of KAI1 with VANGL1 may interfere with the KAI1-integrin interaction, leading to a release of $\alpha3\beta1$ and an inhibition of integrin-mediated invasion [10]. Additionally, KAI1 is associated with protein kinase C (PKC), which mediates phosphorylation of MARCKS (myristoylated alanine-rich C kinase substrate) and ERMs (ezrin, radixin and moesin) resulting in a reorganization of existing actin structures and allowing for reassembly of new actin structures that promote migration [14]. It has been theorized that KAI1 suppresses cell motility through a negative influence on PKC, c-Met and epidermal growth factor receptor (EGFR) [14]. It is possible that the binding of VANGL1 to KAI1 eliminates the KAI1 suppression effects.

The noncanonical Wnt/planar cell polarity (PCP) pathway plays a role in cancer progression. The PCP pathway is activated by the binding of

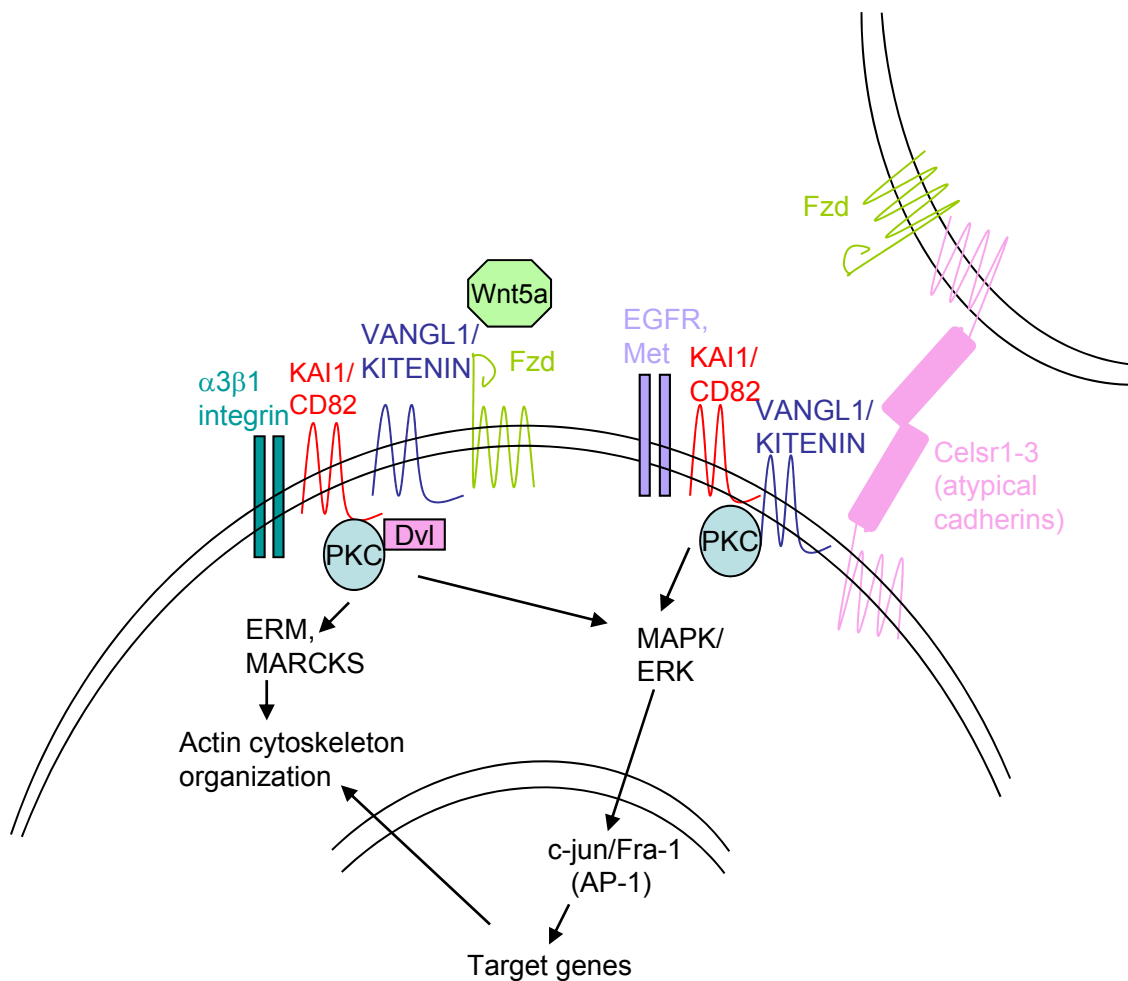


Figure 3.2. VANGL1 cell signalling. VANGL1 interacts with the metastasis-suppressor KAI1. KAI1 interacts with $\alpha 3\beta 1$ integrin to inhibit invasion. KAI1 also negatively influences protein kinase C (PKC), which mediates phosphorylation of ERM and MARCKs, leading to actin cytoskeleton organization and migration. VANGL1 is a core plan cell polarity component of the Wnt/planar cell polarity (PCP) pathway and acts as a scaffolding protein for Dishevelled (Dvl) and PKC. This functional complex promotes motility through signalling with MAPK/ERK to elevate levels of the AP-1 transcription factor. Finally, in mammalian cells, interaction of VANGL1 with the atypical cadherins Celsr1-3 may be involved in establishment of cell polarity in a fashion similar to complexes with Flamingo (Fmi) in *Drosophila*.

noncanonical Wnt molecules, such as Wnt5a, to the Frizzled (Fzd) receptor. VANGL1 is a core planar cell polarity component and acts as a scaffolding protein for Dishevelled (Dvl) and PKC [15] (Figure 3.2). A recent study found that the functional complex formed by VANGL1, Dvl and PKC δ promotes colorectal cancer cell migration and invasion [16]. The increased cell motility is dependent on MAPK/ERK (Mitogen-activated protein kinase/extracellular signal-regulated kinase) signalling, which leads to elevated levels of the AP-1 transcription factor. The AP-1 transcription factor is composed of c-Jun, c-Fos and Fra-1 and regulates expression of matrix metalloproteinases (MMPs), adhesion and cytoskeleton regulators, which control cell motility and invasion. A separate study found that AP-1 activation by VANGL1 causes tumour progression in human gastric cancer [17]. Finally, in *Drosophila*, Vangl1 has been found to assist in the establishment of cell polarity through interaction with the atypical cadherin Flamingo (Fmi) in one cell and a Fmi-Fzd complex in an adjoining cell [14]. In mammalian cells, atypical cadherin Celsr molecules (1,2,3) have been found to complex with VANGL1 and may be involved in cell-cell contacts and polarization similar to Fmi in flies [18-20]. The involvement of VANGL1 in the PCP pathway further points to the role of VANGL1 in malignancy, as well as invasion.

Although a role for VANGL1 has been established in many types of cancer (eg. colonic, gastric, head and neck), the role of VANGL1 in breast cancer has yet to be elucidated. In relation to the 21T human breast epithelial cell line 3D model system of early breast cancer progression, VANGL1 was elevated in 21NT (DCIS-like) cells compared to 21PT (ADH-like) cells. The present study made use of the 21T series cells grown in 3D culture to test the hypothesis that

overexpressing VANGL1 in 21PT cells would result in the cells acquiring characteristics of malignancy, making them more like 21NT (or 21MT-1) cells.

3.1.2. S100A2

S100A2 is a member of the S100 EF-hand calcium binding protein family, several of which have been implicated in cancer progression [21]. S100A2 is an unusual member in that unlike the majority of the S100 family members, S100A2 expression is downregulated in many cancers and it has been shown to be a potential tumour suppressor [21]. The exact mechanisms of the tumour suppressor activity of S100A2 are at present uncertain, although there are several potential regulatory functions suggested based on its involvement in different protein-protein interactions, particularly at the nuclear level. It was recently discovered that S100A2 binds the p53 tumour suppressor and this may be involved in the stimulation of p53 activity by S100A2 [22], resulting in cell cycle arrest and apoptosis (Figure 3.3). A study in lung adenocarcinomas found further functions of S100A2, including induction of RUNX3 (runt-related transcription factor 3), and repression of EGFR and NFkB2 (nuclear factor of kappa light polypeptide gene enhancer in B-cells 2) [23] (Figure 3.3). Runt domain transcription factor RUNX3 (runt-related transcription factor 3) is a gastric and colon tumour suppressor that functions downstream of TGF β (transforming growth factor beta) [24]. EGFR signalling is potentially involved in multiple aspects of malignancy, including tumour growth, inhibition of apoptosis, cell migration and invasion [25], while NFkB2 has been linked to control over tumour cell growth, migration and invasion [26]. The tumour suppressing action of

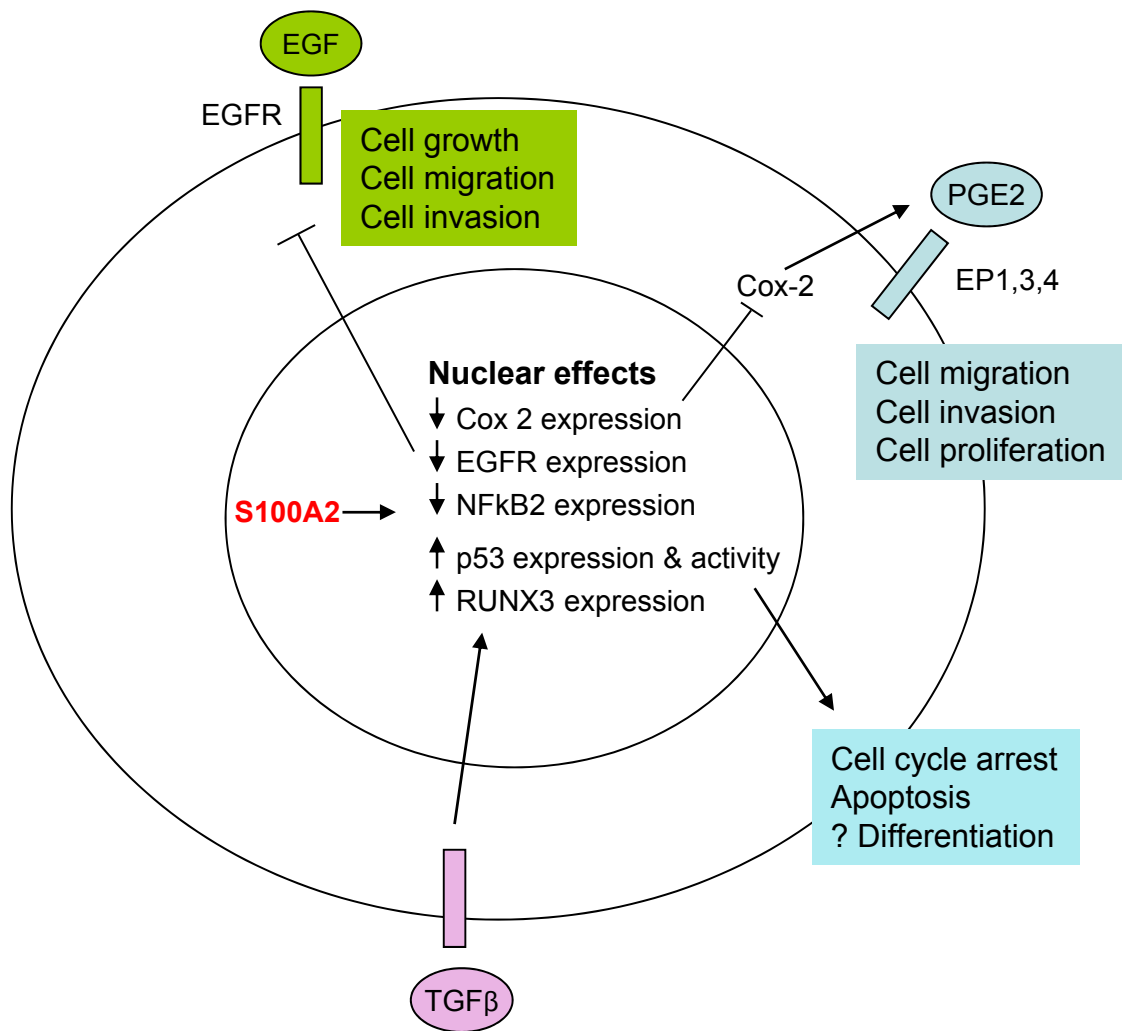


Figure 3.3. Nuclear effects of S100A2. S100A2 has been shown to reduce expression of cyclooxygenase-2 (Cox-2), which normally results in the synthesis and release of prostaglandin E2 (PGE2). PGE2 subsequently promotes cell migration, proliferation and invasion. S100A2 also inhibits epidermal growth factor receptor (EGFR) expression, repressing the cell growth, migration and invasion effects of EGF. Similarly, S100A2 inhibits NFκB2 (nuclear factor of kappa light polypeptide gene enhancer in B-cells 2) expression and its associated downstream signalling. S100A2 also promotes p53 expression and activity, leading to cell cycle arrest and apoptosis. Finally, S100A2 has been found to induce RUNX3 (Runt-related transcription factor 3), which functions downstream of transforming growth factor β (TGFβ).

S100A2 has also been theorized to be in part a result of its ability to reduce cyclooxygenase-2 (Cox-2), the upregulation of which is associated with tumorigenesis in many cancers [27] (Figure 3.3). In fact, it was found that in breast cancer cells, Cox-2 overexpression enhanced cell motility and invasiveness [28]. Cox-2 expression results in the release of the pro-inflammatory mediator prostaglandin E2 (PGE2), which acts on its cell surface receptors EP1, EP2, EP3 and EP4 [29]. In head and neck squamous cell carcinoma (HNSCC), exogenous PGE2 induced cell proliferation and it was concluded that PGE2 produced in the tumour microenvironment, as a result of Cox-2 overexpression, promoted the growth of HNSCC cells in both an autocrine and paracrine fashion by acting on EP receptors, which are widely expressed in most HNSCC cells [29]. Thus, blocking of Cox-2 by S100A2 should result in reduced cell motility, proliferation and invasiveness. Consequently, loss of S100A2 results in tumour progression.

Although various studies have shown S100A2 to be downregulated in malignancy of breast cancer [30, 31], very little is known about the exact functional roles of S100A2 in breast cancer. In relation to the 21T human breast epithelial cell line 3D model system of early breast cancer progression, S100A2 expression was decreased in 21MT-1 (IMC-like) cells compared to 21NT (DCIS-like) cells. The present study used the 21T series cells grown in 3D culture to test the hypothesis that knocking down S100A2 in 21NT cells would result in the cells becoming more invasive, with characteristics similar to the 21MT-1 cells.

3.1.3. *T-box 3 (TBX3)*

TBX3 is a member of the T-box family of transcription factors that play an important role in development of many animal species. Specifically, TBX3 mutant mice have demonstrated that TBX3 is required for expression of Lef-1 and Wnt10b, which induce mammary placodes [32]. In mouse embryo development, a model has emerged in which TBX3 expression is both induced and maintained in early mammary gland initiation by Wnt and FGF (fibroblast growth factor) [33]. Also in mouse development, TBX3 and Sonic hedgehog (Shh) regulate one another and loss of TBX3 results in loss of Shh [32] (Figure 3.4). In humans, ulnar-mammary syndrome (UMS), a congenital autosomal-dominant disorder, is caused by mutations that result in haplo-insufficiency of the TBX3 protein. UMS is characterized by upper-limb anomalies and mammary gland hypoplasia, as well as hair, genital and dental defects [34]. Additionally, TBX3 has been linked to tumorigenesis and is involved in cell cycle control and inhibition of cell senescence, through both p53-dependent and independent pathways [35-37]. The p53-dependent pathway signals through p14 (ARF), a tumour suppressor and cell cycle control protein, which is in turn repressed by TBX3 [35] (Figure 3.4). More recently, it was discovered that the mechanism of TBX3 repression of p14 (ARF) involves recruitment of histone deacetylases (HDACs) [38]. Downregulation or inhibition of p14 (ARF) leads to increased proliferation and immortalization, as well as failure of apoptosis [32]. Apart from the p14 (ARF) dependent function of TBX3, in melanoma it was found that TBX3 repressed E-cadherin expression, which leads to enhanced invasiveness [39] (Figure 3.4). In a similar fashion to that occurring during development, it was

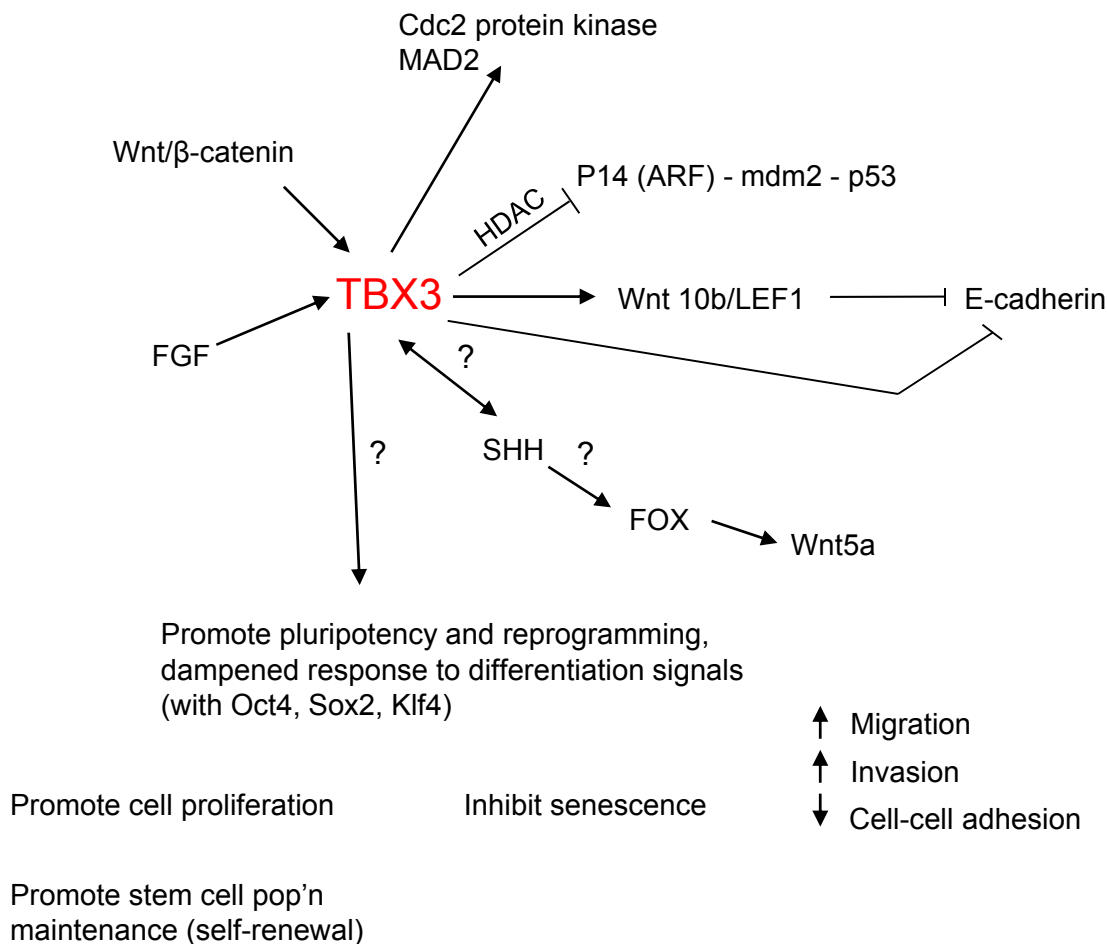


Figure 3.4. Effects and signalling of TBX3. In development, TBX3 is induced and maintained by Wnt and fibroblast growth factor (FGF) signalling. It is also both regulated by Sonic hedgehog (Shh) and regulates Shh. In cancer, TBX3 has been shown to inhibit senescence and promote proliferation through repression of P14 (ARF) and consequently p53. TBX3 has also been shown to be inversely related to E-cadherin, resulting in increased invasiveness and reduced cell-cell adhesion. Finally, in stem cells, TBX3 promotes pluripotency and reprogramming and dampens responsiveness to differentiation signals, a function that has not yet been proven in cancer.

found in liver cancer that TBX3 transcription is activated by Wnt/ β -catenin signalling [40]. This same study found that TBX3 is a mediator of β -catenin activity, influencing cell proliferation and survival. TBX2, and TBX3 by relation, have also been implicated in regulating cell cycle control. TBX2 has been shown to upregulate Cdc2, which promotes entry into mitosis, and MAD2, which is involved in spindle checkpoint activation [32]. A recent study of induced pluripotent stem (iPS) cells found a role for TBX3 in promoting pluripotency [41]. The stem cells are generally generated from mouse embryonic fibroblasts after treatment with a combination of Oc4, Sox2 and Klf4. However, the addition of TBX3 improved the pluripotency and reprogramming potential of the cells, dampening the response to differentiation signals.

Two different isoforms of TBX3 have been identified, TBX3 and TBX3+2a. The TBX3+2a variant has an extra 22 amino acids, encoded by exon 2a, inserted into the T-box domain [34]. It was theorized that since the 2a insertion was inside the highly conserved T-box domain, which is required for deoxyribonucleic acid (DNA)-binding and protein-protein interactions, this variant would have altered DNA-binding properties [42]. In fact, Fan and colleagues [42] did find that the TBX3+2a isoform was unable to bind the consensus T-box DNA-binding site and this resulted in the isoform not inhibiting senescence, as has been shown for TBX3, but instead accelerating senescence. A more recent study, however, has found that TBX3+2a can bind the DNA-binding site and is an anti-senescence factor in melanoma [43]. The original paper that described TBX3 as an anti-senescence factor was published by Brummelkamp and colleagues [35]. Interestingly, the study by Hoogaras et. al. [43] sequenced the cDNA from the

original Brummelkamp paper and found that it was in fact the TBX3+2a splice variant that was used in the study, indicating that Brummelkamp *et al.* [35] provides further evidence that the TBX3+2a variant does in fact exhibit a functional effect. The present study also seeks to examine both TBX3 isoforms. Since most literature refers to TBX3 in general and not in reference to any isoform, for simplicity in this thesis, when we are referring to both isoforms of TBX3 (or when an isoform is not identified), we will state TBX3. The two splice variants will be referred to as TBX3 isoform 1 (TBX3 variant) and TBX3 isoform 2 (TBX3+2a variant).

Very little is known about TBX3 function in breast cancer, although it has potential as a master regulator and clinical studies have shown it to be elevated during progression. In relation to the 21T human breast epithelial cell line 3D model system of early breast cancer progression, TBX3 expression was increased in 21MT-1 (IMC-like) cells compared to 21NT (DCIS-like) cells. The present study used the 21T series cells grown in 3D culture to test the hypothesis that overexpressing both isoforms of TBX3 in 21NT cells would result in the cells acquiring the characteristics of an invasive phenotype, similar to the 21MT-1 cells.

3.2. MATERIALS AND METHODS

3.2.1. Cell Lines and Culture

The 21T series cell lines (21PT, 21NT, 21MT-1) were maintained in culture in α HE media, which consists of α -MEM (minimal essential medium)

supplemented with 2mM L-glutamine (Gibco Life Technologies, Grand Island, NY), insulin (1 µg/mL), epidermal growth factor (12.5 ng/mL), hydrocortisone (2.8 mM), 10 mM 4-(2-hydroxyethyl)-1-piperazineethanesulfonic acid (HEPES), 1 mM sodium pyruvate, 0.1 mM nonessential amino acids and 50mg/mL gentamycin reagent (all from Sigma Chemical, St. Louis, MO). For regular culture conditions, the α HE media was further supplemented with 10% fetal bovine serum (FBS; Gibco Life Technologies) and named α HE10F. Transfected cell lines, created from the parental 21T series cells were also maintained in α HE10F media. Both the VANGL1 transfected cells (21PT+EV, 21PT+VANGL1) and the TBX3 transfected cells (21NT+EV, 21NT+ TBX3 Iso1, 21NT+TBX3 Iso2) had 0.2 mg/mL G418 (Gibco Life Technologies) added to the culture medium as a selection marker, while 0.2 µg/mL Puromycin (Invitrogen Life Technologies, Mississauga, ON) was added to the medium of S100A2 transfected cells (21NT+EV, 21NT+shS100A2) as a selection marker.

3.2.2. VANGL1 Expression Vector

An expression vector for VANGL1 was constructed in order to overexpress VANGL1 protein in 21PT cells and assess its functional role in early breast cancer progression. To construct the expression vector, VANGL1 cDNA was PCR-amplified using a pCMV-SPORT expression vector containing VANGL1 (Genbank accession number: BC065272), provided by the Centre for Applied Genomics at The Hospital for Sick Children (University of Toronto) as the cDNA template. PCR amplification was performed using Phusion High-Fidelity DNA Taq Polymerase (New England BioLabs, Pickering, ON) and the following

conditions: 98°C for 30 sec, followed by 40 cycles of 98°C for 7 sec, 62°C for 15 sec and 72°C for 45 sec and finally a 72°C hold for 8 min. The primers for PCR amplification can be found in Table 3.1. Five separate PCR reactions were completed and run on a 1% agarose gel. Bands at the appropriate size (~1500 kb) were gel extracted, using a QIAquick gel extraction kit (Qiagen, Mississauga, ON) and pooled. Next, the VANGL1 PCR product was incubated with T4 polynucleotide kinase (T4 PNK; New England BioLabs) to phosphorylate the insert. Finally, the VANGL1 PCR product was purified using a QIAquick PCR purification kit (Qiagen), following the manufacturer's protocol and the concentration was determined by spectrophotometry, using a NanoDrop 1000 Spectrophotometer (Thermo Scientific, Mississauga, ON).

VANGL1 was inserted into a pcDNATM3.1/myc-His B plasmid (Invitrogen Life Technologies), such that the myc tag would be fused to the C-terminus of VANGL1. To prepare the plasmid for ligation with the VANGL1 insert, the plasmid was digested with EcoRV (New England BioLabs) to insert the VANGL1 downstream of the pCMV promoter, into the multiple cloning site (Figure 3.5). EcoRV digestion results in a blunt end cut. The plasmid was subsequently incubated with calf intestinal phosphatases (CIP; New England BioLabs) to dephosphorylate the plasmid. The plasmid was then electrophoresed on a 1% agarose gel and extracted using the QIAquick gel extraction kit (Qiagen). The concentration of the processed plasmid was determined using the NanoDrop 1000 Spectrophotometer (Thermo Scientific).

The plasmid and VANGL1 PCR product were incubated overnight with ATP (adenosine triphosphate) and T4 DNA ligase (both from New England

Table 3.1. Primer sequences for VANGL1 cloning, TBX3 cloning and TBX3 qRT-PCR.

Primer Name	Sequence
VANGL1 Cloning Primers	
Forward	5'-GCC ACC ATG GAT ACC GAA TCC ACT-3'
Reverse	5'-AAC GGA TGT CTC AGA CTG TAA GCG-3'
TBX3 Cloning Primers	
Iso2 / Iso1 Frag 1 Forward	5'-GCC ACC ATG AGC CTC TCC ATG AGA-3'
Iso1 Frag1 Reverse	5'-CAT GGA GTT CAA TAT AGT AAA TCC ATG TTT GAC-3'
Iso1 Frag2 Forward	5'-TGG ATT TAC TAT ATT GAA CTC CAT GCA CAA AT-3'
Iso2 / Iso1 Frag2 Reverse	5'-TTC GGG ACC GCC TGC GGG ACC TGT CCG GC-3'
TBX3 qRT-PCR Primers	
Endogenous Forward	5'-GCG GAC TTG TCC CCG GCT GG-3'
Endogenous Iso1 Reverse	5'-CAT GGA GTT CAA TAT AGT AAA TCC ATG TTT GTC TG-3'
Endogenous Iso2 Reverse	5'-CAC TTG GGA AGG CCA AAG TAA ATC CAT G-3'
TBX3-ZsGreen Forward	5'-CAC CGC CAC CCC TTC CTC AAT CTG AAC AC-3'
TBX3-ZsGreen Reverse	5'-GTG GCG ACC GGT AGC AAC TAC GGG GAC GCG-3'

Cloning primers for VANGL1 were used to PCR amplify VANGL1, using a pCMV-SPORT expression vector containing VANGL1 as template. Cloning primers for TBX3 were used to PCR amplify isoforms of TBX3 using a pOTB7 expression vector containing TBX3 as template. A Kozak consensus sequence was added to the forward primer of the cloning primers, immediately upstream of the translation start site of the specific gene (VANGL1 or TBX3), to ensure a high level of translation initiation. Extra amino acids were also added to the reverse primer of the cloning primers to ensure the specific gene (VANGL1 or TBX3) was in frame in relation to the plasmid (VANGL1, pcDNATM3.1/myc-His B; TBX3, pZsGreen-C1). Lastly, the stop codon was removed from the reverse primers so that myc (VANGL1) or ZsGreen (TBX3), fused to the C-terminus, would be transcribed. The two isoforms of TBX3 were PCR-amplified separately. Amplification of TBX3 Iso1 required production of two TBX3 fragments, which were annealed to produce TBX3 Iso1, while the forward primer of fragment 1 (Frag1) and the reverse primer of fragment 2 (Frag2) were used to PCR amplify TBX3 Iso2 (see Figure 3.6). TBX3 qRT-PCR primers were used to amplify endogenous TBX3 Iso1 and Iso2, as well as the TBX3-ZsGreen fusion product. For endogenous TBX3, the forward primer was common for both isoforms and was located within the 5'UTR. The reverse primers for endogenous TBX3 Iso1 spanned the splice junction, while TBX3 Iso2 reverse primer was within the 22 aa insert, thus ensuring specificity of each isoform during PCR amplification. The forward primers for TBX3-ZsGreen were downstream of the splice junction, in order to amplify both isoforms. The reverse primer for TBX3-ZsGreen spanned the junction between TBX3 and ZsGreen.

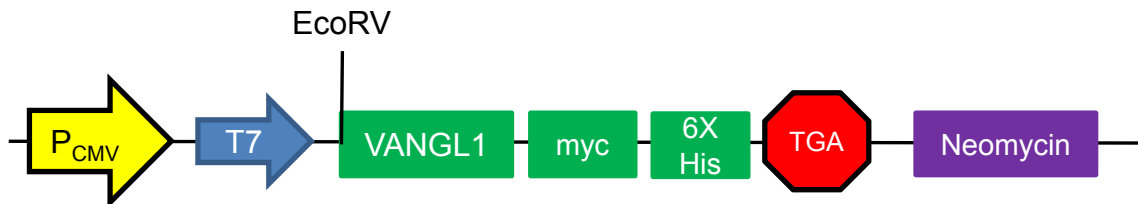


Figure 3.5. Plasmid map for VANGL1 expression vector. Protein expression was driven by a human cytomegalovirus (CMV) promoter. VANGL1 was inserted into the multiple cloning site of a pcDNATM3.1/myc-His B plasmid by restricting enzyme digest with EcoRV, which creates a blunt cut. Insertion into the multiple cloning site allowed insertion in frame with the *myc* epitope, the polyhistide C-terminal tag and the stop codon. The plasmid also contained a Neomycin resistance gene to enable selection of stable transfectants.

BioLabs) at 16 degrees to complete the ligation (Figure 3.5). Competent bacteria (DH5alpha, made in-house) were then transformed with the ligated plasmid and streaked on Luria Bertani (LB) agar (Invitrogen Life Technologies) plates with 50 µg/mL ampicillin (Gibco Life Technologies). Thirty bacteria colonies were picked and expanded in LB+ ampicillin media, and DNA was isolated using a GenElute mammalian genomic DNA miniprep kit (Sigma Chemical). The DNA was digested with KpnI (New England BioLabs) and run on a 1% agarose gel as a preliminary check to see if the insertion was the correct size and in the correct orientation. Seven of the 30 clones were sent to the DNA Sequencing Facility at Robarts Research Institution (London, ON) for sequencing. Clones with the proper sequence were used for stable transfections.

3.2.3. *TBX3* Expression Vector

Two expression vectors for TBX3 were constructed in order to overexpress TBX3 protein in 21NT cells and to subsequently assess its functional role in early breast cancer progression. Since TBX3 has two variants/isoforms, an expression vector was constructed for both, referred to here as TBX3 Isoform 1 (TBX3 Iso1) and TBX3 Isoform 2 (TBX3 Iso2) (also referred to as TBX3+2a). To construct the expression vectors, TBX3 Iso1 and TBX3 Iso2 cDNA was PCR-amplified using a pOTB7 expression vector containing TBX3 Iso2 (Genbank accession number: BC025258; Open Biosystems, Thermo Scientific) as the cDNA template. TBX3 Iso2 has an additional 22 amino acid (66 base pair (bp)) sequence, encoded by exon 2a, inserted into the T-box domain [34]. To obtain TBX3 Iso2, PCR amplification of the whole transcript was performed using

Phusion High-Fidelity DNA Taq polymerase (New England BioLabs) and the following conditions: 98°C for 30 sec, followed by 40 cycles of 98°C for 5 sec, 62°C for 15 sec and 72°C for 1 min and finally a 72°C hold for 8 min. To produce TBX3 Iso1, two PCR product fragments, representing the transcript before (fragment 1) and after (fragment 2) the 66 bp TBX3 Iso2 addition, were PCR amplified (Figure 3.6A), using the same conditions as for TBX3 Iso2. PCR primer sequences for TBX3 Iso2 and both fragments of TBX3 Iso1 can be found in Table 3.1. Three separate PCR reactions were completed for TBX3 Iso2 and each fragment of TBX3 Iso1 and then run on a 1% agarose gel. Bands representing TBX3 Iso2 at approximately 2000 kb were extracted and pooled. For TBX3 Iso1, a band at ~660 kb for fragment 1 and a band at ~1380 kb for fragment 2 were gel extracted and pooled. When designing the PCR primers for the two fragments of TBX3 Iso1, the reverse primer of the upstream amplicon (fragment 1) and the forward primer for the downstream amplicon (fragment 2) had a 20 bp overlap to ensure that the ends of these amplicons would anneal in a subsequent PCR reaction to melt the fragments together. To anneal these two fragments and generate TBX3 Iso1, 100 ng of each fragment was used as template in a PCR reaction without primers, using Phusion High-Fidelity DNA Taq polymerase (New England BioLabs). The cycling conditions were 98°C for 5 min and then 72°C for 15 min. The annealed TBX3 Iso1 PCR product was purified using a QIAquick PCR purification kit (Qiagen) and then complete TBX3 Iso1 was PCR amplified using the annealed product as template. The primers for this PCR amplification were the forward primer for the translational start site for TBX3 (TBX3 Iso2/TBX3 Iso1 fragment 1 forward primer) and the end of the coding sequence immediately

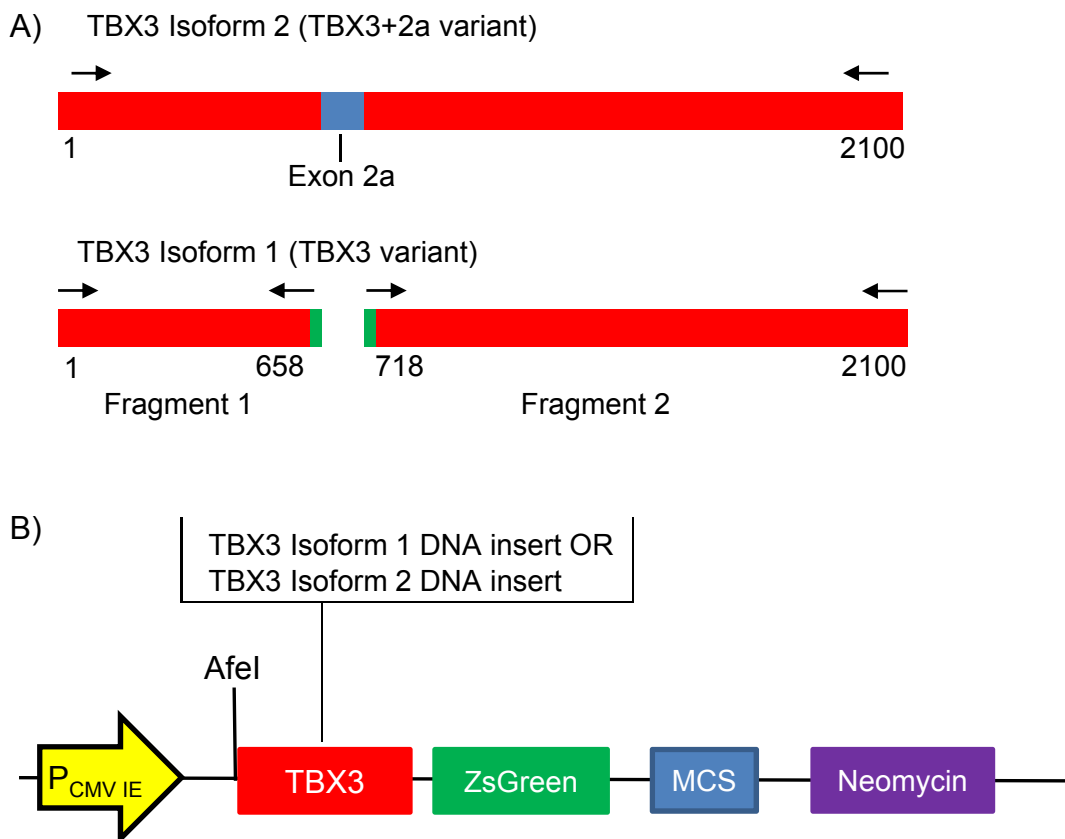


Figure 3.6. Cloning primer design and plasmid map for TBX3 expression vector. A) TBX3 isoform 2 contains a 22 amino acid insert encoded by exon 2a. Since isoform 1 was missing the exon 2a insert, primers were designed to amplify 2 fragments of isoform 1 separately. Fragment 1 encompassed TBX3 before the 2a insert, while Fragment 2 encompassed TBX3 after the 2a insert. In addition, an amino acid linker from the Fragment 2 forward primer was added to the reverse primer for Fragment 1, while an amino acid linker from the Fragment 1 reverse primer (positive strand) was added to the forward primer of Fragment 2. Also, the Fragment 1 forward primer contained a Kozak sequence, while in the Fragment 2 reverse primer, the stop codon was removed and 2 amino acids were added so that the insert would be in frame with ZsGreen. The forward primer for Fragment 1 and reverse primer for Fragment 2 were used to PCR-amplify both isoform 2 and the complete isoform 1 product once the two fragments were annealed together. B) Protein expression was driven by a human (CMV) immediate early (IE) promoter. TBX3 isoforms were inserted into the pZsGreen-C1 plasmid before the ZsGreen coding sequence by restricting enzyme digest with AfeI, which creates a blunt cut. TBX3 was inserted before ZsGreen, instead of in the multiple cloning site (MCS) so that ZsGreen would be fused to the C-terminal of the TBX3 isoforms. The plasmid also contained a Neomycin resistance gene to enable selection of stable transfectants .

upstream of the stop codon (TBX3 Iso2/TBX3 Iso1 fragment 2 reverse primer). The complete TBX3 Iso1 PCR product was then run on a 1% agarose gel and extracted using a QIAquick gel extraction kit (Qiagen). The extracted TBX3 Iso1 and TBX3 Iso2 PCR products were then incubated with T4 PNK (New England BioLabs), PCR purified and the concentration of each was determined by spectrophotometry (NanoDrop 1000 Spectrophotometer, Thermo Scientific).

TBX3 Iso1 and TBX3 Iso2 were inserted separately into pZsGreen-C1 plasmids (Clontech Laboratories, Mountain View, CA), such that the ZsGreen was fused to the C-terminus of TBX3 Iso1 or TBX3 Iso2. To prepare the plasmid for ligation with the TBX3 inserts, the plasmid was digested with AfeI (New England BioLabs) so TBX3 was inserted upstream of the ZsGreen1 coding sequence and not in the multiple cloning site (Figure 3.6B). AfeI digestion results in a blunt end cut. After digestion, the plasmid was incubated with CIP (New England BioLabs) to de-phosphorylate the plasmid. The plasmid was then electrophoresed on a 1% agarose gel and extracted using a QIAquick gel extraction kit (Qiagen). The concentration of the processed pZsGreen-C1 plasmid was determined using a NanoDrop 1000 Spectrophotometer (Thermo Scientific).

The plasmid and TBX3 isoform PCR products were incubated overnight with ATP and T4 DNA ligase (New England BioLabs) at 16°C to complete the ligation (Figure 3.6B). Competent bacteria (DH5alpha) were then transformed with the ligated plasmids and streaked on LB agar (Invitrogen Life Technologies) plates with 50 µg/mL kanamycin (Gibco Life Sciences). Fifteen bacteria colonies per TBX3 isoform were picked and expanded in LB+kanamycin media, and the

DNA was isolated using a GenElute mammalian genomic DNA miniprep kit (Sigma Chemicals). The DNA was digested with the following restriction enzyme pairs: AgeI and KpnI, MfeI and XhoI, NheI and HndIII (New England BioLabs). The resulting fragments were run on a 1% agarose gel as a preliminary check to see if the insertions were the correct size and in the correct orientation. Five clones for each isoform were sent to the DNA Sequencing Facility at Robarts Research Institution (London, ON) for sequencing. Clones with the proper sequence were used for stable transfections.

3.2.4. *shRNA against S100A2*

Short hairpin ribonucleic acid (shRNA) against S100A2 was constructed in order to determine the role of S100A2 in early breast cancer progression. The shRNA was a kind gift from Dr Michael Golding (Texas A&M University). Three separate S100A2 shRNAs in addition to an empty vector shRNA were constructed (Figure 3.7) [44]. Competent bacteria were transformed with the plasmids expressing the shRNA's and streaked on LB agar (Invitrogen Life Technologies) plates with 50 µg/mL ampicillin (Gibco Life Sciences). Ten colonies were chosen for each shRNA plasmid. In order to determine which of the shRNA's against S100A2 knocked down S100A2 gene expression most efficiently, 21NT cells were transiently transfected with all three shRNA's separately. qRT-PCR was used to determine the change in S100A2 mRNA expression, following the same methodology as above. One shRNA construct was able to reduce S100A2 mRNA expression by 45% and was subsequently

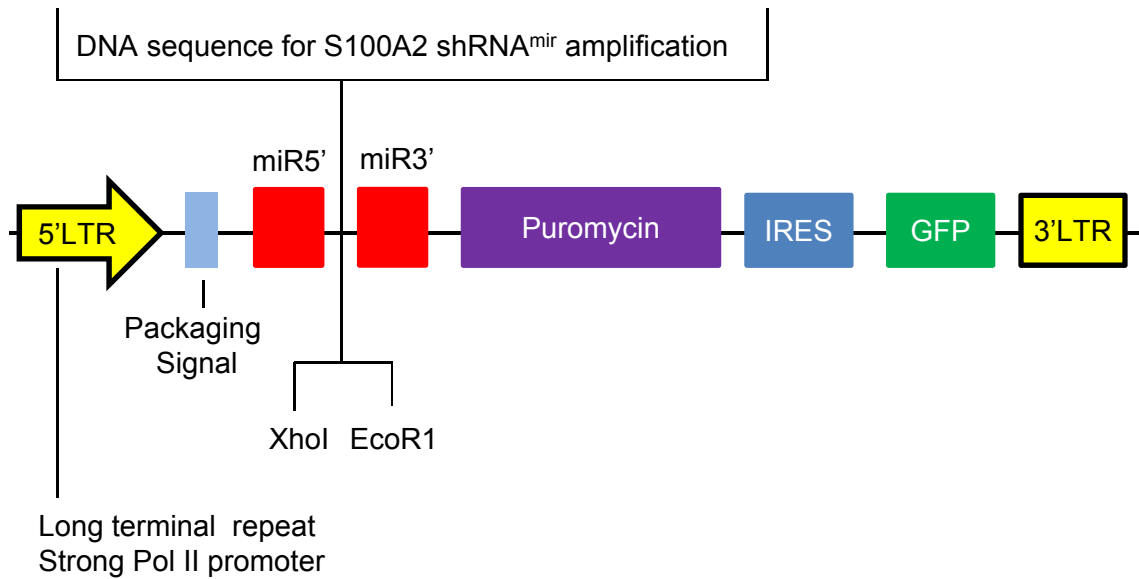


Figure 3.7. Plasmid map for S100A2 shRNA vector. The plasmid was obtained as a kind gift from Dr Michael Golding and the map has been adapted from the one provided by him. This is a miR-based shRNA expression cassette and is driven by an RNA polymerase II (Pol II) promoter. The DNA sequence for S100A2 shRNA^{mir} amplification is cloned in between XhoI and EcoR1 sites. The plasmid contains a Puromycin resistance gene to enable selection of stable transfectants. The plasmid also contains an internal ribosome entry site (IRES) for translational initiation in the middle of the mRNA sequence and a green fluorescent protein (GFP) tag.

used for stable transfections. The sequence of the shRNA chosen for S100A2 knockdown can be found in Appendix C Table 1.

3.2.5. *Transient and Stable Transfections*

Stably transfected cell lines were created to overexpress VANGL1 in 21PT cells and both isoforms of TBX3 in 21NT cells. In addition, 21NT cells were stably transfected with shRNA against S100A2, after preliminary transient transfections with the three S100A2 shRNA constructs mentioned above. For all stable transfections, empty vector controls were also transfected into the appropriate cell line. Lipofectin[®] Reagent (Invitrogen Life Technologies) methodology was used for both stable and transient transfections. The day before transfection, 21PT or 21NT cells were seeded in 6-well plates at a density that would result in 80% confluency the next day (350,000 cells per well). The following day, cells were transfected with 1 μ g of the appropriate expression vector or shRNA DNA, following the manufacturer's protocol. One day after transfection, the transfection media was replaced with α HE10F. Three days following transfection, total RNA was collected from 21NT cells transiently transfected with shRNA against S100A2 using TRIzol (Invitrogen Life Technologies) methodology. Stable transfections were subcultured into T25 culture flasks (Nunc Brand Products, Rochester, NY) three days following transfection. Puromycin (S100A2 shRNA vector) or G418 (VANGL1 and TBX3 expression vectors) selection was added to α HE10F growth medium the day following subculture. Stably transfected cells were expanded and frozen vials were placed at -80°C.

3.2.6. 3D In Vitro Cultures

For all 3D cultures, cells were grown in Matrigel Basement Membrane Matrix (BD Biosciences, Mississauga, ON) for 9 or 15 days. Cultures were created in 24-well plates (Nunc Brand Products) for mRNA and protein extraction and 48-well plates (Nunc Brand Products) for H&E staining and immunohistochemistry. The cultures contained three distinct layers. The bottom layer consisted of undiluted Matrigel for a solid base. The middle layer contained a 1:1 mix of Matrigel and cells (4.0×10^5 for 24-well, 2.0×10^5 for 48-well) in α HE media supplemented with 0.1% bovine serum albumin (BSA; Gibco Life Sciences). These two layers were topped with growth media supplemented with 0.1% BSA.

3.2.7. Collection and Quantification of RNA and Protein from 3D Cultures

After 9 days in 3D culture, cells were removed from Matrigel using Cell Recovery Solution (BD Biosciences), which non-enzymatically dissociates the Matrigel. For each experiment, 3 biological replicates were grown per cell line. Total RNA and protein were either extracted at the same time or separately.

When total RNA was extracted separately, cell pellets were treated with TRIzol (Invitrogen Life Technologies) and RNA was extracted as per the manufacturer's instructions. RNA concentrations were determined by spectrophotometry using a NanoDrop 1000 Spectrophotometer (Thermo Scientific). Aliquots of total RNA were stored at -20°C until conversion to complementary DNA (cDNA).

When only protein was required, cells were washed with RIPA buffer (10 mM Tris-HCl pH 7.5, 1 mM EDTA, 0.5 mM EGTA, 150 mM NaCl, 1% Tx-100, 0.5% DOC, and 0.1% SDS) containing protease inhibitors (1 Complete Mini Protease Inhibitor cocktail tablet /10 mL, Roche; Mannheim, Germany) and passed through a 22-gauge needle several times to lyse the cells. Sterile microcentrifuge tubes, containing the cell lysates were incubated on ice for 10 minutes and then spun down at 4°C. Supernatants were transferred to new microcentrifuge tubes and stored at -20°C. Protein concentrations were determined using the BioRad Bradford Assay (Mississauga, ON) and concentrations were standardized to known BSA concentrations.

When mRNA expression validation was immediately followed by protein expression validation, RNA and protein were extracted from the same cells. For these experiments, RNA and protein were extracted using the GE Healthcare Illustra™ triple prep kit (Baie d'Urfe, QC), following the manufacturer's protocol. RNA and protein concentrations were determined in the same method as above.

3.2.8. Quantitative Real Time-PCR (qRT-PCR) Validation

Complementary DNA was synthesized from 1µg total RNA using Superscript II, with random primers (both from Invitrogen Life Technologies). qRT-PCR was conducted using a Rotor-Gene RG-3000 temperature cycler (Corbett Life Science, San Francisco, CA) and RT2 SYBR-Green qPCR Master Mix (SuperArray Biosciences Corporation, Frederick, MD), following the manufacturer's protocol. Since SYBR-Green binds to the minor groove of all double stranded DNA, RT2 qPCR primers for VANGL1, TBX3, S100A2 and 18S

rRNA were purchased from SuperArray, which were guaranteed to produce minimal primer dimers and non-specific product. Primer sets for the different isoforms of endogenous TBX3 and the TBX3-ZsGreen fusion protein were designed in house and the sequences can be found in Table 3.1. Expression levels of all genes were calculated based on a standard curve for that gene. Standard curves were created with six dilutions from the reverse transcription product (1, 1:5, 1:25, 1:125, 1:625, 1:3125) and in triplicate. Expression levels of the housekeeping gene 18S rRNA was also determined for each sample and quantities were used to normalize values obtained for each gene of interest. All samples were assayed using three biological replicates and in duplicate. All experiments were performed in triplicate with similar results.

3.2.9. Western Blotting

Western blots were conducted using the BioRad Mini Protean II Cell system. Either 10% (VANGL1 and TBX3) or 12% (S100A2) polyacrylamide gels containing sodium dodecyl sulphate (SDS) were loaded with denatured whole cell lysates (25-50 μ g) and 5X reducing loading buffer. Gels were run at 60V for approximately 20 minutes, so the dye front was through the stacking gel and then the voltage was increased to 120 V for approximately 90 minutes. Polyvinylidene fluoride (PVDF) membranes (Amersham, GE Healthcare), which had been activated in methanol, were incubated with gels in cold transfer buffer for at least 10 minutes. Gels and membranes were then transferred at 100 V for 1.5 hours. Membranes were blocked in 5% milk in TBS-T (tris-buffered saline with 0.1% Tween) for one hour. To detect VANGL1, a mouse monoclonal antibody (R&D

Systems, Burlington, ON, catalogue no. MAB5476) was used at 1:1000 in TBS-T. To detect TBX3 a mouse monoclonal antibody (Sigma Chemicals, catalogue no. WH0006926M10) was used at 1:1000. Finally to detect S100A2 a mouse monoclonal antibody (Abgent, San Diego, CA, catalogue no. AT3754a) was used at 1:1000 in TBS-T. Membranes were incubated with primary antibodies overnight at 4°C, while rocking according to the manufacturers' instructions. An antibody against β -tubulin (Invitrogen Life Technologies; catalogue no. 32-2600) was used as a loading control at 1:2000 in TBS-T and was incubated with membranes for 1 hour, while rocking. After the primary antibody, the membranes were washed 3 times for 5 minutes each with TBS-T and then incubated with the secondary anti-mouse antibody, conjugated to HRP (Amersham, catalogue no. NXA931; 1:10 000 in TBS-T), for 1 hour at room temperature, while rocking. After 3 more washes at 5 minutes each with TBS-T, membranes were incubated with ECL Plus Western Blotting Detection System (Amersham) and then exposed to film in a dark room.

Alterations to the above Western blot methodology were made in order to resolve protein bands with the ZsGreen antibody for the TBX3 overexpressing cells. An 8% SDS polyacrylamide gel was overloaded (329 μ g TBX3 Iso1, 203 μ g TBX3 Iso2) and run without denaturing/boiling the lysates and without adding a reducing agent. The gel was run at 65 V for approximately 30 minutes and then the voltage was increased to 125 V for approximately 90 minutes. A PVDF membrane, which had been activated in methanol, was incubated with the gel in cold transfer buffer for at least 10 minutes. The gel and membrane were then transferred at 35 V for 1.5 hours. The membrane was blocked in 0.1% gelatin

(Sigma Chemical) in TBS-T for 1.5 hours. To detect ZsGreen, a rabbit polyclonal antibody (Clonetech Laboratories, catalogue no. 632474) was used at 1:1000 in 0.1% gelatin in TBS-T and incubated with the membrane overnight at 4°C, while rocking. After incubation, the membrane was washed 5 times for 5 minutes each with TBS-T and then incubated with the secondary anti-rabbit antibody conjugated with HRP (Millipore, Billerica, MA, catalogue no. AP132P; 1:10 000 in 0.1% gelatin in TBS-T) for 1.5 hours at room temperature, while rocking. After 3 more washes at 5 minutes each with TBS-T, the membrane was incubated with ECL Plus Western Blotting Detection System and then exposed to film in a dark room as above.

3.2.10. Morphologic Characterization of 3D In Vitro Cultures

After 9 and 15 days growth in Matrigel, 10% neutral buffered formalin was added to the 48-well dishes for 48 hours. Once cultures were stiffened, the cultures were removed as intact Matrigel plugs. The formalin-fixed plugs were then processed, paraffin-embedded and sectioned into 4µm slices for H&E staining and immunohistochemistry.

Histomorphology of the cell lines in 3D culture was determined by examination of H&E stained sections of the Matrigel plugs. Morphologic characterization was based on assessment of extracellular lumen formation, number of groups with polarized cells, spherical (vs. non-spherical) colony formation and proportion of single cells (Appendix B Figure 1). Each of these parameters was assessed in terms of a percentage of total “events” counted. In relation to extracellular lumen formation, number of groups with polarized cells

and spherical colonies, an event was defined as a cell group. In relation to the proportion of single cells seen in the plug, an event was defined as either a single cell or a cell group. For each cell line being studied, 10 high power (400X) fields of view from three replicate Matrigel plugs were examined. This yielded between 200 and 275 events per 10 high power fields.

3.2.11. Proliferation and Apoptosis in 3D Cultures

Matrigel plugs from 9 and 15 days cultures were immunostained for the proliferation marker Ki67, and for the apoptotic marker caspase 3. Ki67 immunohistochemistry was performed as described previously [45] with the Ki67 antibody (Dako, Mississauga, ON, catalogue no. M7240) applied (1/150 dilution) overnight at 4°C. For caspase 3 immunostaining, a microwave oven was used to pretreat deparaffinized sections for epitope retrieval. Caspase 3 antibody, which recognized cleaved caspase 3 (Cell Signaling Technologies, Danvers, MA, catalogue no. 9662) was applied (1/300 dilution) for 15min at room temperature. For both Ki67 and caspase 3, positive staining was detected with an UltraVision LP Detection System HRP Polymer (Thermo Scientific, Waltham, MA) kit, following the manufacturer's protocol. Positive and negative controls were included for both assays. All slides were counterstained with Harris's Hematoxylin.

Both Ki67 and caspase 3 indices were calculated for each cell line. The indices were defined as the number of cells positive for Ki67 or caspase 3 staining divided by the total cells counted. For each cell line being studied, 10 high power (400X) fields of view from three replicate Matrigel plugs were

examined, yielding between 200 and 350 cells. A ratio of proliferation over apoptosis was also calculated for each cell line, in order to determine the balance of dividing cells vs. apoptosing cells.

3.2.12. Transwell Invasion Assay

A transwell system was used to look at the invasion potential of VANGL1 overexpressing cells. The systems consisted of 2 chambers separated by a porous membrane coated with Matrigel. Cells were seeded in the upper chamber of the transwell system and allowed to invade towards a chemoattractant (FBS) in the lower chamber. The day before the assay, transwell inserts with 8 μm pores (Corning Life Sciences, Lowell, MA) were coated with 20 μg Matrigel, diluted in sterile water. Plates were left to dry overnight in the tissue culture hood. The following day, Matrigel coated transwells were reconstituted by adding 100 μL αHE media supplemented with 0.1% BSA. The plates were incubated on a shaker at room temperature for 90 minutes. During this incubation, cells were collected and diluted to 4×10^5 cells/mL in αHE plus 0.1% BSA. In order to determine the invasive ability of the cells, 800 μL of αHE plus 10% FBS was added to the lower chamber of the transwell system. To the upper chamber, 100 μL of the cell suspension was added (final cell concentration of 4×10^4 cells/well). Plates were then incubated for 72 hours at 37°C and 5% CO_2 . After the assay was complete, the upper chambers of the transwells were removed, inverted and fixed for 20 minutes with 1% gluteraldehyde in 1X PBS. The membranes of the upper transwells were then rinsed with sterile water. Cells were stained with Harris' haematoxylin for 15 minutes and then the membranes were rinsed again.

Addition of 1% NH_4OH (in sterile water) for 1 minute was used to intensify the cell staining. The transwell membranes were rinsed one final time with sterile water. Non-invasive cells which were attached to the upper surface of the transwell membranes were removed using a cotton Q-tip. The transwells were then allowed to dry overnight. Once dry, five high powered fields (200X) were photographed per transwell membrane. Cells that invaded to the underside of the membrane were counted from these pictures using the cell counter plug-in on ImageJ (Open source software, National Institute of Health, USA). Three biological replicates were used for this assay and the experiment was completed twice with similar results.

3.2.13. Matrigel Invasion Assay

Time lapse microscopy was used to quantify the invasive ability of S1002 knockdown and TBX3 overexpressing 21NT cells through 6 days of culture in Matrigel. An invasion assay using time lapse microscopy was chosen for genes involved in the 21NT (DCIS) to 21MT-1 (IMC) transition because 21MT-1 cells are unable to pass through the 8 μm pores of a transwell system. On average, 21MT-1 cells are 30 μm in diameter, are often polygonally-shaped and when grown in a transwell system, many cell aggregates form on the upper surface of the transwell membrane. In contrast, 21NT cells are 19 μm in diameter, more spindle-shaped in a transwell system and pass freely through 8 μm pores. Thus, a transwell system would not provide a fair assessment of the invasive ability of the S100A2 knockdown and TBX3 overexpressing 21NT cells compared to the 21MT-1 cells. For the time lapse Matrigel invasion assay, cells were grown 3D

Matrigel in 8-well chamber slides (Nunc Brand Products) for 9 days. Matrigel cultures were made as described previously, with scaled down volumes of the three layers for the 8-well chamber slide. In addition, the number of cells in the middle layer was reduced to 1.5×10^4 . After 9 days, the slides were then moved to an incubated stage platform of a Zeiss Axiovert 200M microscope for time lapse photography. Z-stack microscopy images at 5 positions were taken for each cell line every 12 hours until day 15 of growth. All cells found within the 5 positions per cell line (about 100 cells total) were then followed using AxioVision 4.5 software (Carl Zeiss Imaging Solutions), to determine the percentage of cells that invaded through the Matrigel matrix and the distance the moving cells were able to travel. A cell was defined as moving if any part of the cell was in a different location compared to the image taken 12 hours previously. The minimum distance a cell could travel to be termed as moving was 5 μm . The distance a moving cell travelled was measured using the AxioVision 4.5 software.

3.2.14. Confocal Microscopy

Confocal microscopy was used to detect protein levels of the TBX3-ZsGreen fusion product transfected cells. 21NT, 21NT+TBX3 Iso1, 21NT+TBX3 Iso2 and 21NT+EV cells were grown on 22 mm round tissue culture grade coverslips (VWR, Mississauga, ON) inside 6-well plates (Nunc Brand Products) for 24 hours. Cell medium was removed and cells were fixed with 2% formalin for 10 minutes. Wells were rinsed with 1X PBS and then permeabilization buffer (0.05% saponin, 0.10% BSA, 0.075% glycine) was added for 10 minutes. After rinsing with PBS, the cells were blocked with 10% normal goat serum (Invitrogen

Life Technologies) for 30 minutes. Without removing the goat serum, primary antibodies were added in more goat serum. To detect TBX3, the same mouse monoclonal antibody (Sigma Chemicals) used for Western blotting was used at a concentration of 1:400. To detect vimentin, a mouse monoclonal antibody (Dako, Burlington, ON; clone 3B4, catalogue no. 632474) was used at a concentration of 1:250. To detect E-cadherin, a mouse monoclonal antibody (BD Biosciences, catalogue no. 610181) was used at 1:650. Finally, an IgG1 k isotype control mouse monoclonal antibody (BD Pharmingen, catalogue no. BD554121) was used at 1:300. Primary antibodies were incubated with cells overnight at 4°C. After primary antibody was removed and wells were rinsed with 1X PBS, AlexaFluor 594 goat anti-mouse IgG (Invitrogen Life Technologies, catalogue no A-11005; 1:1000 in goat serum) was incubated with cells for 1.5 hours. Wells were rinsed again and Hoechst 33342 (Invitrogen Life Technologies, catalogue no. H1399; 1:5000 in PBS) was added for 45 minutes in the dark. After rinsing the wells one final time with PBS, coverslips were mounted onto glass slides for confocal microscopy.

Confocal laser scanning microscopy was performed using an Olympus FluoView™ FV1000 coupled to the IX81 Motorized Inverted System Microscope at The Victoria Research Laboratory Confocal Microscope Core Facility. Sequential channel scans of each stained section were optimized for maximum signal to noise ratio and minimal laser power output. Image analysis and processing were performed with ImageJ software (NIH).

3.2.15. Statistical Analysis

The differences between experimental groups were analyzed using one-way analysis of variance (ANOVA), followed by Tukey's test for post hoc analysis. Statistical analysis was performed using GraphPad InStat 3 (La Jolla, CA). For all statistics, a p-value of less than 0.05 was considered statistically significant. In all bar graphs, bars labeled with letters that are not the same indicate this significant difference. Alternately, bars labeled with the same letters are not significantly different from each other.

3.3. RESULTS

3.3.1. VANGL1

In work described in Chapter 2, VANGL1 was found to be elevated in 21NT (DCIS-like) cells compared to 21PT (ADH-like) cells [8]. To determine the functional role of VANGL1 in this transition (ADH to DCIS), VANGL1 was transfected into 21PT cells and the cells were analyzed using several functional assays, including colony profile (spherical vs. irregular), lumen formation, cell polarization, proportion of single cells, proliferation index, apoptosis index and cell invasion.

3.3.1.1. VANGL1 mRNA Expression Levels are Altered in 21NT Compared to 21PT Cells

Since the 21T series model of early breast progression was created in a 3D system, before generating transfectants, we first wanted to determine whether

the differential expression of VANGL1 mRNA (between 21PT and 21NT) could also be seen in 2D culture. Using qRT-PCR, we determined that when grown in 2D culture, VANGL1 is in fact elevated 1.8-fold in 21NTci compared to 21PTci cells (Figure 3.8). However, this was less of an increase than that seen for 3D culture (2.2-fold; Figure 3.8). Thus, the progression stage-specific expression of VANGL1 is more pronounced when cells are grown in 3D than in 2D.

Additionally, the 21PT and 21NT cells used for the microarray analysis contained an empty neo-selection vector (21PTci, 21NTci). Since we planned to transfect VANGL1 into the 21PT cells, we decided to use the parental 21PT and 21NT cells, to eliminate any issues that may arise with two transfected vectors. To ensure that VANGL1 mRNA was similarly altered in the parental cell lines, qRT-PCR was used to determine the difference in VANGL1 mRNA expression between the parental lines. It was found that VANGL1 mRNA is increased 2.6-fold in 21NT parental cells compared to 21PT parental cells (Figure 3.9). From these data, it was determined that VANGL1 mRNA is elevated in parental 21NT (DCIS-like) cells compared to parental 21PT (ADH-like) cells.

3.3.1.2. *VANGL1-Transfected 21PT Cells Show mRNA and Protein Levels Similar to 21NT Cells*

A myc-tagged VANGL1 expression vector was constructed and transfected into 21PT cells (21PT+VANGL1). In addition, a control empty vector was also transfected into 21PT cells (21PT+EV). Both qRT-PCR and Western blotting were used to determine if levels of VANGL1 were increased in 21PT+VANGL1 cells and how these levels compared to 21PT and 21NT

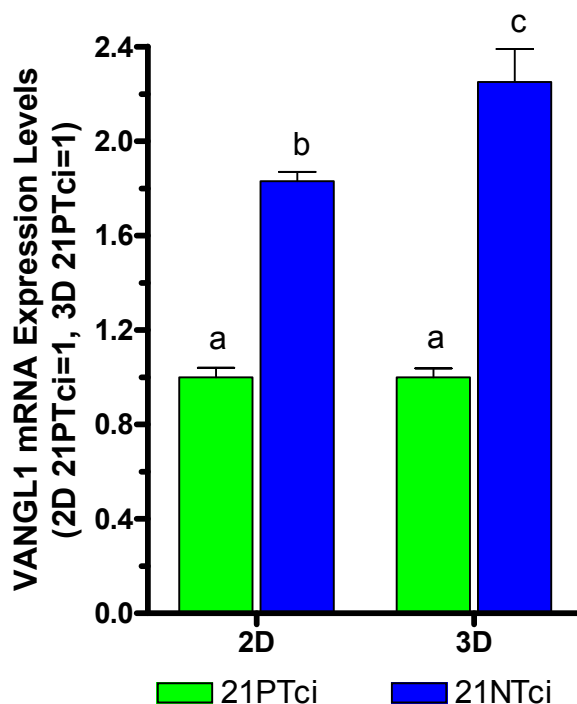


Figure 3.8. mRNA expression levels of VANGL1 in 21PTci and 21NTci cells grown in 2D and 3D culture. For ease of comparison, the mRNA expression level for 21PTci was set to 1 for both 2D and 3D. In 2D culture, VANGL1 mRNA is 1.8-fold higher in 21NTci compared to 21PTci cells, while in 3D culture, the difference in mRNA expression is 2.1-fold. For 2D culture, cells were grown in 6-well plates for 72 hours, while for 3D culture, cells were grown in Matrigel for 9 days. mRNA expression levels were calculated as a ratio with 18S rRNA, a housekeeping gene. In this figure and all subsequent figures, bars labeled with letters that are not the same indicate significant difference between the bars at a p-value of at least <0.05 (i.e. 'a' vs 'b', 'a' vs 'c' and 'b' vs 'c'). Statistics were performed before levels were modified to set 21PTci levels as 1.

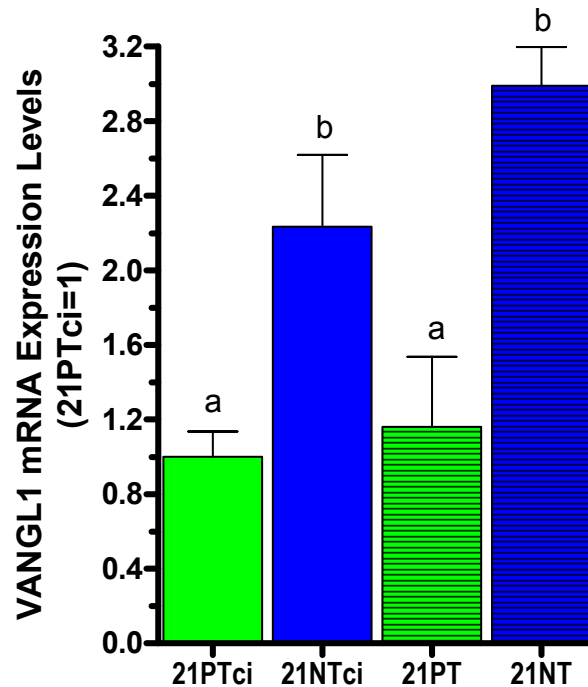


Figure 3.9. mRNA expression levels of VANGL1 in 21PTci, 21NTci, 21PT and 21NT cells grown in 3D culture. For ease of comparison, the mRNA expression level for 21PTci was set to 1. VANGL1 mRNA was expressed at the same level in both 21PTci and the parental 21PT cell lines. The mRNA expression is 2.2-fold higher in 21NTci cells compared to 21PTci cells. For the parental cell lines, VANGL1 mRNA is 2.6-fold higher in 21NT cells vs. 21PT cells. Cells were all grown in 3D Matrigel for 9 days before RNA was extracted. mRNA expression levels were calculated as a ratio with 18S rRNA, a housekeeping gene. Bars labeled with letters that are not the same indicate significant difference between the bars at a p-value of at least <math><0.05</math>. Statistics were performed before levels were modified to set 21PTci levels as 1.

(parental) cells. It was found that VANGL1 mRNA and protein levels were indeed increased in transfected cells to the same levels as 21NT cells (Figure 3.10).

3.3.1.3. 3D In Vitro Cultures of 21PT+VANGL1 Cells Display Features of More Advanced Progression than 21PT+EV Cells

In order to assess the ability of VANGL1 to alter morphologic characteristics of 21PT cells in 3D, VANGL1 transfected cells, as well as control, 21PT, 21NT and 21MT-1 cells, were grown in Matrigel matrix for 9 and 15 days. By day 15, it was apparent that 21PT+VANGL1 cells had a reduced ability to form extracellular lumina and polarized cells compared to 21PT+EV (and 21PT parental) cells (Figure 3.11). In fact, 21PT+VANGL1 cells did not form any lumina. Additionally, the reduced ability to form polarized cells was even more pronounced than for the 21MT-1 (IMC-like) cells (29% compared to 43%). These findings suggest that the 21PT+VANGL1 cells were less organized than the 21PT+EV cells, or even 21NT and 21MT-1 cells. In addition, 21PT+VANGL1 cells had a reduced ability to form spherical colonies over that of the 21PT+EV control and parental 21PT cells, as well as both the 21NT and 21MT-1 cells (Figure 3.11). A higher proportion of single cells compared to 21PT+EV cells were also noted in the 21PT+VANGL1 Matrigel plugs (Figure 3.11). Reduced ability to form spherical colonies and a greater proportion of single cells are characteristics consistent with more invasive phenotype, a feature that was directly tested as described in section 3.3.14. Similar 3D morphologic trends were seen in day 9 cultures (Appendix C, Figure 1).

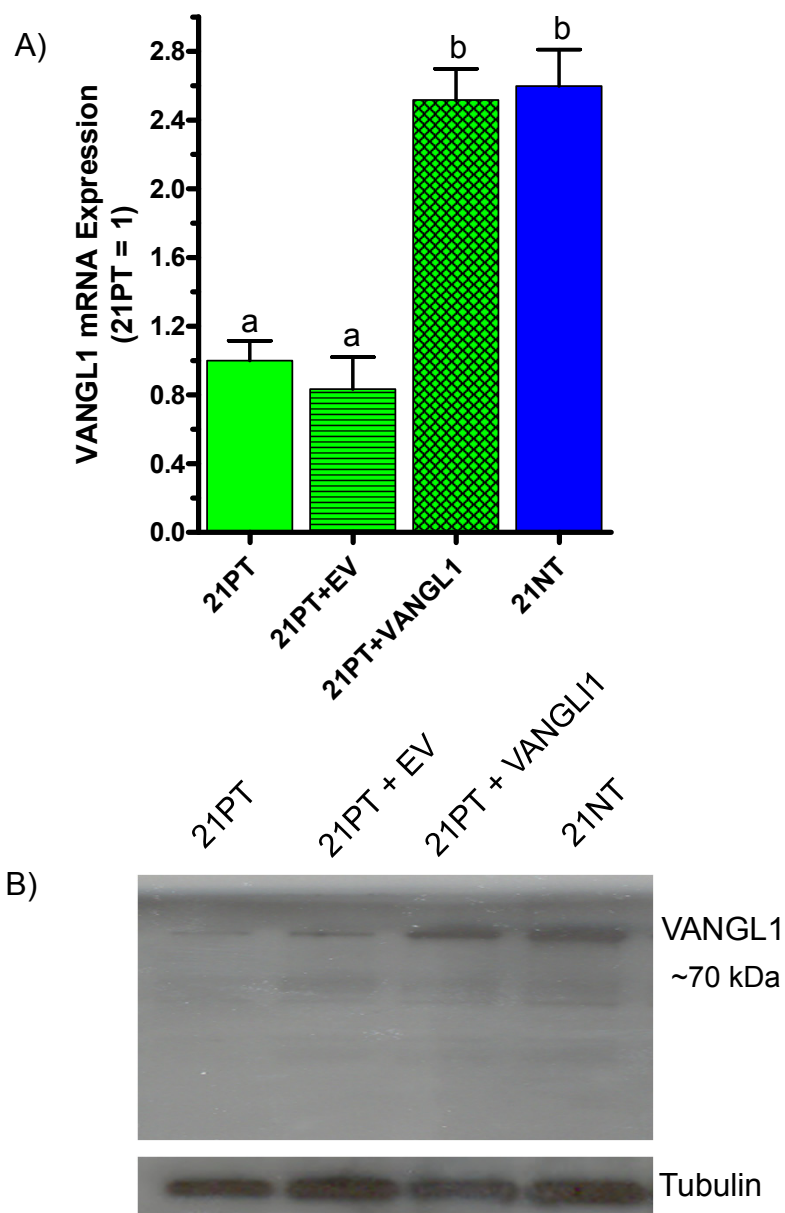


Figure 3.10. mRNA and protein levels of VANG1 after transfection into 21PT cells. VANG1 was fused to a myc-tag and stably transfected into 21PT cells using Lipofectin Reagent. mRNA and protein were extracted from cells grown in Matrigel for 9 days. A) VANG1 mRNA levels are highest in 21PT+VANG1 cells and 21NT cells. Control 21PT+empty vector (EV) cells had the same mRNA level of VANG1 as 21PT cells. mRNA levels were obtained using real-time quantitative PCR. Bars labeled with letters that are not the same indicate significant difference between the bars at a p-value of at least <0.05 . Western blotting (B) shows a similar increase in VANG1 (70kDa) protein expression in 21NT+VANG1 cells. Proteins were detected with a monoclonal anti-VANG1 antibody.

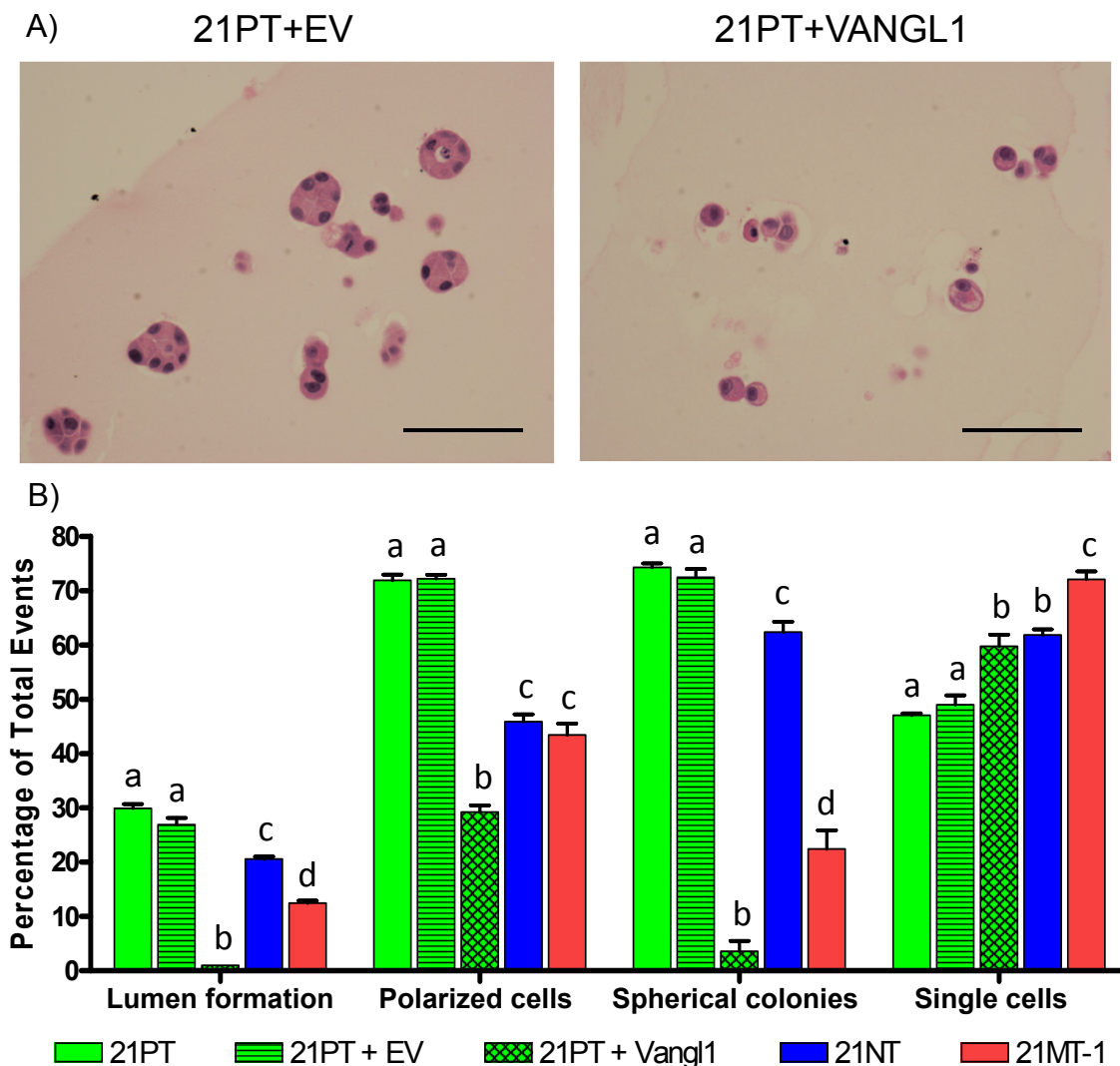


Figure 3.11. Characteristics of 21T and VANGL1 overexpressing cells after 15 days growth in 3D Matrigel. 21PT+VANGL1 cells show no lumen formation and fewer polarized cells than 21PT+EV cells, indicating that the VANGL1 cells are more disorganized. In addition, VANGL1 transfected cells also formed far fewer spherical colonies, with the percentage being lower than even 21MT-1 cells. The percentage of single cells seen in Matrigel plugs for 21PT+VANGL1 cells was at the same level as 21NT cells. 21PT+EV cells show no differences from 21PT cells. For (A), all sections were H&E stained and the scale bar represents 50 μ m. In (B) for 'single cells', an event is either a single cell or a cell group, whereas for the 'lumen formation', 'polarized cells' and 'spherical colonies' comparisons, an 'event' was defined as a cell group only. Bars labeled with letters that are not the same indicate significant difference between the bars at a p-value of at least <0.05 . Statistics for each comparison were calculated separately from the other comparisons.

3.3.1.4. Altered Proliferation, Apoptosis and Invasive Ability of 21PT+VANGL1 Cells Indicate Conversion to a Later Stage of Progression

Proliferation and apoptosis indices were calculated for the VANGL1 overexpressing cells. Ki67 immunohistochemistry for proliferation was conducted for cells grown in Matrigel for 9 and 15 days. By day 15, proliferation rates for 21PT+VANGL1 were 17.5%, compared to only 2% for 21PT+EV cells and 3.5% for 21NT cells (Figure 3.12A). Assessment of apoptosis by caspase 3 was done on cells grown in Matrigel for 9 and 15 days, and showed that by day 15, 21PT+VANGL1 cells had an increased apoptosis index compared to 21PT+EV cells (Figure 3.12B). However, this increase in apoptosis mirrored that of 21NT cells. The ratios of proliferation/apoptosis were calculated for 21PT, 21PT+EV, 21PT+VANGL1 and 21NT cell lines grown in Matrigel, using the Ki67 (proliferation) divided by the caspase 3 (apoptosis) index. Results indicate that at day 15, 21PT+VANGL1 cells have a much higher ratio of proliferation/apoptosis, compared to 21PT, 21PT+EV or 21NT cells ($p < 0.001$) (Figure 3.12C). Similar results were seen at day 9 (Appendix C, Figure 2).

To assess the invasive ability of the VANGL1 overexpression cells, invasion assays were conducted using a transwell system. 21PT, 21PT+EV, 21PT+VANGL1 and 21NT cells were all seeded in the upper chamber of the transwell system and allowed to invade through Matrigel to reach the FBS chemoattractant in the lower chamber of the transwell system. It was found that significantly more 21PT+VANGL1 cells were able to invade through the Matrigel than either the 21PT (or 21PT+EV) or 21NT cells (Figure 3.13). These results

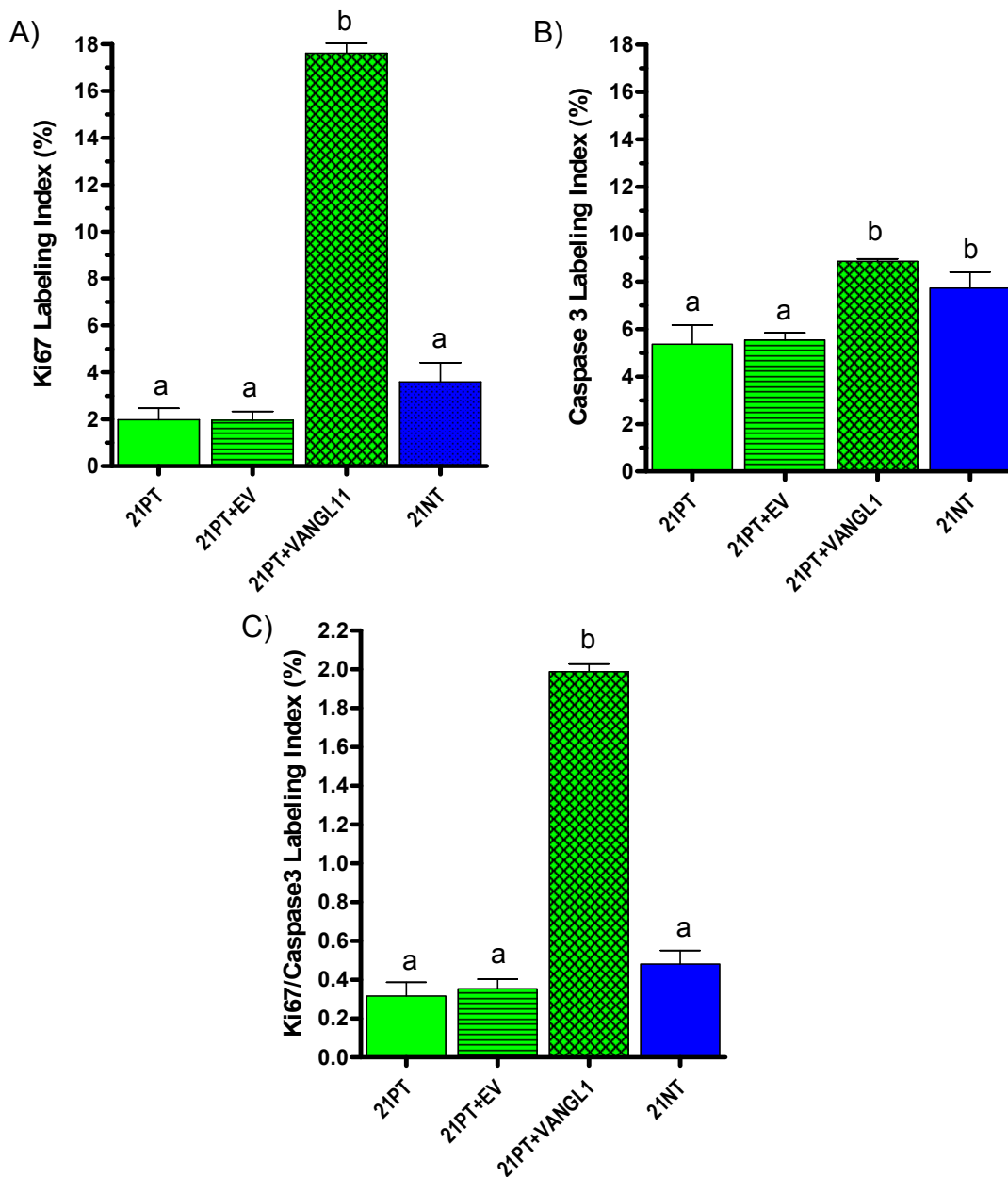


Figure 3.12. Proliferative and apoptotic activity of 21T and VANG11 overexpressing cell lines after 15 days growth in 3D Matrigel. Proliferation (A) was quantified by Ki67 immunohistochemical staining of Matrigel plugs, while apoptosis (B) was quantified by caspase 3 immunohistochemistry. 21PT+VANG11 cells showed a large increase in proliferation (A) over 21PT+EV cells, while apoptosis levels (B) increased to 21NT cell levels. When the ratio of proliferation/apoptosis was calculated (C), VANG11 overexpressing cells showed a much higher ratio than the 21PT+EV and even the 21NT cells. 21PT+EV cells showed no differences from the 21PT cells. Bars labeled with letters that are not the same indicate significant difference between the bars at a p-value of at least <math><0.05</math>.

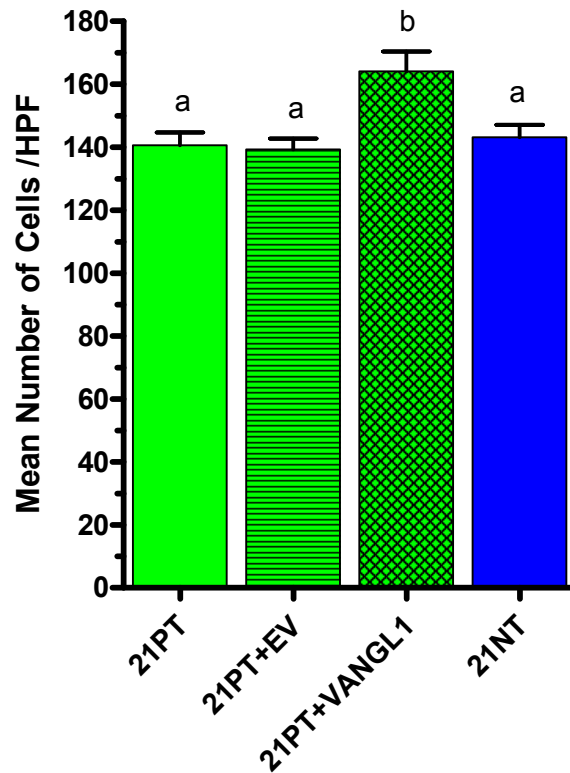


Figure 3.13. Invasion of VANGL1 overexpressing cells using a transwell system. VANGL1 overexpressing cells, as well as 21PT, 21PT+EV and 21NT cells were seeded in the upper chamber of the transwell system and allowed to invade through 20 μ g of Matrigel, towards FBS. After 72 hours, more 21PT+VANGL1 cells were able to invade than any of the other 21T cell lines. For each cell line, 5 high power fields (HPF) were counted per three replicated. Bars labeled with letters that are not the same indicate significant difference between the bars at a p-value of at least <0.05 .

indicate that the VANGL1 overexpressing cells are more invasive than 21PT or 21NT cells.

3.3.2. S100A2

As described in Chapter 2, S100A2 was found to be reduced in 21MT-1 (IMC-like) cells compared to 21NT (DCIS-like) cells [8]. To determine the functional role of S100A2 in the transition to an invasive phenotype, shRNA against S100A2 was transfected into 21NT cells and the cells were analyzed using several functional parameters, including colony profile (spherical vs. irregular), lumen formation, cell polarization, proportion of single cells, proliferation index, apoptosis index and cell invasion by time lapse microscopy.

3.3.2.1. S100A2 mRNA Expression Levels are Altered in 21MT-1 Compared to 21NT Cells

Since the 21T series breast cell line model of early breast cancer progression was created in a 3D system, prior to generating transfectants we wanted to determine whether this differential expression of S100A2 mRNA between 21NTci and 21MT-1 would also be seen when the 21T series cells were grown in 2D culture. Using qRT-PCR, we determined that when cells are grown in 2D, S100A2 is in fact decreased 3.4-fold in 21MT-1 compared to 21NTci cells (Figure 3.14). This reduction in S100A2 mRNA is comparable to the 3.2-fold reduction seen in 21MT-1 cells grown in 3D (Figure 3.14). From these data, it was determined that the stage-specific gene expression pattern of S100A2 can be found in cells grown in both 2D and 3D culture.

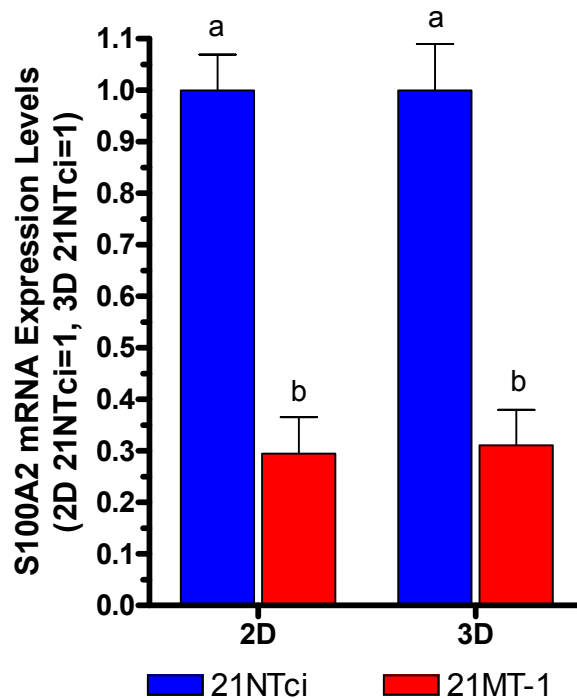


Figure 3.14. mRNA expression levels of S100A2 in 21NTci and 21MT-1 cells grown in 2D and 3D culture. For ease of comparison, the mRNA expression level for 21NTci was set to 1 for both 2D and 3D. In 2D culture, S100A2 mRNA is 3.4-fold lower in 21MT-1 compared to 21NTci cells, which is not significantly different from the 3.2-fold difference seen in 3D culture. For 2D culture, cells were grown in 6-well plates for 72 hours, while for 3D culture, cells were grown in Matrigel for 9 days. mRNA expression levels were calculated as a ratio of 18S rRNA, a housekeeping gene. Bars labeled with letters that are not the same indicate significant difference between the bars at a p-value of at least <0.05 . Statistics were performed before levels were modified to set 21NTci levels as 1.

The previous microarray analysis used 21NT cells containing an empty neo-selection vector (21NTci). Since we planned to knockdown S100A2 in the 21NT cells, we decided to use the parental 21NT cells, to eliminate any issues that may arise with two transfection vectors in the same cell line. qRT-PCR was used to determine the differential expression of S100A2 in 21MT-1 cells vs. the parental 21NT cell line. It was found that S100A2 mRNA is decreased 3.5-fold in 21MT-1 cells compared to 21NT parental cells (Figure 3.15). Thus, S100A2 mRNA is indeed reduced in 21MT-1 (IMC-like) cells compared to parental 21NT (DCIS-like) cells.

3.3.2.2. 21NT+shS100A2 Cells Show mRNA and Protein Levels Similar to 21MT-1 Cells

Short hairpin (sh) RNA against S100A2 was obtained and transfected into 21NT cells (21NT+shS100A2). In addition, a control empty shRNA vector was also transfected into 21NT cells (21NT+EV). Both qRT-PCR and Western blotting were used to determine if levels of S100A2 were decreased in 21NT+shRNA cells and how these levels compared to 21NT and 21MT-1 cells. It was found that S100A2 mRNA and protein levels were indeed decreased in transfected cells to the same levels as 21MT-1 cells (Figure 3.16).

3.3.2.3. 3D In Vitro Cultures of 21NT+shS100A2 Cells Display Features of a Later Stage of Progression

3D *in vitro* cultures were used to assess the ability of S100A2 to alter morphologic characteristics of 21NT cells. S100A2 knockdown cells, as well as

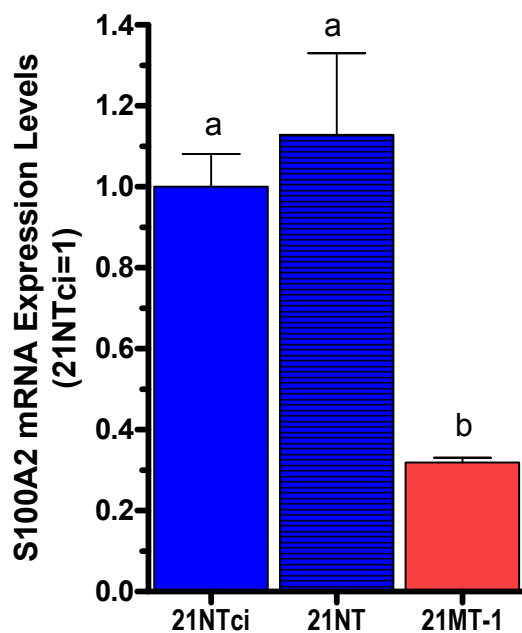


Figure 3.15. mRNA expression levels of S100A2 in 21NTci and 21NT cells compared to 21MT-1 cells. For ease of comparison, the mRNA expression level for 21NTci was set to 1. S100A2 mRNA was expressed at the same level in both 21NTci and the parental 21NT cell lines. The mRNA expression is decreased 3.2-fold in 21MT-1 cells compared to 21NTci cells and 3.5-fold compared to 21NT parental cells. Cells were all grown in 3D Matrigel for 9 days before RNA was extracted. mRNA expression levels were calculated as a ratio with 18S rRNA, a housekeeping gene. Bars labeled with letters that are not the same indicate significant difference between the bars at a p-value of at least <0.05 . Statistics were performed before levels were modified to set 21NTci levels as 1.

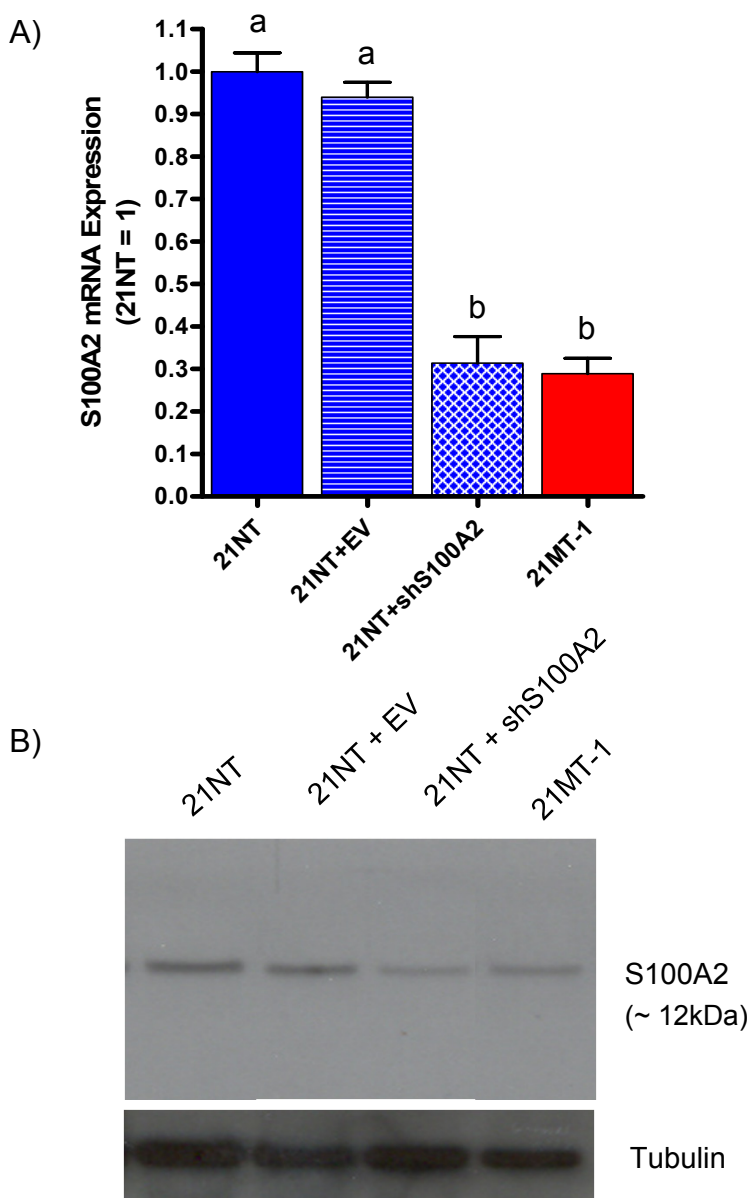


Figure 3.16. mRNA and protein levels of S100A2 after shRNA transfection into 21NT cells. An shRNA vector against S100A2 was stably transfected into 21NT cells using Lipofectin Reagent. mRNA and protein were extracted from cells grown in Matrigel for 9 days. A) S100A2 mRNA is knocked down in 21NT+shS100A2 cells to 21MT-1 levels. Control 21NT+empty vector (EV) cells had the same mRNA level of S100A2 as 21NT cells. mRNA levels were obtained using real-time quantitative PCR. Bars labeled with letters that are not the same indicate significant difference between the bars at a p-value of at least <math><0.05</math>. B) Western blotting shows a similar decreased in S100A2 (12kDa) expression in 21NT+shS100A2 cells. Proteins were detected with a monoclonal anti-S100A2 antibody.

control vector transfected 21NT, 21NT parental and 21MT-1 cells, were grown in Matrigel matrix for 9 and 15 days. By day 15, it was obvious that 21NT+shS100A2 cells had completely lost the ability to form extracellular lumina (Figure 3.17). In addition, S100A2 knockdown cells had a reduced ability to form polarized cells compared to 21NT+EV, 21NT and 21MT-1 cells (Figure 3.17). These findings suggest that the 21NT+shS100A2 cells were less organized than 21NT cells, or even 21MT-1 cells. The ability to form spherical colonies was also reduced in 21NT+shS100A2 cells, to the same level as the invasive 21MT-1 cell line (Figure 3.17). Additionally, the proportion of single cells seen in 21NT+shS100A2 Matrigel plugs was the same as those seen for 21MT-1 cells (Figure 3.17). Thus, the S100A2 knockdown cells possessed several characteristics consistent with increased invasiveness, similar to 21MT-1 cells. Similar trends were seen in day 9 cultures (Appendix C, Figure 3). Alteration in invasiveness of 21NT+shS100A2 cells was then directly assessed as described in 3.3.2.4.

3.3.2.4. 21NT+shS100A2 Cells Exhibit Characteristics of a More Aggressive Phenotype Including Alterations in Proliferation, Apoptosis and Invasion

Assessment of proliferative rates by Ki67 immunohistochemistry and apoptosis rates by caspase 3 were performed for the S100A2 knockdown cells. Immunohistochemistry for proliferation and apoptosis was conducted on Matrigel plugs from cells grown in Matrigel for 9 and 15 days. By day 15, proliferation rates for 21NT+shS100A2 were 11.5%, compared to 3.5% for 21NT+EV cells and 6% for 21MT-1 cells (Figure 3.18A). The apoptosis index showed that at day

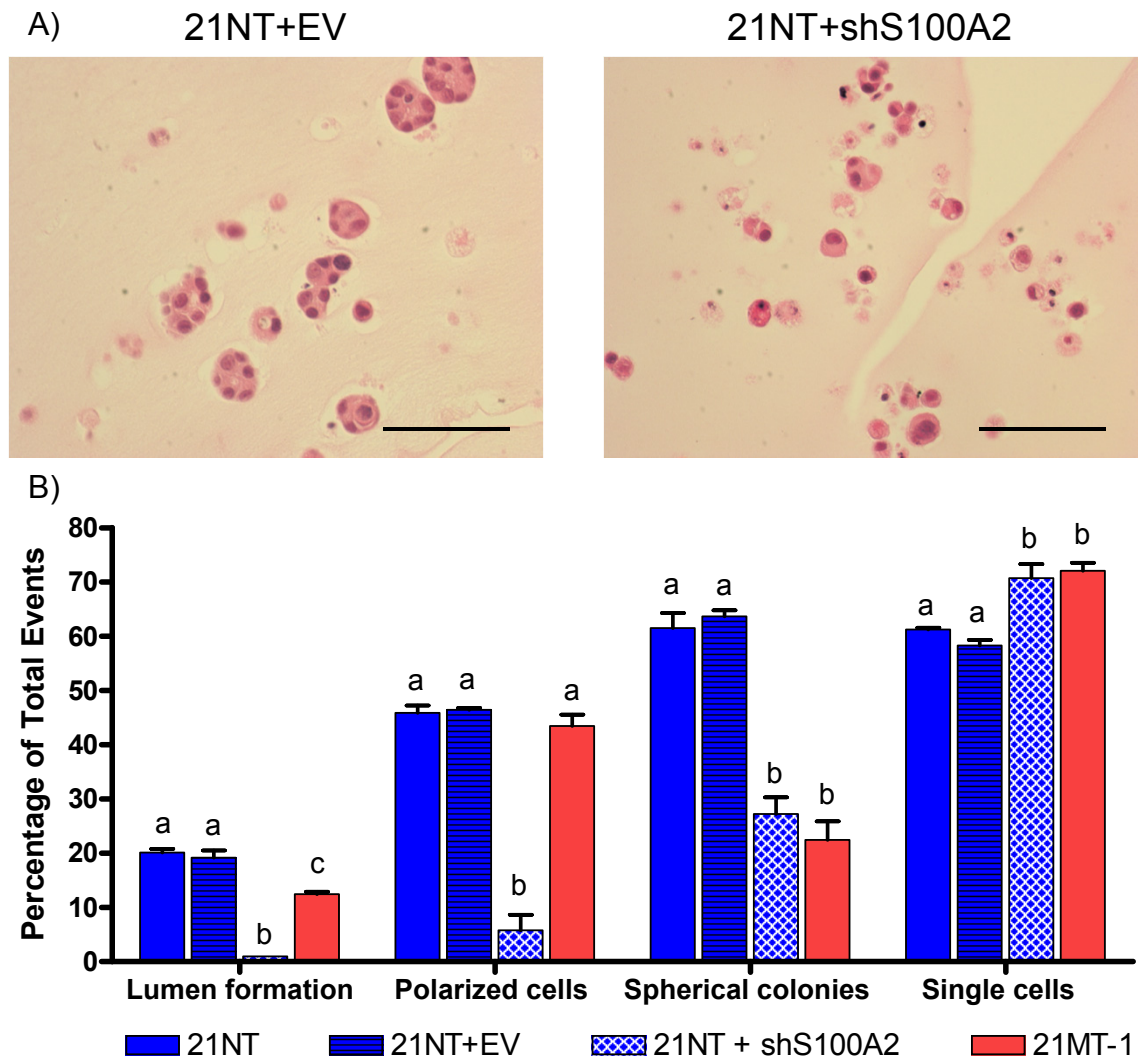


Figure 3.17. Characteristics of 21T and S100A2 knockdown cells after 15 days growth in 3D Matrigel. 21NT+shS100A2 cells show complete loss of lumen forming ability and fewer polarized cells than 21NT+EV or 21MT-1 cells, indicating that the S100A2 knockdown cells are less organized. In addition, S100A2 shRNA cells also formed fewer spherical colonies than 21NT+EV cells and in line with 21MT-1 cells. The percentage of single cells seen in Matrigel plugs for 21NT+shS100A2 cells was at the same level as 21MT-1 cells. 21NT+EV cells show no differences from 21NT cells. For (A), all sections were H&E stained and the scale bar represents 50 μ m. In (B) for 'single cells', an event is either a single cell or a cell group, whereas for the 'lumen formation', 'polarized cells' and 'spherical colonies' comparisons, an 'event' was defined as a cell group only. Bars labeled with letters that are not the same indicate significant difference between the bars at a p-value of at least <0.05 . Statistics for each comparison were calculated separately from the other comparisons.

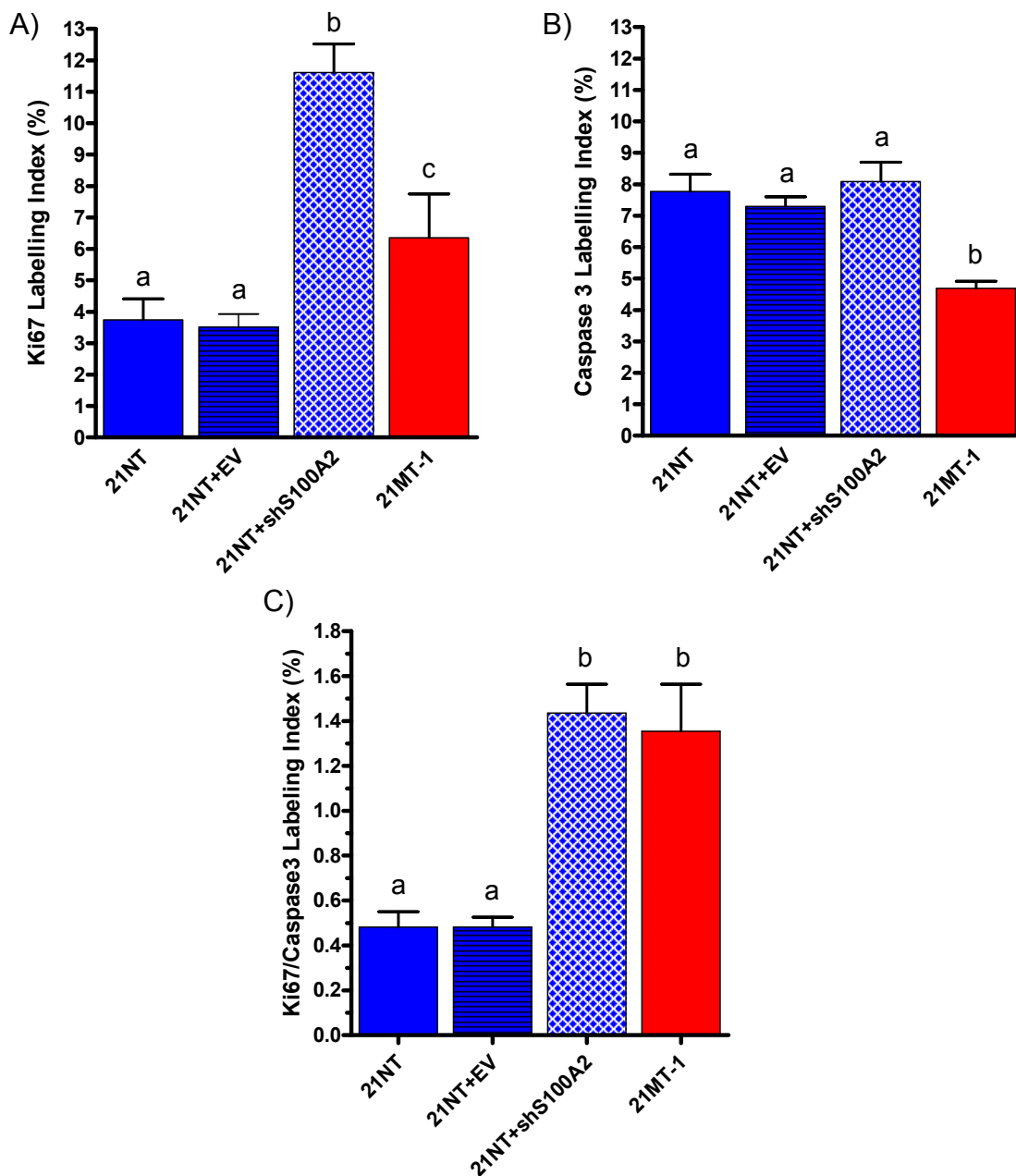


Figure 3.18. Proliferative and apoptotic activity of 21T and S100A2 knockdown cell lines after 15 days growth in 3D Matrigel. Proliferation (A) was quantified by Ki67 immunohistochemical staining of Matrigel plugs, while apoptosis (B) was quantified by caspase 3 immunohistochemistry. 21NT+shS100A2 cells showed an increase in proliferation (A) over 21NT+EV and 21MT-1 cells, while apoptosis levels (B) of S100A2 shRNA cells were not different from 21NT+EV cells. When the ratio of proliferation/apoptosis was calculated (C), S100A2 knockdown 21NT cells showed a ratio in line with 21MT-1 cells. 21NT+EV cells showed no differences from the 21NT cells. Bars labeled with letters that are not the same indicate significant difference between the bars at a p-value of at least <math><0.05</math>.

15, there was no difference in apoptosis rates between 21NT+EV and 21NT+shS100A2 cells (Figure 3.18B). However, 21MT-1 cells have a lower apoptosis rate at day 15 compared to 21NT, 21NT+EV and S100A2 21NT knockdowns. Ratios of proliferation/ apoptosis were calculated for 21NT, 21NT+EV, 21NT+shS100A2 and 21MT-1 cell lines grown in Matrigel, using the Ki67 (proliferation) vs. the caspase 3 (apoptosis) index. The ratios indicate that at day 15, 21NT+shS100A2 cells have a proliferation/apoptosis ratio that is the same as 21MT-1 cells and higher than 21NT+EV and 21NT cells (Figure 3.18C). Similar results were seen at day 9 (Appendix C, Figure 4). These results indicate that S100A2 knockdown cells have a similar growth profile to the invasive 21MT-1 (IMC-like) cells.

To assess the invasive ability of the S100A2 knockdown cells, 21NT, 21NT+EV, 21NT+shS100A2 and 21MT-1 cells were grown in Matrigel for 9 days and then followed with time lapse microscopy until day 15. It was found that similarly to 21MT-1 cells, 100% of 21NT+shS100A2 cells were able to travel through the Matrigel in both horizontal and vertical directions, compared to only ~30% of 21NT+EV cells (Figure 3.19). In addition, S100A2 knockdown cells traveled 212 μm on average over the six days, which was significantly ($p < 0.01$) farther than 21NT+EV cells (15 μm) cells, but similar to 21MT-1 cells (205 μm). These results indicate that the S100A2 knockdown cells invade in a manner similar to 21MT-1 cells.

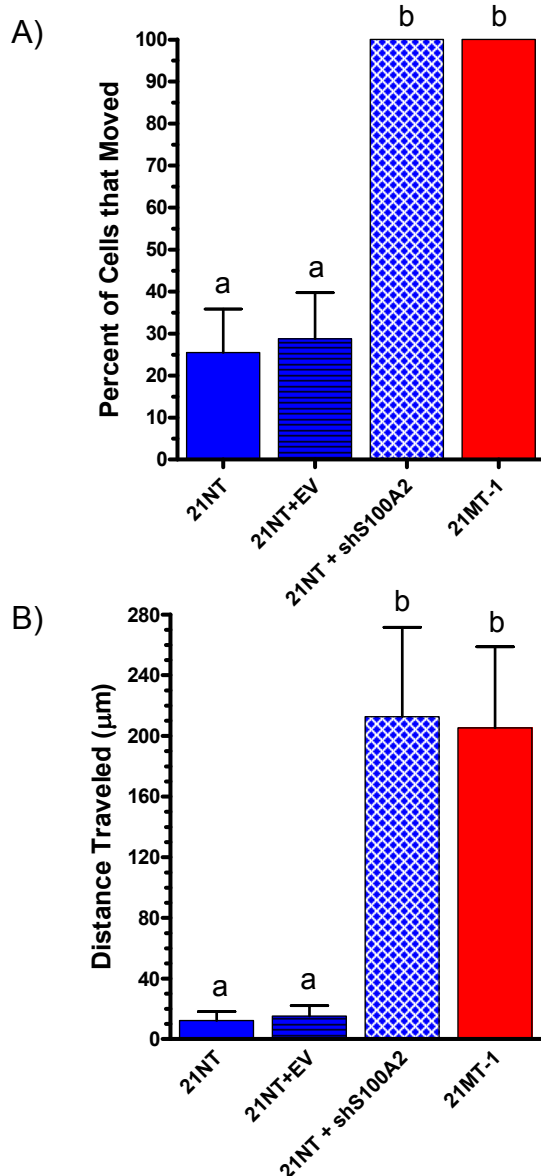


Figure 3.19. Cell invasion through Matrigel matrix for 21T and S100A2 knockdown cells. Cells were grown in Matrigel for 9 days and then transferred to the incubator stage platform of a time lapse microscope until day 15. Z-stack images were taken every 12 h and all cells were followed for the entire 6-day incubation. (A) Percentage of total cells that invaded (moved) through the Matrigel matrix. A higher percentage of 21NT+shS100A2 cells were able to move than 21NT or 21NT+EV cells. The percentage of S100A2 knockdown cells that were able to invade through Matrigel was 100%, similar to 21MT-1 cells. Similarly, when looking at the distance (μm) moving cells are able to travel through the matrix (B), S100A2 knockdown cells were able to travel as far as 21MT-1 cells. Bars labeled with letters that are not the same indicate significant difference between the bars at a p-value of at least <0.05 .

3.3.3. TBX3

In work described in Chapter 2, TBX3 was found to be increased in 21MT-1 (IMC-like) cells compared to 21NT (DCIS-like) cells [8]. There are two isoforms of TBX3, created by alternative splicing. TBX3 isoform 2 (TBX3 Iso2), also known as TBX3+2a is the full transcript, while TBX3 Isoform 1 (TBX3 Iso1), also known as TBX3 (common form), has 22 amino acids spliced out of exon 2. To determine the functional role of both isoforms of TBX3 in the transition to an invasive phenotype, the isoforms were transfected separately into 21NT cells. Functional assays including colony profile (spherical vs. irregular), lumen formation, cell polarization, proportion of single cells, proliferation index, apoptosis index, cell invasion and presence of epithelial to mesenchymal transition (EMT) markers were then used to analyze the cells.

3.3.3.1. TBX3 mRNA Expression Levels are Altered in 21MT-1 Compared to 21NT Cells

Since the 21T series model of early breast cancer progression was created in a 3D system, prior to generating transfectants, we first wanted to determine whether the differential expression of TBX3 between 21NTci and 21MT-1 cells was specific to 3D culture. Using qRT-PCR, we determined that when 21NTci and 21MT-1 cells are grown in 2D culture, TBX3 is elevated 1.7-fold in 21MT-1 compared to 21NTci cells (Figure 3.20). This was less of an increase than that seen for 3D culture (2.8-fold; Figure 3.20). Thus, the stage-specific gene expression pattern of TBX3 is more pronounced when cells are grown in 3D than in 2D.

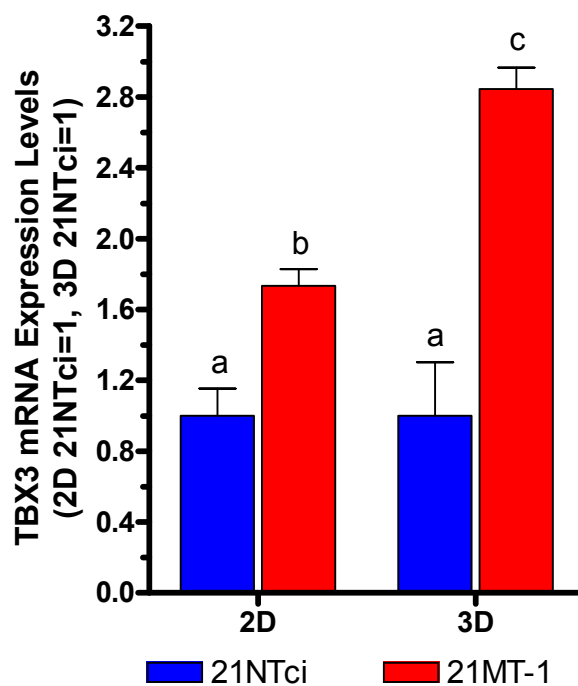


Figure 3.20. mRNA expression levels of TBX3 in 21NTci and 21MT-1 cells grown in 2D and 3D culture. For ease of comparison, the mRNA expression level for 21NTci was set to 1 for both 2D and 3D. In 2D culture, TBX3 mRNA is 1.7-fold higher in 21MT-1 compared to 21NTci cells, while TBX3 mRNA expression is increased 2.7-fold in 21MT-1 cells compared to 21NTci cells when grown in 3D culture. For 2D culture, cells were grown in 6-well plates for 72 hours, while for 3D culture, cells were grown in Matrigel for 9 days. mRNA expression levels were calculated as a ratio with 18S rRNA, a housekeeping gene. Bars labeled with letters that are not the same indicate significant difference between the bars at a p-value of at least <math><0.05</math>. Statistics were performed before levels were modified to set 21NTci levels as 1.

When microarray analysis was completed with the 21T series cells, the 21NT cells contained an empty neo-selection vector (21NTci). Since we planned to transfect TBX3 into the 21NT cells, we decided to use the parental 21NT cells, to eliminate any issues that may arise with two transfected vectors. To ensure that TBX3 mRNA levels were similarly altered in the parental cell lines, qRT-PCR was used to determine the increase in TBX3 mRNA expression in 21MT-1 cells compared to both the 21NTci and parental 21NT cell lines. It was found that TBX3 mRNA was increased 2.9-fold in 21MT-1 cells compared to 21NT parental cells (Figure 3.21). From these data, it was determined that TBX3 mRNA was elevated in 21MT-1 (IMC-like) cells compared to parental 21NT (DCIS-like) cells.

3.3.3.2. 21NT+TBX3 Iso1 and 21NT+TBX3 Iso2 Cells Show mRNA and Protein Levels Increased Over 21NT+EV Cells

Expression vectors containing TBX3 isoform 1 fused to ZsGreen and TBX3 isoform 2 fused to ZsGreen were constructed and transfected into 21NT cells (21NT+TBX3 Iso1, 21NT+TBX3 Iso2). In addition, a control expression vector containing only ZsGreen was also transfected into 21NT cells (21NT+EV). Quantitative RT-PCR was used to determine the endogenous mRNA levels of the two TBX3 isoforms in transfected cells, as well as empty vector control, 21NT (parental) and 21MT-1 cells. In addition, the mRNA level of the TBX3-ZsGreen fusion product was determined. To quantify and distinguish the endogenous transcript from the transgene, a forward primer for the endogenous forms targeting 5'UTR (untranslated region) was designed, while reverse primers which either spanned (TBX3 Iso1) or were within the splice junction (TBX3 Iso2) were

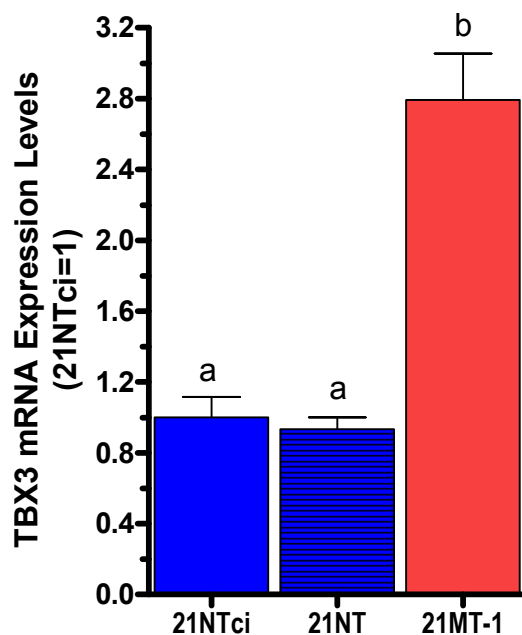


Figure 3.21. mRNA expression levels of TBX3 in 21NTci and 21NT cells compared to 21MT-1 cells. For ease of comparison, the mRNA expression level for 21NTci was set to 1. TBX3 mRNA was expressed at the same level in both 21NTci and the parental 21NT cell lines. The mRNA expression is 2.8-fold higher in 21MT-1 cells compared to 21NTci cells and 2.9-fold higher compared to 21NT parental cells. Cells were all grown in 3D Matrigel for 9 days before RNA was extracted. mRNA expression levels were calculated as a ratio with 18S rRNA, a housekeeping gene. Bars labeled with letters that are not the same indicate significant difference between the bars at a p-value of at least <0.05 . Statistics were performed before levels were modified to set 21NTci levels as 1.

designed, to ensure the isoforms were amplified separately (Table 3.1). For quantitation of only the TBX3-ZsGreen transgene, forward primers were designed to anneal to a sequence downstream of the splice junction, while the reverse primer was designed to anneal to a sequence specific to the TBX3-ZsGreen junction (Table 3.1). Results indicate that 21NT+TBX3 Iso1 and 21NT+TBX3 Iso2 cells both have increased TBX3-ZsGreen mRNA expression for their respective isoform over that of 21NT+EV cells (Figure 3.22A), although the levels in 21NT+TBX3 Iso2 transfectants are higher than 21NT+TBX3 Iso1 (6.6-fold over 21NT+EV, compared to 3.5-fold). Also, mRNA of endogenous TBX3 isoform 1 is increased 2.0-fold in 21NT+TBX3 Iso1 cells and 1.6-fold in 21NT+TBX3 Iso2 cells (Figure 3.22A). Similarly, mRNA of endogenous TBX3 isoform 2 is increased 1.8-fold in 21NT+TBX3 Iso1 cells and 2.9-fold in 21NT+TBX3 Iso2 cells (Figure 3.22A). Endogenous TBX3 isoform 1 mRNA is increased in 21MT-1 cells 3.7-fold compared to 21NT+EV cells, while isoform 2 mRNA is increased 2.6-fold in 21MT-1 cells compared to 21NT+EV cells (Figure 3.22A). Thus, via mRNA it appears that both isoforms of TBX3 are increased in transfected cells over 21NT cells.

Western blots using a monoclonal antibody against TBX3 were also performed to determine the protein level of TBX3 in the transfected cell lines, as well as 21NT, 21NT+EV and 21MT-1 cells. A band at 80kDa was resolved, which corresponds to endogenous TBX3 (Figure 3.22B). Since the two isoforms are only 22 amino acids different in size, separate bands for each isoforms could not be resolved. TBX3 protein at this size was increased in 21NT+TBX3 Iso1 and 21NT+TBX3 Iso2 compared to 21NT (and 21NT+EV) cells (Figure 3.22B).

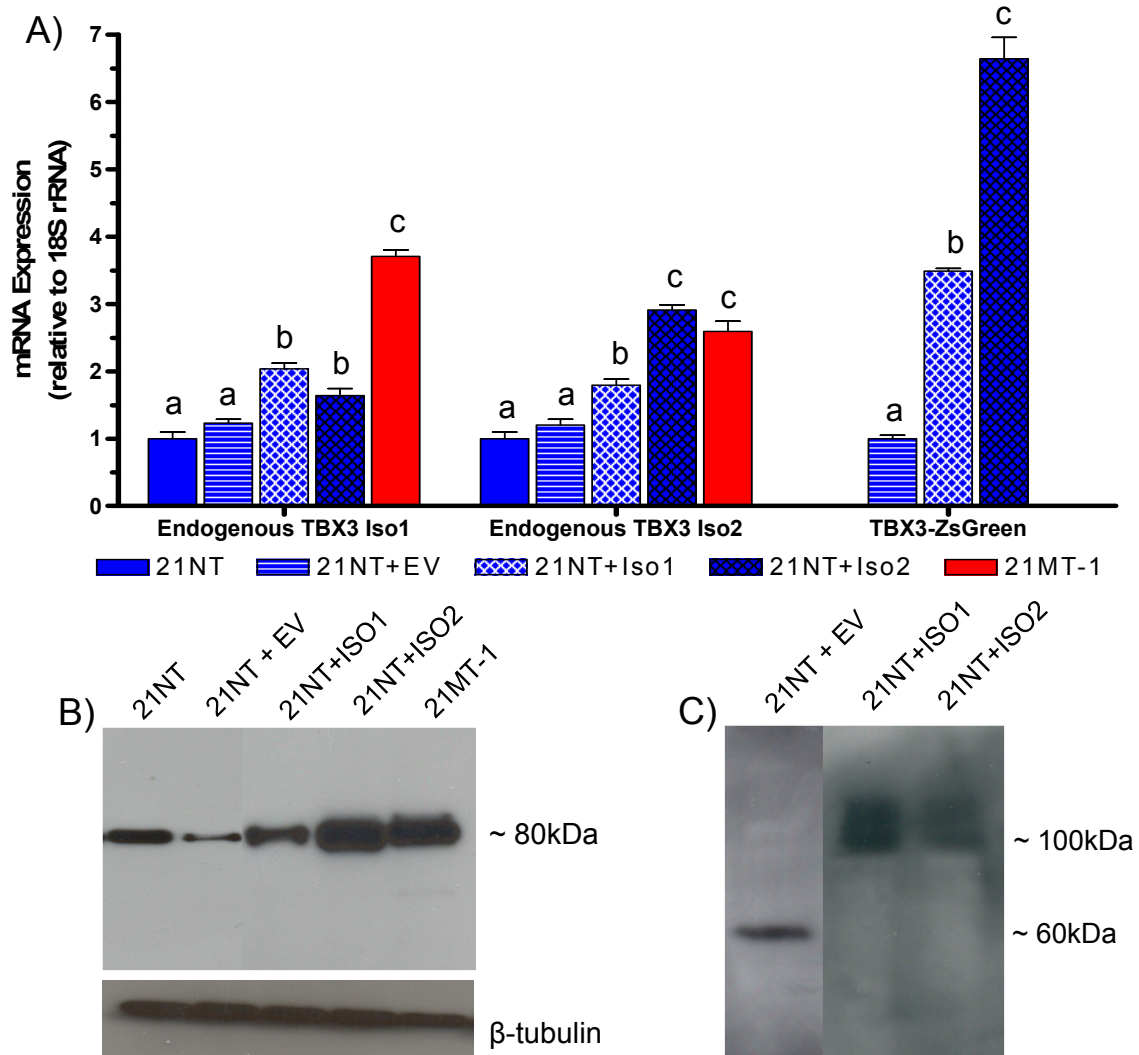


Figure 3.22. mRNA and protein levels of endogenous TBX3 and TBX3-ZsGreen after transfection into 21NT cells. The two isoforms of TBX3 (TBX3 Iso1, TBX3 Iso2) were separately fused to ZsGreen protein and stably transfected into 21NT cells. mRNA and protein were extracted from cells grown in Matrigel for 9 days. In cells transfected with only TBX3 Iso1, (A) endogenous TBX3 Iso1 mRNA is increased as well as the TBX3-ZsGreen fusion product. Similarly, cells transfected with TBX3 Iso2 alone (A) show increased endogenous TBX3 Iso2 as well as TBX3-ZsGreen mRNA. Control 21NT+empty vector (EV) cells had the same mRNA level of both TBX3 isoforms and TBX3-ZsGreen, compared to 21NT cells. mRNA levels were obtained using real-time quantitative PCR. For ease of comparison, the mRNA expression level for 21NT was set to 1 for endogenous TBX3, while 21NT+EV was set to 1 for the fusion product. Bars labeled with letters that are not the same indicate significant difference between the bars at a p-value of at least <math><0.05</math>. Western blotting (B) shows similar increases in endogenous TBX3 (80kDa) protein for both transfected cell lines and presence (C) of a TBX3-ZsGreen fusion protein (100 kDa) in 21NT+TBX3 Iso1 and 21NT+TBX3 Iso2 transfected cells. The 21NT+EV cell lines also show a ZsGreen product. A β -tubulin loading control was used in (B), however different amounts of protein were loaded in (C) to resolve bands. Thus, (C) is not used to compare amounts of TBX3-ZsGreen protein but to show expression only. Proteins were detected with a monoclonal anti-TBX3 antibody (B) or a polyclonal anti-ZsGreen antibody (C).

However, since the transfected TBX3 was fused to ZsGreen, which is approximately 20kDa, the fusion protein should have been resolved at approximately 100kDa. No band was resolved at this location (Figure 3.22b) when using the TBX3 antibody, even after altering many blot conditions, including amount of protein loaded, concentration of primary and secondary antibody, incubation time with primary and secondary antibody, transfer time and exposure time. Instead, immunoblotting with a polyclonal antibody against ZsGreen was used in order to resolve the protein band corresponding to the TBX3-ZsGreen fusion protein. 21NT+TBX3 Iso1 and 21NT+TBX3 Iso2 cells both showed protein banding at approximately 100kDa (Figure 3.22C), corresponding to the size expected for TBX3 (80 kDa) plus ZsGreen (20 kDa). The empty vector control cells (21NT+EV) showed a protein band resolved at approximately 60kDa (Figure 3.22C). Although the predicted protein size of ZsGreen is ~20kDa, this 60kDa band could represent a trimeric form of ZsGreen because this blot was performed under non-denaturing and non-reducing conditions.

Confocal microscopy was also employed to determine the relationship between TBX3 and ZsGreen. Both 21NT+TBX3 Iso1 and 21NT+TBX3 Iso2 cell lines showed increased TBX3 and ZsGreen compared to 21NT cells (Figure 3.23). Much of the TBX3 and ZsGreen signal also colocalized, indicating that the increased TBX3 was a result of the transfected ZsGreen fusion protein. Thus, TBX3 is increased in the transfected cell line compared to 21NT cells. It is also worth noting that a proportion of the ZsGreen signal was confined to the nuclear volume (34% of total signal for TBX3 Iso1, 23% of total signal for TBX3 Iso2), consistent with TBX3's action as a transcription factor.

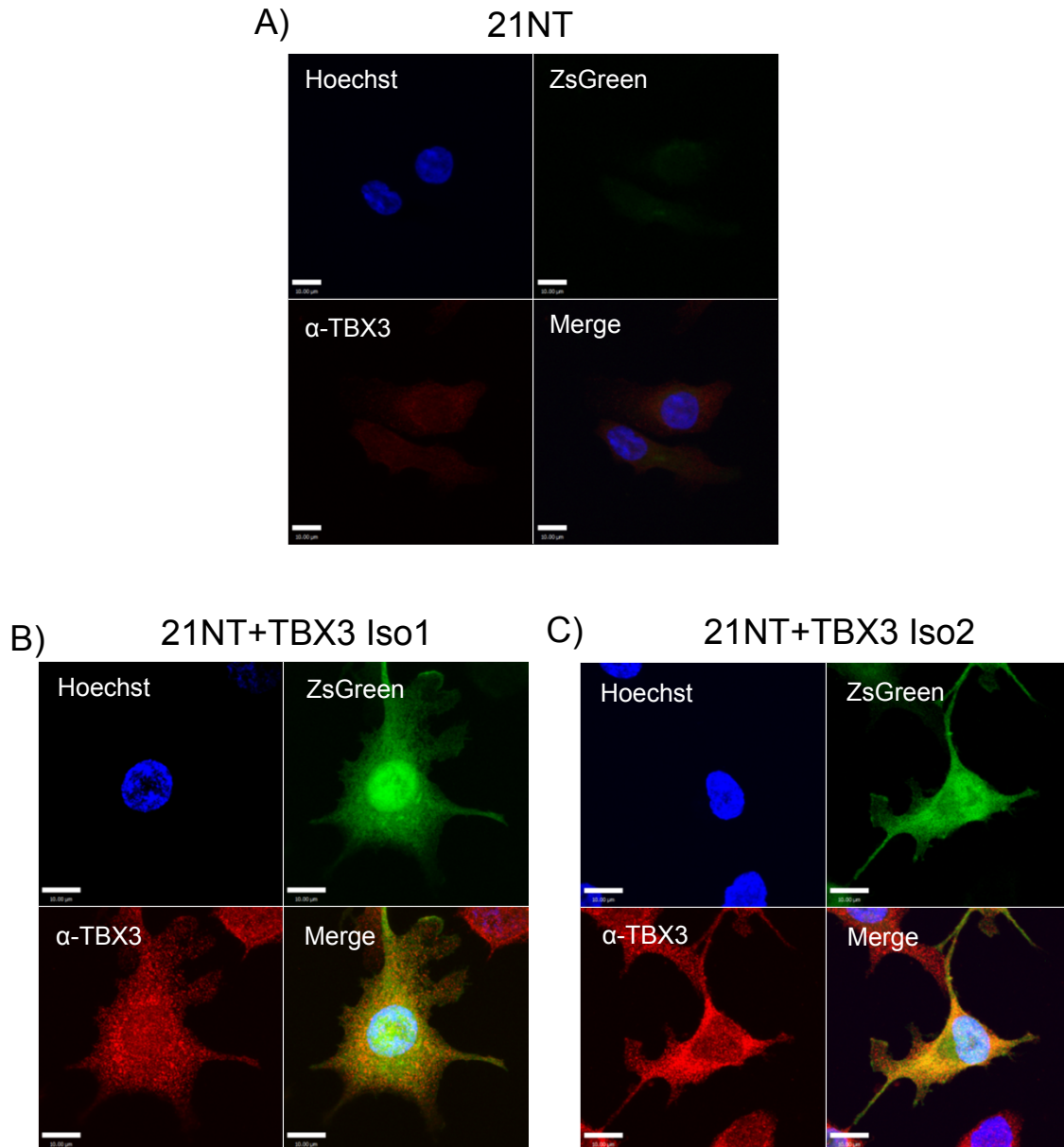


Figure 3.23. Relationship between TBX3 and ZsGreen using confocal microscopy. 21NT (A), 21NT+TBX3 Iso1 (B) and 21NT+TBX3 Iso2 (C) cells were grown on coverslips for 24 hrs. Cells were fixed and stained with an anti-TBX3 antibody. In order to incorporate fluorescence, the secondary was conjugated to Alexa488 (red). Cells were also stained with Hoechst (blue) for nuclear detection. The 21NT cell line (A) lacked ZsGreen expression. The transfected cell lines (B, C) show more TBX3 than the 21NT (A) cells. In the TBX3-ZsGreen transfected cell lines (B, C), the majority of the TBX3 and ZsGreen signal colocalized, indicating that most of the increased TBX3 is a result of the transfected ZsGreen fusion protein. Scale bar represents 10 μm.

3.3.3.3. 3D In Vitro Cultures of 21NT+TBX3 Cells Display Features of a More Advanced Stage of Progression

To assess the ability of TBX3 to alter morphologic characteristics of 21NT cells, TBX3-transfected cells (both isoforms), as well as control, 21NT and 21MT-1 cells, were grown in Matrigel matrix for 9 and 15 days. At day 15, it was apparent that both 21NT+TBX3 Iso1 and 21NT+TBX3 Iso2 cells had a reduced ability to form extracellular lumina and polarized cells compared to 21NT+EV cells (Figure 3.24). For TBX3 isoform 1 overexpressing cells, ability to form extracellular lumina were reduced to the same levels as 21MT-1 cells; however, for TBX3 isoform 2 overexpressing cells, the ability to form extracellular lumina was reduced past 21MT-1 levels (Figure 3.24). Overexpression of both isoforms resulted in reduced ability to form polarized cells past levels seen for 21MT-1 cells (Figure 3.24). These findings suggest that both 21NT+TBX3 Iso1 and 21NT+TBX3 Iso2 cells were less differentiated than 21NT+EV cells and perhaps even less differentiated than 21MT-1 cells. Both TBX3 variant overexpressing cells also had a reduced ability to form spherical colonies compared to 21NT+EV cells, although not lower than 21MT-1 cells (Figure 3.24). Similarly to 21MT-1 cells, 21NT+TBX3 Iso1 and 21NT+TBX3 Iso2 cell Matrigel plugs showed a higher proportion of single cells compared to 21NT+EV control cells (Figure 3.24). Matrigel plugs of TBX3 overexpressing cells also showed a small percent of very large, irregularly shaped, loosely packed aggregates, unlike any seen with 21T series cells in 3D culture before (Figure 3.24). These results are consistent with the conclusion that the TBX3 overexpressing cells acquired characteristics of invasive behaviour, similar to those seen with 21MT-1 cells. Similar trends were

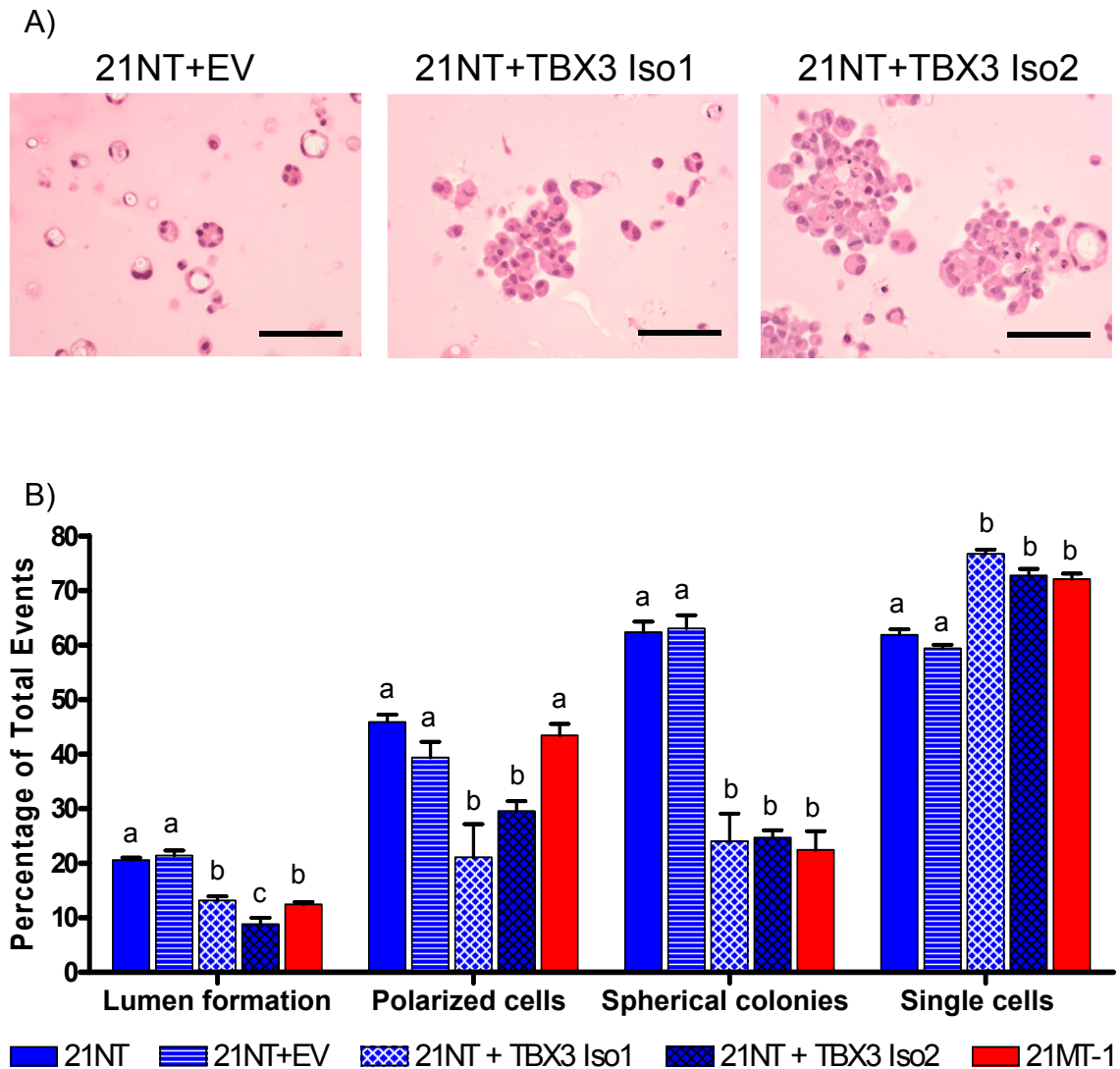


Figure 3.24. Characteristics of 21T and TBX3 transfected cells after 15 days growth in 3D Matrigel. 21NT +TBX3 Iso1 and Iso2 cells form fewer lumens and polarized cells than 21NT+EV cells, indicating that the TBX3 cells are less organized. In addition, TBX3 transfected cells also formed less spherical colonies, in line with the invasive 21MT-1 cell line and more single cells, also similarly to 21MT-1 cells. 21NT+EV cells show no differences from 21NT cells. For (A), all sections were H&E stained and the scale bar represents 50 μ m. In (B) for 'single cells', an event is either a single cell or a cell group, whereas for the 'lumen formation', 'polarized cells' and 'spherical colonies' comparisons, an 'event' was defined as a cell group only. Bars labeled with letters that are not the same indicate significant difference between the bars at a p-value of at least <0.05 . Statistics for each comparison were calculated separately from the other comparisons.

seen in day 9 cultures (Appendix C, Figure 5). Invasive ability of the TBX3 transfectants was then directly tested as described in section 3.3.3.4.

3.3.3.4. *Altered Proliferation, Apoptosis and Invasive Ability Indicate 21NT+TBX3 Cells Exhibit Characteristics of a More Invasive Phenotype*

Proliferation and apoptosis rates were calculated for the TBX3 overexpressing cells after growth in 3D Matrigel for 9 and 15 days. Immunohistochemistry using Ki67 was used to calculate proliferation indices, while caspase 3 immunohistochemistry was used to calculate apoptosis indices. By day 15, proliferation rates for 21NT+TBX3 Iso1 and 21NT+TBX3 Iso2 were greatly increased over 21NT, 21NT+EV or 21MT-1 levels (Figure 3.25A). In fact 21NT+TBX3 Iso1 cells had 61.0% proliferating cells, while 21NT+TBX3 Iso2 had 58.8% proliferating cells, compared to 3.5% seen for 21NT+EV cells and 6% for 21MT-1 cells. The apoptosis index showed that at day 15, there was no difference in apoptosis rates between 21NT+EV (and 21NT) and 21NT+TBX3 Iso1 or 21NT+TBX3 Iso2 cells (Figure 3.25B). However, 21MT-1 cells have a lower apoptosis rate at day 15 compared to 21NT+EV and TBX3 overexpressing cells. Ratios of proliferation/apoptosis were then calculated for 21NT, 21NT+EV, 21NT+TBX3 Iso1, 21NT+TBX3 Iso2 and 21MT-1 cell lines grown in Matrigel, using the Ki67 vs. the caspase 3 index. The ratios indicate that at day 15, both TBX3 overexpressing cell lines have proliferation/apoptosis ratios that are greatly increased compared to 21NT+EV ($p < 0.001$) and 21MT-1 ($p < 0.001$) cells (Figure 3.25C). Similar results were seen at day 9 (Appendix C, Figure 6).

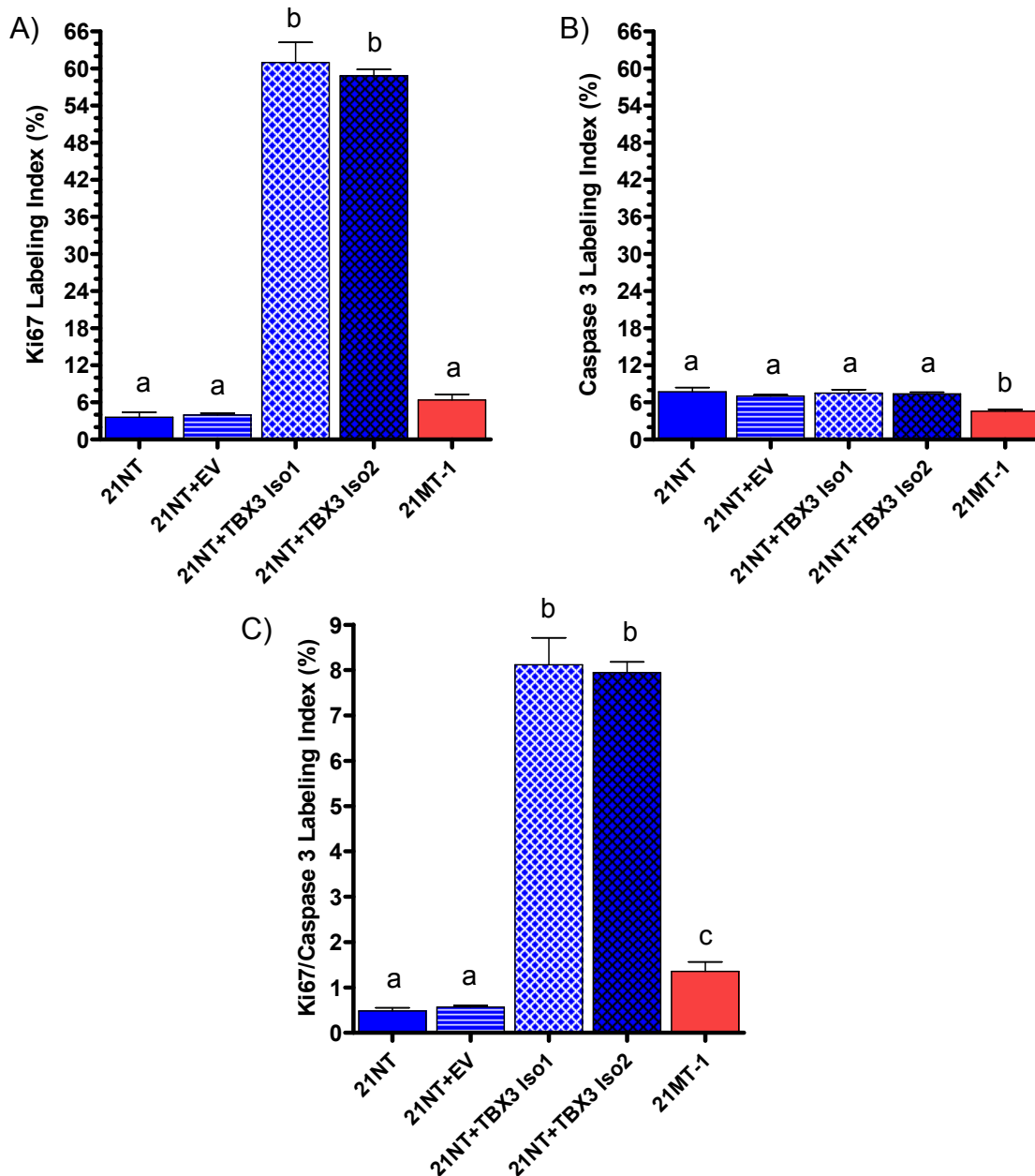


Figure 3.25. Proliferative and apoptotic activity of 21T and TBX3 transfected cell lines after 15 days growth in 3D Matrigel. Proliferation (A) was quantified by Ki67 immunohistochemical staining of Matrigel plugs, while proliferation (B) was quantified by caspase 3 immunohistochemistry. 21NT+TBX3 Iso1 and Iso2 cells showed a large increase in proliferation (A) over 21NT+EV cells, while apoptosis levels (B) remained similar to the 21T cells. When the ratio of proliferation/apoptosis was calculated (C), TBX3 transfected cells showed a much higher ratio than the 21NT+EV and even the 21MT-1 cells. 21NT+EV cells showed no differences from the 21NT cells. Bars labeled with letters that are not the same indicate significant difference between the bars at a p-value of at least <0.05 .

In order to assess the invasive ability of the TBX3 overexpressing cells, 21NT, 21NT+EV, 21NT+TBX3 Iso1, 21NT+TBX3 Iso2 and 21MT-1 cells were grown in Matrigel for 9 days and followed with time lapse microscopy until day 15. It was found that 83.7% of TBX3 isoform 1 overexpressing cells were able to travel through the Matrigel, while 92.7% of TBX3 isoform 2 overexpressing cells were able to invade (Figure 3.26). This is significantly more than 21NT+EV cells ($p < 0.001$) and not significantly different from the 100% of 21MT-1 cells that are able to invade through Matrigel. In addition, 21NT+TBX3 Iso1 cells traveled 154 μm on average over the seven days, while 21NT+TBX3 Iso2 cells traveled 182 μm , both of which were significantly ($p < 0.01$) farther than the 15 μm traveled by 21NT+EV cells, but similar to 21MT-1 cells (212 μm). These results indicate that the TBX3 overexpressing cells (both isoform 1 and 2) are as invasive as 21MT-1 cells.

3.3.3.5. 21NT+TBX3 Cells Show Vimentin and E-Cadherin Alterations Consistent with EMT

While maintaining the TBX3 cells (21NT+TBX3 Iso1, 21NT+TBX3 Iso2) in 2D culture, it was noted that the cells had a more mesenchymal-like or spindled appearance than the 21NT or 21NT+EV control cells. To determine if the cells had undergone an EMT conversion, confocal microscopy was used to analyze expression of two EMT markers, vimentin and E-cadherin. Since we had already established that TBX3 colocalized with ZsGreen, ZsGreen presence was used to determine cells with increased TBX3 expression. The confocal microscopy demonstrated that E-cadherin is greatly reduced in both 21NT+TBX3 Iso1 and

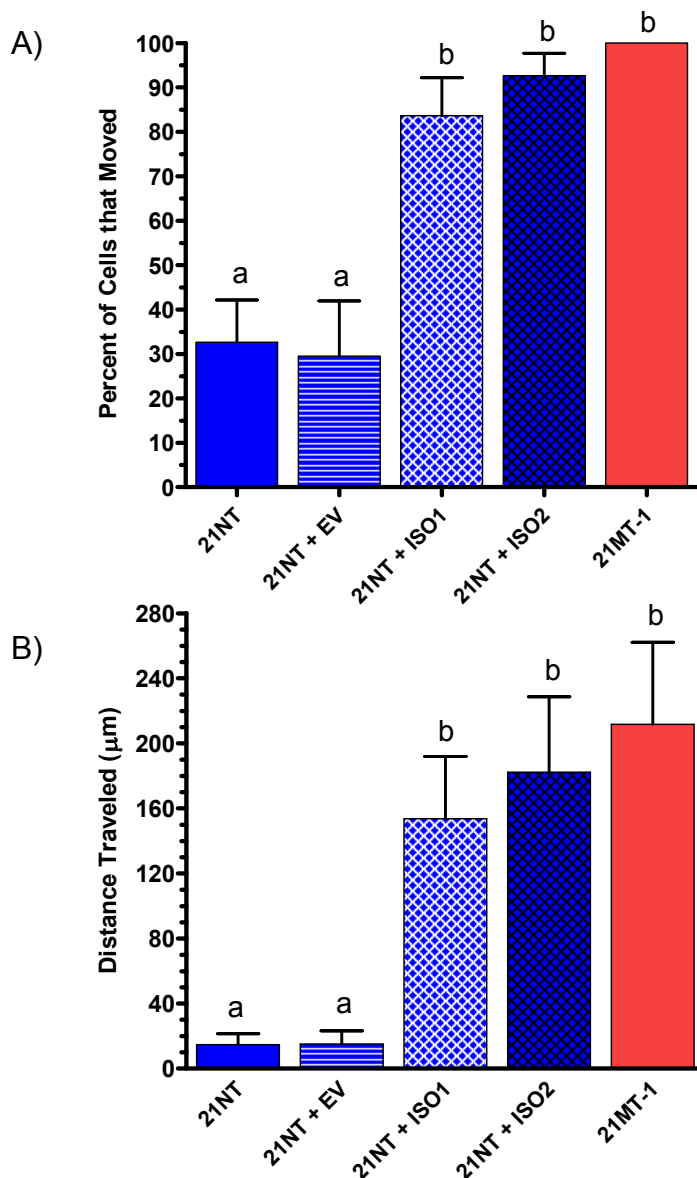


Figure 3.26. Cell invasion through Matrigel matrix for 21T and TBX3 transfected cells. Cells were grown in Matrigel for 9 days and then transferred to the incubator stage platform of a time lapse microscope until day 15. Z-stack images were taken every 12 h and all cells were followed for the entire 6-day incubation. (A) Percentage of total cells that invaded (moved) through the Matrigel matrix. A higher percentage of 21NT+TBX3 Iso1 and Iso2 cells were able to invade than 21NT or 21NT+EV cells. In fact, the percentage of TBX3 cells that were able to invade through Matrigel was not significantly different from the invasive 21MT-1 cells. Similarly, when looking at the distance (μm) moving cells are able to travel through the matrix (B), TBX3 transfected cells were able to travel as far as 21MT-1 cells and significantly further than 21NT+EV or parental 21NT cells. Bars labeled with letters that are not the same indicate significant difference between the bars at a p-value of at least <0.05 .

21NT+TBX3 Iso2 cells compared to 21NT+EV cells (Figure 3.27). Isoform 1 overexpressing cells appear to have an even greater E-cadherin reduction than the isoform 2 overexpressing cells. In contrast, vimentin is greatly increased in the TBX3 overexpressing cells compared to 21NT+EV controls (Figure 3.28). These results indicate that TBX3 may have indeed induced an EMT conversion in the overexpressing cells.

3.4. DISCUSSION

Gene expression profiling of clinical breast cancer specimens has yielded abundant differences between stages of progression (eg. [46-50]). However, this gene profiling has not elucidated which of these differently expressed genes are key players in functionally regulating the transitions through stages of breast cancer. Moreover, there are few model systems, *in vitro* or *in vivo*, that can be used to test the influence of candidate genes on human breast cancer progression. The 21T human breast epithelial cell line 3D model system of early breast cancer progression which we have previously described (Chapter 2 and [8]) has been used in the present study to functionally characterize gene targets identified as stage-specifically altered between ADH, DCIS and IMC. A major advantage of this system lies in the isogenic background of these cells, eliminating individual genetic background variability, which can cloud results when comparing across cell lines of different patient origin. A second major advantage hinges on the ability of the cells to represent specific stages of progression when grown in 3D *in vitro* culture [8]. Use of a 3D system allows us to rapidly (9-15 days) test multiple functional characteristics of candidate genes to

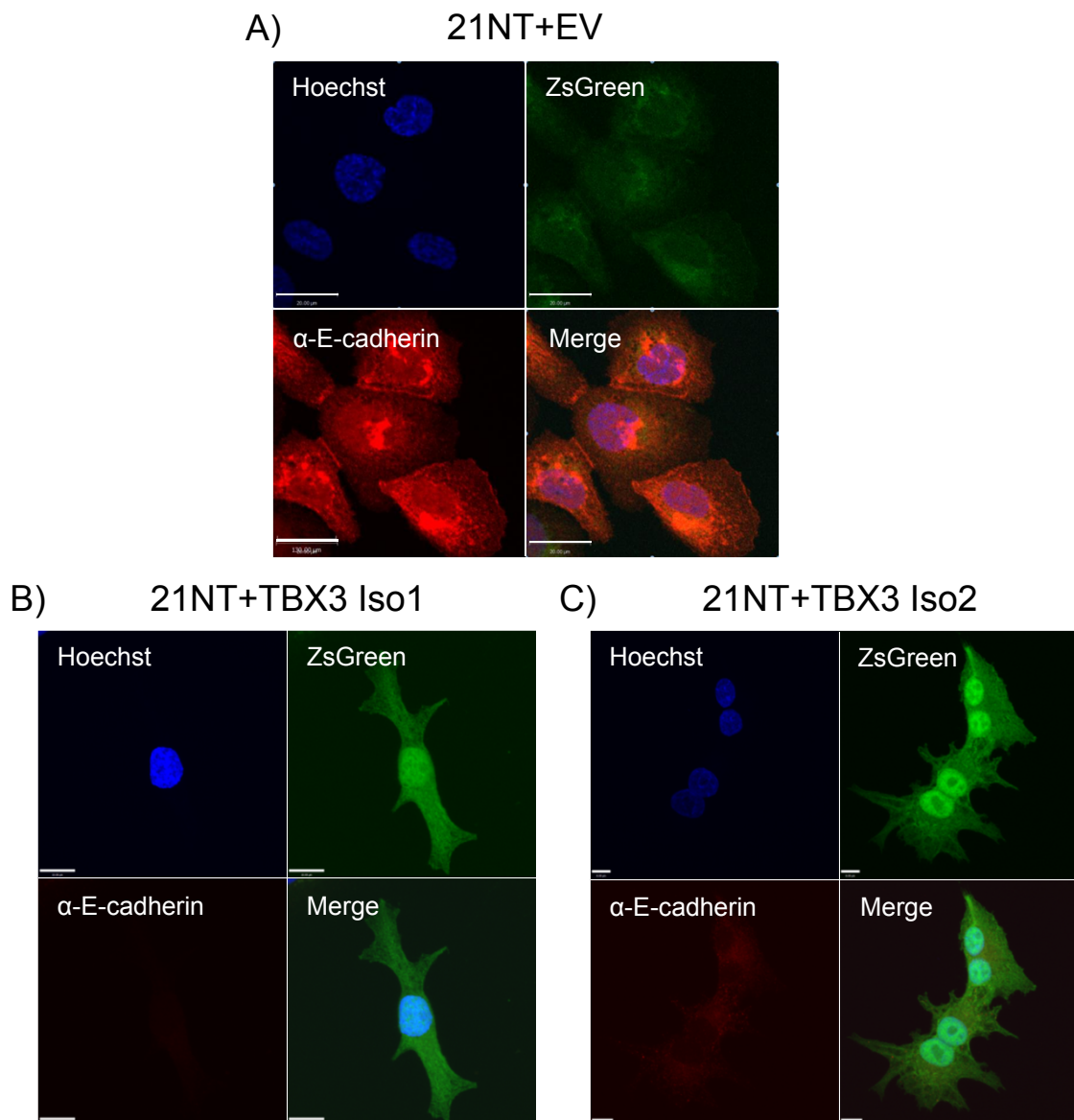


Figure 3.27. Levels of E-cadherin in TBX3-ZsGreen transfected cells using confocal microscopy. 21NT+EV (A), 21NT+TBX3 Iso1 (B) and 21NT+TBX3 Iso2 (C) cells were grown on coverslips for 24hrs. Cells were fixed and stained with an anti-E-cadherin antibody. In order to incorporate fluorescence, the secondary was conjugated to Alexa488 (red). Cells were also stained with Hoechst (blue) for nuclear detection. Both cells transfected with TBX3 Iso1 (B) and TBX3 Iso2 (C) show reduced levels of E-cadherin compared to empty vector control cells (21NT+EV; A). Scale bar represents (A) 20 μm , (B) 10 μm and (C) 8 μm .

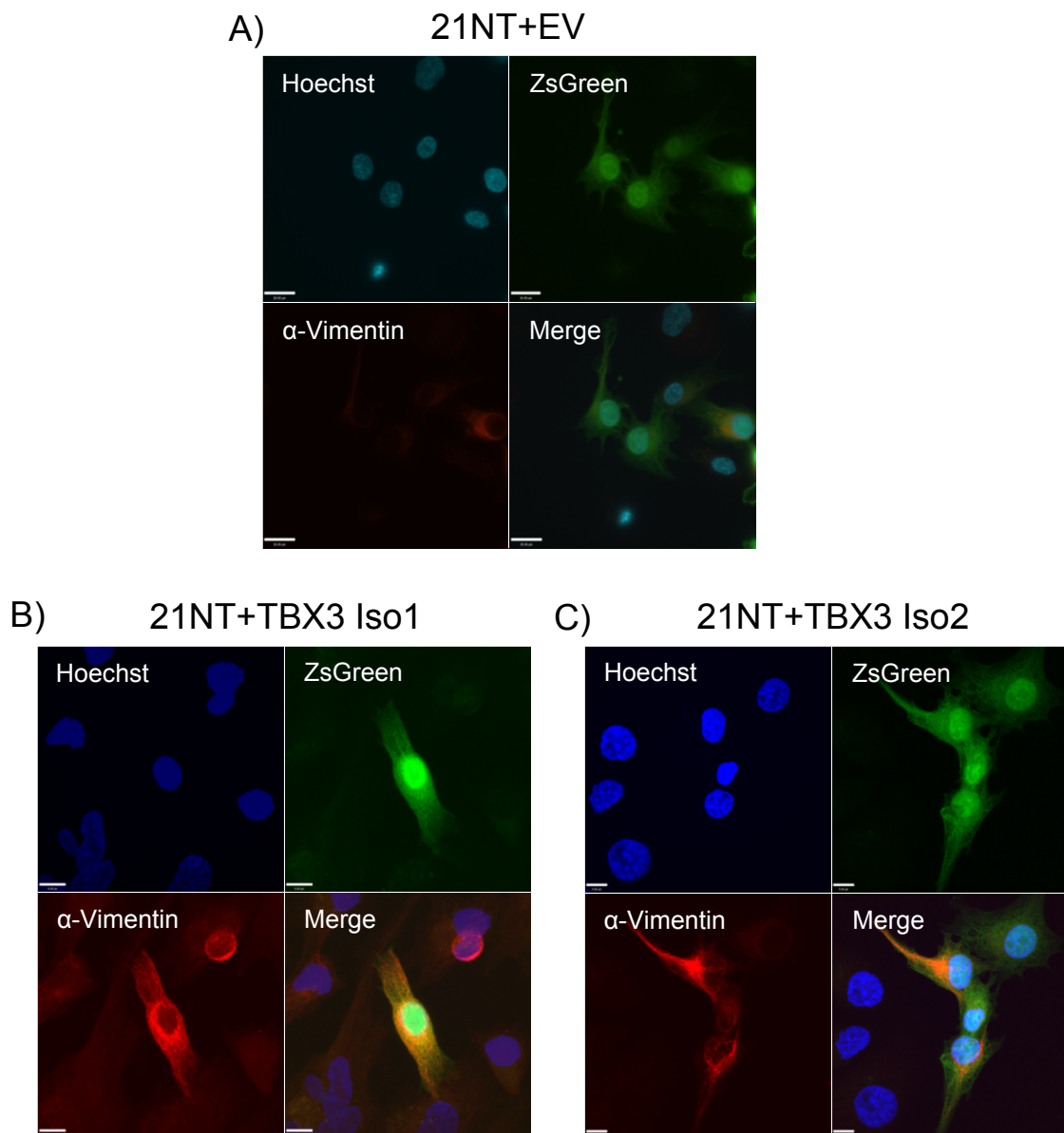


Figure 3.28. Levels of vimentin in TBX3-ZsGreen transfected cells using confocal microscopy. 21NT+EV (A), 21NT+TBX3 Iso1 (B) and 21NT+TBX3 Iso2 (C) cells were grown on coverslips for 24 hrs. Cells were fixed and stained with an anti-vimentin antibody. In order to incorporate fluorescence, the secondary was conjugated to Alexa488 (red). Cells were also stained with Hoechst (blue) for nuclear detection. Both cells transfected with TBX3 Iso1 (B) and TBX3 Iso2 (C) show increased levels of vimentin compared to empty vector control cells (21NT+EV; A). Scale bar represents (A) 20 μm and (B,C) 9 μm .

determine their role in regulating the transitions through the stages of breast cancer.

3.4.1. VANGL1 Promotes the Transition from ADH to Invasive Malignancy

VANGL1 was overexpressed in 21PT (ADH-like) cells to learn if the transfected cells would acquire attributes of a malignant (DCIS and or invasive) phenotype. We compared the 21PT+VANGL1 cells to parental 21PT (and control 21PT+EV) cells, as well 21NT cells, which represent DCIS, to determine the role of VANGL1 in this early transition. When grown in 3D Matrigel, the VANGL1 overexpressing cells appeared less organized. This was based on the cells' complete loss of the ability to form extracellular lumina and the decreased ability to form polarized cells. In fact the reduction in ability to form polarized cells was decreased beyond even that of the 21MT-1 cells, which are invasive and actually represent IMC when grown in 3D culture and *in vivo*. The VANGL1 overexpressing cells also had a greatly reduced ability to form spherical colonies compared to the parental 21PT cells (even more reduced than for the 21MT-1 cells) and showed an increased percentage of single cells. These features would suggest that VANGL1 overexpressing cells did acquire characteristics of malignancy, that were at least progressed to the point of a DCIS-like (21NT-like) phenotype, and for some features suggestive of an invasive (21MT-1-like) phenotype. This increased invasive ability was substantiated by the invasion assay, which showed that the VANGL1 overexpressing cells were indeed more invasive than 21NT cells. Proliferation rate, as visualized by immunohistochemical staining with Ki67, demonstrated that VANGL1

overexpressing 21PT cells had a greatly increased rate of cell growth compared to the 21PT parental line, the 21PT+EV control cells and the 21NT line. In fact this increase in proliferation was past the levels observed for 21MT-1 cells in other experiments (see Figure 3.17 and 3.24 for documented rates). However, the apoptosis rate for VANGL1 transfected 21PT cells was also increased, but only to levels usual for 21NT cells. When we calculated a ratio of proliferating over apoptosing cells, we saw that the ratio for VANGL1 overexpressing cells was much higher than for 21PT, 21PT+EV or 21NT cells, indicating that the VANGL1 overexpressing cells have a growth advantage.

The characteristics of invasive ability seen with the VANGL1 overexpressing cells may be a result of the ability of VANGL1 to negatively interact with the metastasis suppressing actions of its binding partner, KAI1. Previous studies have shown that VANGL1 increases metastatic ability through its interaction with KAI1 [10, 11]. Additionally, the role of VANGL1 in the PCP (planar cell polarity) pathway may elucidate the reason we see progression past DCIS (21NT cells) with VANGL1 overexpressing cells. The role of the PCP pathway in cancer development is controversial. Previously it has been shown that the canonical Wnt/ β -catenin pathway is upregulated in tumourigenesis and that there is antagonism between canonical Wnt signalling and noncanonical Wnt signalling, leading to a belief that PCP signalling should suppress tumourigenesis [51]. Moreover, Wnt5a, a noncanonical Wnt, is downregulated in many types of cancer [52-56] and a tumour suppressing role for Wnt5a, as an antagonist of Wnt/ β -catenin signalling has evolved [15]. However, in other studies, especially in cancer of advanced stage, Wnt5a is upregulated and associated with invasion,

metastasis and angiogenesis [15, 57-59]. From this, a new theory involving a biphasic role for the PCP pathway has emerged [15]. It was theorized that at early stages activated Wnt/ β -catenin signalling is involved in the transformation from normal cells to neoplastic ones, while PCP signalling, which is often mediated by Wnt5a, inhibits progression by antagonizing Wnt/ β -catenin signalling. However, tumours are still able to develop by escaping the inhibition of PCP signalling, either by downregulation of PCP signalling or upregulation of downstream effectors of canonical Wnt signalling. As the tumour progresses, the role of PCP signalling becomes altered to promote migration and invasion and support angiogenesis, which all contribute to metastasis in advanced stage cancers [15]. As was mentioned previously, the binding of non-canonical Wnt molecules, such as Wnt5a, to the Fzd receptor, activates the PCP pathway [15]. Interestingly, we previously found that Wnt5a mRNA is moderately high in 21PT, low in 21NT and very high in 21MT-1 (see real-time validation in Chapter 2 (Table 2.3) and [8]). Hence the theory of a dual role for the PCP pathway fits with the 21T model system. At early stages of progression VANGL1 is low even though Wnt5a is slightly elevated, potentially resulting in low PCP signalling and reduced antagonism of Wnt/ β -catenin signalling. By the stage of DCIS, VANGL1 is increased, potentially resulting in increased PCP signalling (which may require VANGL1). Finally, in IMC, Wnt5a levels increase (with further activation of the PCP pathway), while VANGL1 remains elevated. Thus, the effects of a non-canonical pathway signal (such as that from Wnt5a) may differ depending on whether or not the cells are expressing VANGL1 (tumour suppressing in the absence of VANGL1, promoting of malignancy in the presence of VANGL1).

These results also suggest that the increased expression of VANGL1 promotes progression to both *in situ* and invasive mammary carcinoma.

3.4.2. S100A2 Inhibits the Transition to an Invasive Phenotype

S100A2 was knocked-down in 21NT (DCIS-like) cells to determine if the transfected cells would undergo a transition to a more invasive phenotype. We compared the 21NT+shS100A2 cells to 21NT, 21NT+EV and 21MT-1 (IMC-like) cells, to evaluate the role of S100A2 in this later transition. When cultured in 3D Matrigel, the S100A2 knockdown cells showed a more disorganized pattern of growth than both 21NT (and 21NT+EV) and 21MT-1 cells, with complete loss of the ability to form extracellular lumina and a lack of cell polarization. In terms of spherical colonies formed and presence of single cells, the S100A2 knockdown 21NT cells showed levels altered from that of the parental DCIS-like 21NT (or 21NT+EV) cells and similar to the levels of IMC-like, 21MT-1 cells. The 3D invasive characteristics of S100A2 knockdown cells were directly assessed by invasion assay using time lapse microscopy. Not only were 100% of S100A2 knockdown 21NT cells able to invade through Matrigel, but these cells were also able to travel as far through Matrigel as 21MT-1 cells. Immunohistochemical staining for Ki67 (proliferation) and caspase 3 (apoptosis), performed on Matrigel plugs, showed that the proliferation rate of S100A2 knockdown cells was increased over both 21NT (and 21NT+EV) and 21MT-1 cells, while the apoptosis rate for the transfected cells did not differ from the 21NT parental cells or 21NT+EV control cells. When we calculated a ratio of proliferation to apoptosis

we found that the growth profile of the S100A2 knockdown cells matched that of 21MT-1 cells.

Previous studies have theorized that the tumour suppressing ability of S100A2 is a direct consequence of its ability to block Cox-2 [27]. Since in the present study, we are knocking down S100A2, the enhanced cell motility, invasiveness, and proliferation effects associated with Cox-2 activity [28, 29] should be present and we do see these characteristics in the S100A2 knockdown cells. However, the mRNA expression of Cox-2 is not significantly higher in 21MT-1 cells compared to 21NT cells [8]. Thus, at least for the 21T model system of early breast cancer progression, S100A2 may be enhancing the invasiveness characteristics via a Cox-2-independent pathway.

A possible alternative mechanism of S100A2 effects is via regulation of RUNX3. The 21T microarray analysis (Chapter 2 and [8]) has shown that there is decreased RUNX3 in 21MT-1 cells. RUNX3 signals downstream in the TGF β pathway, which has been shown to play a complex role in breast cancer. It has been demonstrated that during early breast tumour outgrowth, elevated TGF β is tumour suppressive, while at later stages there is a switch towards induction of malignancy and progression [60-62]. Since previous literature has indicated that S100A2 can induce RUNX3 [23] and as there are reduced levels of S100A2 in 21MT-1 cells, it is possible that the tumour suppressing abilities of RUNX3 [24], and consequently TGF β signalling are inhibited due to loss of S100A2.

Similarly, previous literature has shown that S100A2 represses NF κ B2 [23], and we have previously shown that 21MT-1 cells have increased NF κ B2 (Chapter 2 and [8]). It may be then that low levels of S100A2 in 21MT-1 cells

result in a lack of repression and overactivity of NFkB2, perhaps resulting in NFkB2 being able to exert its oncogenic control over apoptosis, cell cycle, migration and differentiation [26]. The lack of apoptosis alteration in S100A2 knockdown cells was surprising, considering S100A2 is thought to stimulate p53 activity [22]. However, the 21T series cells do all have a p53 mutation [63], which may have altered the sensitivity of the p53 pathway to S100A2 effects.

3.4.3. *TBX3 Promotes the Transition to an Invasive Phenotype*

We transfected constitutive expression vectors of both isoforms of TBX3 into 21NT (DCIS-like) cells to determine if the transfected cells would acquire attributes of an invasive phenotype. We compared the 21NT+TBX3 Iso1 and 21NT+TBX3 Iso2 cells to both 21NT+EV (and 21NT) cells and invasive 21MT-1 cells, to determine the role of TBX3 in this stage of progression (from *in situ* to invasive disease). Western blotting with a combination of a monoclonal mouse antibody against TBX3 and a polyclonal rabbit antibody against ZsGreen was able to resolve protein banding indicating that 21NT transfectants did indeed express the TBX3-ZsGreen fusion protein. Due to the design of the TBX3 expression vector, the empty vector control cells (21NT+EV) were able to produce ZsGreen. Western blotting of the control cells with the ZsGreen antibody resolved a protein band at 60 kDa, which is three times larger than the expected 20 kDa size of ZsGreen. It is believed that since this Western blot was performed under non-denaturing and non-reducing conditions that the 60 kDa product was a ZsGreen trimeric complex. As further evidence that 21NT transfectants expressed the TBX3-ZsGreen fusion protein, PCR primers, which

distinguished between endogenous TBX3 and the fusion protein were designed and the PCR results indicated that transfected cells of both TBX3 variant-ZsGreen fusion constructs had increased mRNA expression of the fusion TBX3-ZsGreen protein. Further analysis using confocal microscopy and the TBX3 antibody, as well as ZsGreen signal, showed that the transfected cells had increased TBX3 and that much of the TBX3 signal colocalized with ZsGreen signal. These three experiments determined that the transfected TBX3 overexpressing cells did have increased TBX3. Although TBX3 overexpressing cells were transfected with isoform specific TBX3 fused to ZsGreen, an increase in endogenous TBX3 observed by qPCR and Western blotting reveals that TBX3 transgene expression can induce increased endogenous TBX3 expression in 21NT cells. We theorize that TBX3 works in a feed forward manner such that increased TBX3 leads to induction of TBX3 transcription. This induction appears to not be specific for either isoform, as overexpression of one isoform leads to transcriptional induction of both isoforms, with the specific overexpressed isoform being induced at a higher level than the alternate isoform.

When grown in 3D Matrigel, 21NT cells overexpressing both TBX3 isoforms appeared more disorganized, based on the cells' reduced ability to form extracellular lumina and polarized groups, compared to either the empty vector 21NT control cells, or 21MT-1 cells. In addition, in 21NT cells transfected with both TBX3 isoforms, several very large, highly disorganized and irregular shaped cell aggregates were seen in 3D Matrigel colonies. Both TBX3 overexpressing cell lines had reduced ability to form spherical colonies, similar to 21MT-1 cells. Also similar to 21MT-1 levels, TBX3 Iso1 and TBX3 Iso2 overexpressing cells

had a higher percentage of single cells present in the Matrigel plugs than 21NT cells. Since the TBX3 overexpressing cells acquired 3D colony morphologies more closely related to 21MT-1 cells than 21NT cells, it appeared that both isoforms of TBX3 were able to drive transfected 21NT cells to an invasive phenotype. This was directly confirmed by invasion assay in 3D Matrigel using time lapse microscopy. A large proportion of TBX3 Iso1 and TBX3 Iso2 overexpressing cells were able to invade through Matrigel. In addition, these invading cells were able to travel as far through Matrigel as 21MT-1 cells. When we examined proliferation and apoptosis rates of the TBX3 overexpressing cells, we found that the proliferation rate of both TBX3 isoform transfectants was greatly increased over 21NT+EV and 21MT-1 cells. Interestingly, in the large irregular cell aggregates, that were previously mentioned, more than 90% of the cells stained positive for Ki67. The apoptosis rates for the TBX3 overexpressing cells were not significantly different from the parental 21NT cells or 21NT+EV control cells. Not surprisingly, when we calculated a ratio of proliferation over apoptosis, the ratio for both isoforms of TBX3 overexpressing cells was much higher than for 21NT+EV and 21MT-1 cells, indicating that the TBX3 overexpressing cells have a growth advantage.

In apparent agreement with the study by Hoogaars and colleagues [43], we have found that transfection of both isoforms of TBX3 show similar functional effects, inducing an invasive phenotype. However, in our work, transfection of one TBX3 isoform did result in low level increase in expression of the alternate isoform, such that functional effects seen could have been the result of some combination of the two. Previous studies have determined that TBX3 achieves

senescence bypass through both p53-dependent and independent pathways [35, 37]. The p53-dependent pathway signals through p14 (ARF), which is repressed by TBX3 [35]. Interestingly, regarding the 21T microarray data from Chapter 2, that we have previously published [8], we did not see a decrease in p14 (ARF) in 21MT-1 cells (compared to 21NT cells) represented on our list of genes with significantly altered expression (Supplemental Table 2). However, upon examination of the raw microarray data, we have found that p14 (ARF) mRNA was reduced 1.4-fold in the 21MT-1 cells, compared to 21NT cells, just missing our 1.5-fold changed cut off, such that whether or not TBX3 may be acting functionally through repression of p14 (ARF) in these cells requires further investigation. TBX3-induced invasiveness may also be a result of its ability to repress E-cadherin, which has been shown in the past [39] and in the present study.

The present study builds on the limited evidence that there is a potential role of TBX3 in EMT [39]. EMT is a process by which epithelial cells alter their phenotype and acquire mesenchymal-like properties, through disruption of intercellular adhesion, leading to enhancement of cell motility [64]. Mesenchymal cells, in contrast to epithelial cells, have the ability to migrate as individual cells, thus the aim of this phenotype modulation is to grant the otherwise stationary epithelial cells the ability to break away from the primary site, penetrate into surrounding tissues and move to distant sites [65, 66]. *In vitro* functional markers for EMT include increased migration, invasion, scattering and elongation of cell shape [64], all of which we see for the TBX3 overexpressing cells. In addition, it has been well documented that cells that have undergone EMT have decreased

E-cadherin, as well as increased vimentin [64], both of which we also see in the TBX3 overexpressing cells (both isoforms). These findings indicate that TBX3 may induce EMT. A more thorough analysis looking at other markers of EMT, including increased fibronectin, snail1, snail2 (slug) and accumulation of β -catenin in the nucleus, would further this theory.

3.4.4. Genes Identified by the 21T Series Model System are Involved in Controlling the Transitions Between Stages of Progression

The present study has made use of the 21T human breast epithelial cell line 3D model system to functional characterize genes previously identified as altered between stages of early breast cancer progression [8]. We determined that VANGL1 drives cells towards a more malignant and a more invasive phenotype and promotes the transition from ADH through DCIS to IMC (Figure 3.29). Loss of S100A2, as well as elevated TBX3 promotes invasive characteristics and promotes the transition from DCIS to IMC (Figure 3.29). The 21T 3D model system is thus a powerful tool that not only is able to identify targets with potential significance in breast cancer progression, but also provides a rapid and manipulatable system to test the functional characteristics of the targets.

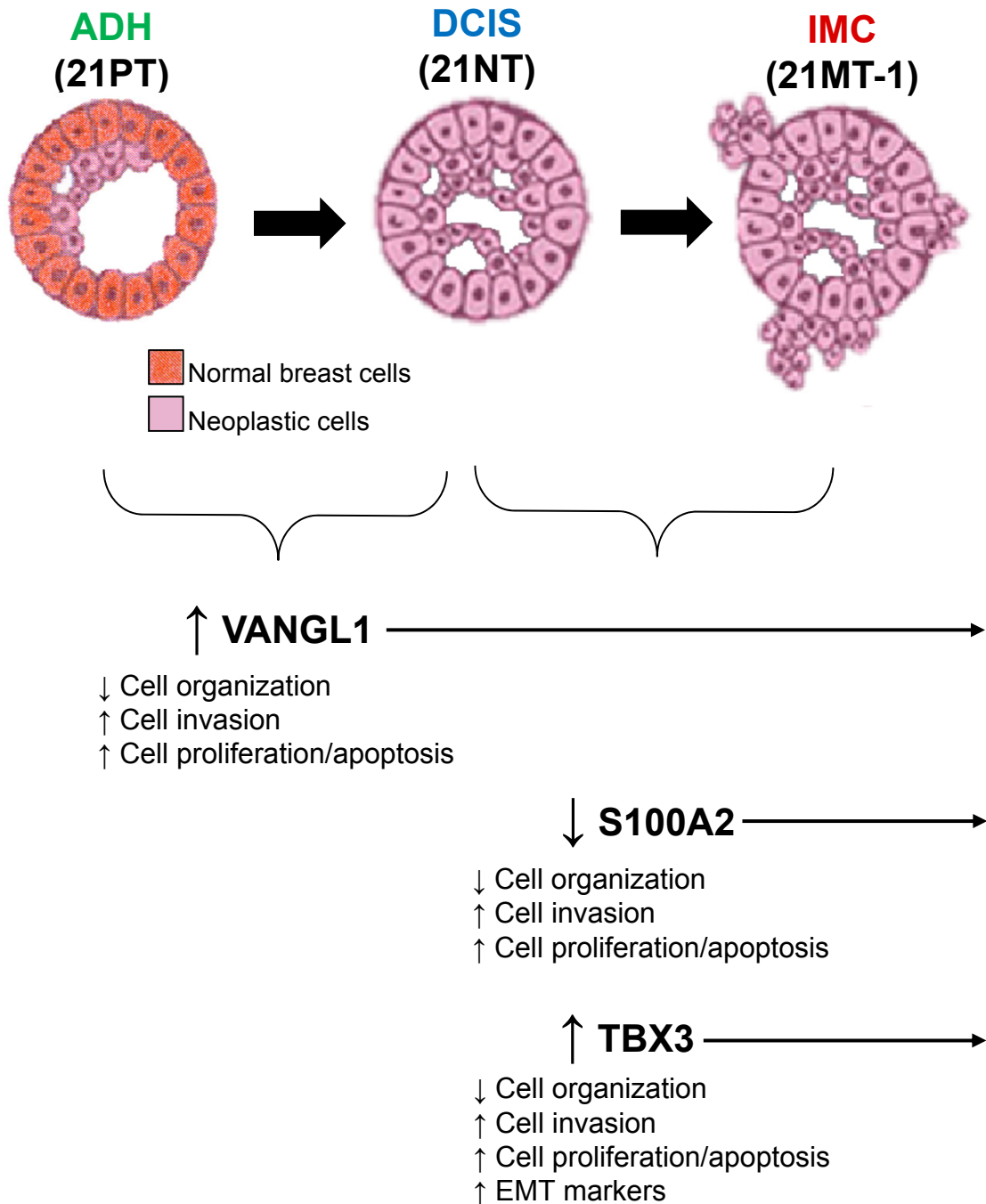


Figure 3.29. The roles of VANGL1, S100A2 and TBX3 in early breast cancer progression. VANGL1 drives cells towards a more malignant and a more invasive phenotype and promotes the transition from ADH through DCIS and in some respects to IMC. Loss of S100A2 promotes invasive characteristics and the transition from DCIS to IMC. Similarly, TBX3 (both isoforms) promotes characteristics of invasiveness and the transition from DCIS to IMC.

3.5. REFERENCES

1. Tang P, Hajdu SI, Lyman GH: **Ductal carcinoma in situ: a review of recent advances.** Curr Opin Obstet Gynecol 2007, **19**(1):63-67.
2. Arpino G, Laucirica R, Elledge RM: **Premalignant and in situ breast disease: biology and clinical implications.** Ann Intern Med 2005, **143**(6):446-457.
3. Bodian CA, Perzin KH, Lattes R, Hoffmann P: **Reproducibility and validity of pathologic classifications of benign breast disease and implications for clinical applications.** Cancer 1993, **71**(12):3908-3913.
4. Carter CL, Corle DK, Micozzi MS, Schatzkin A, Taylor PR: **A prospective study of the development of breast cancer in 16,692 women with benign breast disease.** Am J Epidemiol 1988, **128**(3):467-477.
5. Dupont WD, Parl FF, Hartmann WH, Brinton LA, Winfield AC, Worrell JA, Schuyler PA, Plummer WD: **Breast cancer risk associated with proliferative breast disease and atypical hyperplasia.** Cancer 1993, **71**(4):1258-1265.
6. Allred DC, Wu Y, Mao S, Nagtegaal ID, Lee S, Perou CM, Mohsin SK, O'Connell P, Tsimelzon A, Medina D: **Ductal carcinoma in situ and the emergence of diversity during breast cancer evolution.** Clin Cancer Res 2008, **14**(2):370-378.
7. Allred DC, Mohsin SK, Fuqua SA: **Histological and biological evolution of human premalignant breast disease.** Endocr Relat Cancer 2001, **8**(1):47-61.
8. Souter LH, Andrews JD, Zhang G, Cook AC, Postenka CO, Al-Katib W, Leong HS, Rodenhiser DI, Chambers AF, Tuck AB: **Human 21T breast epithelial cell lines mimic breast cancer progression in vivo and in vitro and show stage-specific gene expression patterns.** Lab Invest 2010, **90**(8):1247-1258.
9. Band V, Zajchowski D, Swisshelm K, Trask D, Kulesa V, Cohen C, Connolly J, Sager R: **Tumor progression in four mammary epithelial cell lines derived from the same patient.** Cancer Res 1990, **50**(22):7351-7357.
10. Lee JH, Park SR, Chay KO, Seo YW, Kook H, Ahn KY, Kim YJ, Kim KK: **KAI1 COOH-terminal interacting tetraspanin (KITENIN), a member of the tetraspanin family, interacts with KAI1, a tumor metastasis suppressor, and enhances metastasis of cancer.** Cancer Res 2004, **64**(12):4235-4243.

11. Lee JK, Bae JA, Sun EG, Kim HD, Yoon TM, Kim K, Lee JH, Lim SC, Kim KK: **KITENIN increases invasion and migration of mouse squamous cancer cells and promotes pulmonary metastasis in a mouse squamous tumor model.** FEBS Lett 2009, **583**(4):711-717.
12. Lee JK, Yoon TM, Seo DJ, Sun EG, Bae JA, Lim SC, Choi YD, Lee JH, Joo YE, Kim KK: **KAI1 COOH-terminal interacting tetraspanin (KITENIN) expression in early and advanced laryngeal cancer.** Laryngoscope 2010, **120**(5):953-958.
13. Lee JH, Cho ES, Kim MY, Seo YW, Kho DH, Chung IJ, Kook H, Kim NS, Ahn KY, Kim KK: **Suppression of progression and metastasis of established colon tumors in mice by intravenous delivery of short interfering RNA targeting KITENIN, a metastasis-enhancing protein.** Cancer Res 2005, **65**(19):8993-9003.
14. Miranti CK: **Controlling cell surface dynamics and signaling: how CD82/KAI1 suppresses metastasis.** Cell Signal 2009, **21**(2):196-211.
15. Wang Y: **Wnt/Planar cell polarity signaling: a new paradigm for cancer therapy.** Mol Cancer Ther 2009, **8**(8):2103-2109.
16. Kho DH, Bae JA, Lee JH, Cho HJ, Cho SH, Lee JH, Seo YW, Ahn KY, Chung IJ, Kim KK: **KITENIN recruits Dishevelled/PKC delta to form a functional complex and controls the migration and invasiveness of colorectal cancer cells.** Gut 2009, **58**(4):509-519.
17. Ryu HS, Park YL, Park SJ, Lee JH, Cho SB, Lee WS, Chung IJ, Kim KK, Lee KH, Kweon SS, Joo YE: **KITENIN is associated with tumor progression in human gastric cancer.** Anticancer Res 2010, **30**(9):3479-3486.
18. Katoh M, Katoh M: **Comparative integromics on non-canonical WNT or planar cell polarity signaling molecules: transcriptional mechanism of PTK7 in colorectal cancer and that of SEMA6A in undifferentiated ES cells.** Int J Mol Med 2007, **20**(3):405-409.
19. Formstone CJ, Mason I: **Expression of the Celsr/flamingo homologue, c-fmi1, in the early avian embryo indicates a conserved role in neural tube closure and additional roles in asymmetry and somitogenesis.** Dev Dyn 2005, **232**(2):408-413.
20. Curtin JA, Quint E, Tsipouri V, Arkell RM, Cattanach B, Copp AJ, Henderson DJ, Spurr N, Stanier P, Fisher EM, Nolan PM, Steel KP, Brown SD, Gray IC, Murdoch JN: **Mutation of Celsr1 disrupts planar polarity of inner ear hair cells and causes severe neural tube defects in the mouse.** Curr Biol 2003, **13**(13):1129-1133.

21. Salama I, Malone PS, Mihaimeed F, Jones JL: **A review of the S100 proteins in cancer.** *Eur J Surg Oncol* 2008, **34**(4):357-364.
22. van Dieck J, Teufel DP, Jaulent AM, Fernandez-Fernandez MR, Rutherford TJ, Wyslouch-Cieszynska A, Fersht AR: **Posttranslational modifications affect the interaction of S100 proteins with tumor suppressor p53.** *J Mol Biol* 2009, **394**(5):922-930.
23. Matsubara D, Niki T, Ishikawa S, Goto A, Ohara E, Yokomizo T, Heizmann CW, Aburatani H, Moriyama S, Moriyama H, Nishimura Y, Funata N, Fukayama M: **Differential expression of S100A2 and S100A4 in lung adenocarcinomas: clinicopathological significance, relationship to p53 and identification of their target genes.** *Cancer Sci* 2005, **96**(12):844-857.
24. Lee CW, Ito K, Ito Y: **Role of RUNX3 in bone morphogenetic protein signaling in colorectal cancer.** *Cancer Res* 2010, **70**(10):4243-4252.
25. Grandis JR, Sok JC: **Signaling through the epidermal growth factor receptor during the development of malignancy.** *Pharmacol Ther* 2004, **102**(1):37-46.
26. Orłowski RZ, Baldwin AS, Jr: **NF-kappaB as a therapeutic target in cancer.** *Trends Mol Med* 2002, **8**(8):385-389.
27. Tsai WC, Tsai ST, Jin YT, Wu LW: **Cyclooxygenase-2 is involved in S100A2-mediated tumor suppression in squamous cell carcinoma.** *Mol Cancer Res* 2006, **4**(8):539-547.
28. Singh B, Berry JA, Shoher A, Ramakrishnan V, Lucci A: **COX-2 overexpression increases motility and invasion of breast cancer cells.** *Int J Oncol* 2005, **26**(5):1393-1399.
29. Abrahao AC, Castilho RM, Squarize CH, Molinolo AA, dos Santos-Pinto D, Jr, Gutkind JS: **A role for COX2-derived PGE2 and PGE2-receptor subtypes in head and neck squamous carcinoma cell proliferation.** *Oral Oncol* 2010, **46**(12):880-887.
30. Wicki R, Franz C, Scholl FA, Heizmann CW, Schafer BW: **Repression of the candidate tumor suppressor gene S100A2 in breast cancer is mediated by site-specific hypermethylation.** *Cell Calcium* 1997, **22**(4):243-254.
31. Liu D, Rudland PS, Sibson DR, Platt-Higgins A, Barraclough R: **Expression of calcium-binding protein S100A2 in breast lesions.** *Br J Cancer* 2000, **83**(11):1473-1479.

32. Rowley M, Grothey E, Couch FJ: **The role of Tbx2 and Tbx3 in mammary development and tumorigenesis.** J Mammary Gland Biol Neoplasia 2004, **9**(2):109-118.
33. Eblaghie MC, Song SJ, Kim JY, Akita K, Tickle C, Jung HS: **Interactions between FGF and Wnt signals and Tbx3 gene expression in mammary gland initiation in mouse embryos.** J Anat 2004, **205**(1):1-13.
34. Bamshad M, Le T, Watkins WS, Dixon ME, Kramer BE, Roeder AD, Carey JC, Root S, Schinzel A, Van Maldergem L, Gardner RJ, Lin RC, Seidman CE, Seidman JG, Wallerstein R, Moran E, Sutphen R, Campbell CE, Jorde LB: **The spectrum of mutations in TBX3: Genotype/Phenotype relationship in ulnar-mammary syndrome.** Am J Hum Genet 1999, **64**(6):1550-1562.
35. Brummelkamp TR, Kortlever RM, Lingbeek M, Trettel F, MacDonald ME, van Lohuizen M, Bernards R: **TBX-3, the gene mutated in Ulnar-Mammary Syndrome, is a negative regulator of p19ARF and inhibits senescence.** J Biol Chem 2002, **277**(8):6567-6572.
36. Brummelkamp TR, Kortlever RM, Lingbeek M, Trettel F, MacDonald ME, van Lohuizen M, Bernards R: **TBX-3, the gene mutated in Ulnar-Mammary Syndrome, is a negative regulator of p19ARF and inhibits senescence.** J Biol Chem 2002, **277**(8):6567-6572.
37. Carlson H, Ota S, Song Y, Chen Y, Hurlin PJ: **Tbx3 impinges on the p53 pathway to suppress apoptosis, facilitate cell transformation and block myogenic differentiation.** Oncogene 2002, **21**(24):3827-3835.
38. Yarosh W, Barrientos T, Esmailpour T, Lin L, Carpenter PM, Osann K, Anton-Culver H, Huang T: **TBX3 is overexpressed in breast cancer and represses p14 ARF by interacting with histone deacetylases.** Cancer Res 2008, **68**(3):693-699.
39. Rodriguez M, Aladowicz E, Lanfrancone L, Goding CR: **Tbx3 represses E-cadherin expression and enhances melanoma invasiveness.** Cancer Res 2008, **68**(19):7872-7881.
40. Renard CA, Labalette C, Armengol C, Cougot D, Wei Y, Cairo S, Pineau P, Neuveut C, de Reynies A, Dejean A, Perret C, Buendia MA: **Tbx3 is a downstream target of the Wnt/beta-catenin pathway and a critical mediator of beta-catenin survival functions in liver cancer.** Cancer Res 2007, **67**(3):901-910.
41. Han J, Yuan P, Yang H, Zhang J, Soh BS, Li P, Lim SL, Cao S, Tay J, Orlov YL, Lufkin T, Ng HH, Tam WL, Lim B: **Tbx3 improves the germ-line competency of induced pluripotent stem cells.** Nature 2010, **463**(7284):1096-1100.

42. Fan W, Huang X, Chen C, Gray J, Huang T: **TBX3 and its isoform TBX3+2a are functionally distinctive in inhibition of senescence and are overexpressed in a subset of breast cancer cell lines.** *Cancer Res* 2004, **64**(15):5132-5139.
43. Hoogaars WM, Barnett P, Rodriguez M, Clout DE, Moorman AF, Goding CR, Christoffels VM: **TBX3 and its splice variant TBX3 + exon 2a are functionally similar.** *Pigment Cell Melanoma Res* 2008, **21**(3):379-387.
44. Silva JM, Li MZ, Chang K, Ge W, Golding MC, Rickles RJ, Siolas D, Hu G, Paddison PJ, Schlabach MR, Sheth N, Bradshaw J, Burchard J, Kulkarni A, Cavet G, Sachidanandam R, McCombie WR, Cleary MA, Elledge SJ, Hannon GJ: **Second-generation shRNA libraries covering the mouse and human genomes.** *Nat Genet* 2005, **37**(11):1281-1288.
45. Luzzi KJ, MacDonald IC, Schmidt EE, Kerkvliet N, Morris VL, Chambers AF, Groom AC: **Multistep nature of metastatic inefficiency: dormancy of solitary cells after successful extravasation and limited survival of early micrometastases.** *Am J Pathol* 1998, **153**(3):865-873.
46. Ma XJ, Salunga R, Tuggle JT, Gaudet J, Enright E, McQuary P, Payette T, Pistone M, Stecker K, Zhang BM, Zhou YX, Varnholt H, Smith B, Gadd M, Chatfield E, Kessler J, Baer TM, Erlander MG, Sgroi DC: **Gene expression profiles of human breast cancer progression.** *Proc Natl Acad Sci U S A* 2003, **100**(10):5974-5979.
47. Abba MC, Drake JA, Hawkins KA, Hu Y, Sun H, Notcovich C, Gaddis S, Sahin A, Baggerly K, Aldaz CM: **Transcriptomic changes in human breast cancer progression as determined by serial analysis of gene expression.** *Breast Cancer Res* 2004, **6**(5):R499-513.
48. Schuetz CS, Bonin M, Clare SE, Nieselt K, Sotlar K, Walter M, Fehm T, Solomayer E, Riess O, Wallwiener D, Kurek R, Neubauer HJ: **Progression-specific genes identified by expression profiling of matched ductal carcinomas in situ and invasive breast tumors, combining laser capture microdissection and oligonucleotide microarray analysis.** *Cancer Res* 2006, **66**(10):5278-5286.
49. Nishidate T, Katagiri T, Lin ML, Mano Y, Miki Y, Kasumi F, Yoshimoto M, Tsunoda T, Hirata K, Nakamura Y: **Genome-wide gene-expression profiles of breast-cancer cells purified with laser microbeam microdissection: identification of genes associated with progression and metastasis.** *Int J Oncol* 2004, **25**(4):797-819.
50. Milovanovic T, Planutis K, Nguyen A, Marsh JL, Lin F, Hope C, Holcombe RF: **Expression of Wnt genes and frizzled 1 and 2 receptors in normal breast**

- epithelium and infiltrating breast carcinoma.** *Int J Oncol* 2004, **25**(5):1337-1342.
51. Veeman MT, Axelrod JD, Moon RT: **A second canon. Functions and mechanisms of beta-catenin-independent Wnt signaling.** *Dev Cell* 2003, **5**(3):367-377.
52. Liang H, Chen Q, Coles AH, Anderson SJ, Pihan G, Bradley A, Gerstein R, Jurecic R, Jones SN: **Wnt5a inhibits B cell proliferation and functions as a tumor suppressor in hematopoietic tissue.** *Cancer Cell* 2003, **4**(5):349-360.
53. Kremenevskaja N, von Wasielewski R, Rao AS, Schofl C, Andersson T, Brabant G: **Wnt-5a has tumor suppressor activity in thyroid carcinoma.** *Oncogene* 2005, **24**(13):2144-2154.
54. Leris AC, Roberts TR, Jiang WG, Newbold RF, Mokbel K: **WNT5A expression in human breast cancer.** *Anticancer Res* 2005, **25**(2A):731-734.
55. Liu XH, Pan MH, Lu ZF, Wu B, Rao Q, Zhou ZY, Zhou XJ: **Expression of Wnt-5a and its clinicopathological significance in hepatocellular carcinoma.** *Dig Liver Dis* 2008, **40**(7):560-567.
56. Ying J, Li H, Yu J, Ng KM, Poon FF, Wong SC, Chan AT, Sung JJ, Tao Q: **WNT5A exhibits tumor-suppressive activity through antagonizing the Wnt/beta-catenin signaling, and is frequently methylated in colorectal cancer.** *Clin Cancer Res* 2008, **14**(1):55-61.
57. Weeraratna AT, Jiang Y, Hostetter G, Rosenblatt K, Duray P, Bittner M, Trent JM: **Wnt5a signaling directly affects cell motility and invasion of metastatic melanoma.** *Cancer Cell* 2002, **1**(3):279-288.
58. Kurayoshi M, Oue N, Yamamoto H, Kishida M, Inoue A, Asahara T, Yasui W, Kikuchi A: **Expression of Wnt-5a is correlated with aggressiveness of gastric cancer by stimulating cell migration and invasion.** *Cancer Res* 2006, **66**(21):10439-10448.
59. Pukrop T, Klemm F, Hagemann T, Gradl D, Schulz M, Siemes S, Trumper L, Binder C: **Wnt 5a signaling is critical for macrophage-induced invasion of breast cancer cell lines.** *Proc Natl Acad Sci U S A* 2006, **103**(14):5454-5459.
60. Silberstein GB, Daniel CW: **Reversible inhibition of mammary gland growth by transforming growth factor-beta.** *Science* 1987, **237**(4812):291-293.

61. Siegel PM, Shu W, Cardiff RD, Muller WJ, Massague J: **Transforming growth factor beta signaling impairs Neu-induced mammary tumorigenesis while promoting pulmonary metastasis.** Proc Natl Acad Sci U S A 2003, **100**(14):8430-8435.
62. Derynck R, Akhurst RJ, Balmain A: **TGF-beta signaling in tumor suppression and cancer progression.** Nat Genet 2001, **29**(2):117-129.
63. Liu XL, Band H, Gao Q, Wazer DE, Chu Q, Band V: **Tumor cell-specific loss of p53 protein in a unique in vitro model of human breast tumor progression.** Carcinogenesis 1994, **15**(9):1969-1973.
64. Lee JM, Dedhar S, Kalluri R, Thompson EW: **The epithelial-mesenchymal transition: new insights in signaling, development, and disease.** J Cell Biol 2006, **172**(7):973-981.
65. Boyer B, Valles AM, Edme N: **Induction and regulation of epithelial-mesenchymal transitions.** Biochem Pharmacol 2000, **60**(8):1091-1099.
66. Guarino M, Micheli P, Pallotti F, Giordano F: **Pathological relevance of epithelial and mesenchymal phenotype plasticity.** Pathol Res Pract 1999, **195**(6):379-389.

CHAPTER 4. GENERAL DISCUSSION

4.1. THESIS SUMMARY

The work described in this thesis has addressed the need to identify molecular factors that drive cells to transition through the stages of early breast cancer progression. Early breast cancer progression involves advancement through specific morphologic stages including atypical ductal hyperplasia (ADH), ductal carcinoma in situ (DCIS) and invasive mammary carcinoma (IMC), although not necessarily always in a linear fashion [1-5]. Although the pathology of these distinct stages is well described, the underlying molecular events controlling progression remain unclear. Model systems are required to study the molecular events and determine the molecular changes that are driving progression. This thesis made use of the 21T series human breast epithelial cell lines grown in a 3D Matrigel system. I hypothesized that when grown in 3D culture, the 21T series cells could be used to identify genes involved in the transition from ADH to DCIS and the transition from DCIS to IMC. Additionally, it was hypothesized that the 3D model system could be further used to determine the role of the identified genes in early breast cancer progression. In order to address these hypotheses, three objectives were defined. First, it was necessary to determine the growth characteristics of the 21T series cell lines in 3D *in vitro* culture. Next, the 3D system was used to identify genes potentially involved in the transition from ADH to DCIS and in the transition from DCIS to IMC. Finally, the validated genes were functionally characterized in the 3D system to determine their role in induction of tumor progression.

The 21T series cell lines, all originally derived from a single patient with metastatic breast cancer, have been previously proposed to represent a mammary tumour progression series [6]. In Chapter 2 (and [7]), we reported that the 21T cell lines indeed mimicked specific stages of human breast cancer progression when grown in the mammary fat pad of nude mice, albeit after a year. More specifically, the 21PT-derived cells developed lesions with morphologic features of ADH, while the 21NT-derived cells formed lesions of DCIS and the 21MT-1 cells lesions of IMC. In order to develop a more rapid, readily manipulatable *in vitro* assay for examining the biologic differences between these cell lines, we have used a 3D Matrigel system. When the three cell lines were grown in 3D Matrigel, they showed characteristic morphologies in which quantifiable aspects of stage-specific *in vivo* behaviours (i.e. differences in acinar structure formation, cell polarization, colony morphology, cell proliferation, cell invasion) were recapitulated in a reproducible fashion. Additionally, in order to determine differential gene expression profiles between the 21T series cell lines, *in vitro* expression arrays were performed on cells grown in 3D culture. Genes that were significantly altered ($p < 0.05$) at least 1.5-fold in either the transition from ADH to DCIS, or DCIS to IMC, were further considered. In order to assess whether these alterations were clinically relevant, we compared our list of differentially expressed genes with a database we generated from established literature on gene expression profiling of breast cancer clinical cancer specimens [8-19]. Ingenuity Pathways Analysis was then used to choose genes involved in the most highly altered canonical pathway and functional categories. Finally, GeneCards (www.genecards.org) was used to further explore the potential role of

the genes in breast cancer. Nineteen genes (Table 2.3) were then chosen for real-time qRT-PCR validation, with seventeen genes showing the same expression trend as the microarray. These genes were specifically altered in either the transition from pre-malignant (ADH: 21PT cells) to malignant growth (DCIS: 21NT cells), or the transition from growth within a duct (DCIS: 21NT cells) to invasion at the primary site (IMC: 21MT-1 cells).

From the PCR validated list, three genes were chosen for functional testing in the 21T series 3D model system. For the transition from ADH to DCIS, VANGL1 was functionally characterized to determine its role in promoting conversion to malignancy (in situ and/or invasive disease). Two genes differentially expressed in the DCIS to IMC transition were chosen for functional characterization, S100A2 and TBX3, to determine their role in progression to an invasive phenotype. Experimental studies focusing on these three genes were the basis for the work in Chapter 3.

VANGL1 was found to be elevated in 21NT (DCIS-like) cells compared to 21PT (ADH-like) cells. To determine the functional role of VANGL1 in the malignant transition, a myc-tagged VANGL1 expression vector was constructed and transfected into 21PT cells. The resulting VANGL1 overexpressing cells were functionally characterized according to colony profile (spherical vs. irregular), lumen formation, cell polarization, proportion of single cells, proliferation index, apoptosis index and cell invasion. The cells were found to have lost characteristics of the parental 21PT cells and gained some of those typically seen for 21NT or 21MT-1 cells. The VANGL1 overexpressing 21PT cultures were found to be more disorganized (less polarized cell groups, less

extracellular lumen formation) than 21NT or even 21MT-1 cells. Additionally, when a ratio of proliferation over apoptosis was calculated for the VANGL1 overexpressing cells, these cells had a higher ratio than 21NT cells. Furthermore, direct examination of invasiveness using transwell assay showed that the VANGL1 transfected 21PT cells had gained a significant level of invasiveness. Thus, the introduction of VANGL1 into 21PT cells induced change from a more ADH-like phenotype, beyond the stage of a DCIS, to a clearly invasive phenotype, without the need for any further experimental intervention.

S100A2 was found to be reduced in 21MT-1 (IMC-like) cells compared to 21NT (DCIS-like) cells. To determine the functional role of S100A2 in the transition to an invasive phenotype, shRNA against S100A2 was transfected into 21NT cells and the cells were analyzed using several functional parameters, including colony profile (spherical vs. irregular), lumen formation, cell polarization, proportion of single cells, proliferation index, apoptosis index and cell invasion by time lapse microscopy. The S100A2 knockdown 21NT cells were found to have lost characteristics of parental 21NT cells and gained those of 21MT-1 cells. The cells formed more disorganized groups (less polarized, less extracellular lumen formation) than either 21NT or 21MT-1 cells and showed a growth profile (ratio of proliferation to apoptosis) similar to 21MT-1 cells. In addition, knockdown S100A2 in 21NT cells resulted in cells that were invasive in 3D Matrigel to a degree comparable to 21MT-1 cells. Thus, loss of S100A2 in these cells originally mimicking DCIS, promotes their progression to the invasive phenotype.

TBX3 was found to be increased in 21MT-1 (IMC-like) cells compared to 21NT (DCIS-like) cells. To determine the functional role of both isoforms of TBX3

in the transition to an invasive phenotype, expression vectors of the isoforms fused to ZsGreen were transfected separately into 21NT cells. Functional assays including colony profile (spherical vs. irregular), lumen formation, cell polarization, proportion of single cells, proliferation index, apoptosis index, cell invasion and presence of EMT markers were then used to analyze the cells. The TBX3 overexpressing 21NT cells obtained characteristics more similar to 21MT-1 cells than to the parental 21NT cells. Both TBX3 overexpressing isoform variant cells formed more disorganized colonies (less polarization, less extracellular lumen formation) and had a much higher proliferation vs. apoptosis ratio than any of the parental 21T cell lines (including 21MT-1). In addition, assays in 3D Matrigel showed the TBX3 overexpressing cells (both isoforms) to be more invasive than the 21MT-1 cells. Thus, overexpression of either isoform of TBX3 is capable of inducing a transition of the DCIS-like 21NT cells to a clearly invasive phenotype.

Together, these studies have revealed that the 21T cell series 3D model system is a powerful tool that not only is able to identify targets with potential significance in breast cancer progression, but also provides a rapid and manipulatable system to test the functional characteristics of the targets.

4.2. DISCUSSION

Much interest surrounds the need to determine new molecular targets for breast cancer therapy. To this end, information from clinical studies examining pre-invasive lesions vs. invasive mammary carcinoma has yielded abundant gene expression profile differences between stages of progression (eg. [8-12]). The limitation we are facing is appropriate processing and synthesis of this data.

Several of these studies looked at specimens from different patients, leading to genetic differences that can mask the importance of specific gene targets. Also testing the involvement of individual genes in progression takes time, especially when using *in vivo* culture.

The 21T series 3D model system is of great advantage in this regard. As was discussed in Chapter 2, the parental cell lines stably represent three distinct stages of breast cancer. This is advantageous over the HMT-3522 and MCF10AT breast epithelial cell line systems, since both show mixed phenotypes and lack stability after culture [20-24]. Additionally, the 21T series cell lines are all derived from one patient, thus having an isogenic background. As a result, targets identified by the system are more likely to be those associated with cancer progression, as opposed to variation between individuals. Finally, the ability of the 21T series cell lines to represent the stages of progression in a 3D *in vitro* system allows us to rapidly test multiple functional characteristics of candidate genes to determine their role in regulating the transitions through the stages of breast cancer. The three targets examined in this thesis were VANGL1, S100A2 and TBX3, all of which have been identified as genes altered during progression in expression array profiling of clinical specimens, but for which very little functional information in relation to a role in breast cancer progression is currently available.

VANGL1 is a transmembrane protein that has been implicated in promoting malignancy and invasion of gastric, squamous, colon and laryngeal cancer [25-30]; however, no functional information is available in relation to breast cancer progression. The tumour enhancing ability of VANGL1 is believed

to be a result of both the negative interaction of VANGL1 with KAI1, a metastasis suppressor, and through the PCP signalling pathway, which is influenced by VANGL1. The microarray data from Chapter 2 identified VANGL1 as increased in 21NT (DCIS-like) compared to 21PT (ADH-like) cells. Consequently, in Chapter 3, we investigated the role of VANGL1 in the transition from ADH to DCIS. The 3D functional assays indicate that cells overexpressing VANGL1 did acquire characteristics of malignancy; however, several of the criteria examined indicated that the cells had progressed even further and had acquired characteristics of invasion. The present data implicates a role for VANGL1 in early breast cancer progression. This role may be achieved through the interaction of VANGL1 with KAI1, which blocks inhibitor effects of KAI1 on signalling and/or through the interaction of VANGL1 with the Wnt5a/Fzd/Dvl complex to alter signalling via the noncanonical Wnt/PCP pathway. Future studies that focus on these interactions would more fully elucidate the role of VANGL1 in early breast cancer (see section 5.3).

S100A2 is a member of the S100 calcium binding family and has been implicated in tumour suppression [31]. The tumour suppressing abilities have been noted in several forms of cancer and are theorized to be partly obtained through the interaction of S100A2 with the Cox-2 pathway [32], p53 signalling [33], RUNX3, EGFR and NFkB2 signalling [34]. In Chapter 3, we characterized the role of S100A2 in the transition from DCIS to IMC. S100A2 was knocked-down in 21NT (DCIS-like) cells to mimic the decreased S100A2 mRNA levels in 21MT-1 compared to 21NT cells that were discovered in Chapter 2. The 3D functional assays indicate that S100A2 knockdown cells did acquire

characteristics of invasion. These results give evidence for the first time that S100A2 may indeed be a gatekeeper of the invasive phenotype in breast cancer progression, such that downregulation of S100A2 allows the transition from the in situ to the invasive phenotype. The potential mechanisms of this phenomenon warrant further study (as described in section 5.3).

TBX3 is a member of the T-box family of transcription factors, previously linked to tumourigenesis and senescence bypass [35-37]; however, very little is known about the function of TBX3 in breast cancer. There are two isoforms of TBX3, which are created by alternative splicing [38]. Although TBX3 Iso1 (TBX3 splice variant) has been consistently implicated in senescence inhibition, there is controversy over whether TBX3 Iso2 (TBX3+2a variant) is also tumour promoting in action [39, 40]. Our interest in TBX3 in the transition from DCIS to IMC arose as a result of the microarray data in Chapter 2 that demonstrated that TBX3 was increased in 21MT-1 (IMC-like) cells compared to 21NT (DCIS-like) cells. In Chapter 3, we overexpressed both isoforms of TBX3 in 21NT (DCIS-like) cells to see if the transfected cells would acquire attributes of an invasive phenotype. When grown in 3D Matrigel, cells overexpressing both TBX3 isoforms did acquire attributes of the invasive phenotype, indicating for the first time that TBX3 (both isoforms) may influence the progression of breast cancer from the in situ to invasive phenotype. This data also provides evidence in the controversy over function of the two TBX3 isoforms, indicating that both isoforms show function in this system (consistent with Hoogaars and colleagues [40]). Other mechanisms of TBX3 effect include repression of p14 (ARF) [36] and induction of EMT through repression of E-cadherin [41]. These mechanisms could be explored in future

work (as discussed in section 5.3) to determine a more exact mechanism for the functional effect seen here.

The 21 human epithelial cell line 3D model system is a powerful tool. The system represents distinct stages of early breast cancer progression and has been shown to correctly predict molecular targets capable of affecting the transitions through these stages. In addition to identifying the targets, this model also provides a rapid and manipulatable system to test the functional characteristics of the targets. In this way, we are identifying genes as potential key regulators in the transitions of early breast progression, ideal for development as targets for preventative therapies directed at attacking cancer at its roots (before the development of invasive disease). At the same time, further use of this system will continue to provide insight into the molecular processes that drive early progression.

5.3. FUTURE DIRECTIONS

This thesis demonstrated that the 21T series 3D model system, which represents distinct stages in early breast cancer progression, can be used not only to identify genes which are involved in controlling the transitions between stages of progression, but also provides a means to functionally characterize the gene targets. The results from these studies raise a number of experimental questions that may form the basis of interesting continuation projects designed to further our understanding of early breast cancer progression.

First, choosing potential genes to further study from microarray data is challenging. We originally chose nineteen genes to validate with PCR and

determined that seventeen of the genes showed the same expression alteration trend by PCR as by microarray (Table 2.3). Only three of these seventeen genes were characterized, leaving fourteen genes ready for functional characterization. Also, several rules and guidelines were used in Chapter 2. These rules were used to ensure that genes chosen for further study were clinically relevant and involved in highly altered canonical pathways and functional categories; however, this does not mean that all genes important in progression were caught. Thus, the array data still holds much potential for further mining to identify genes involved in progression.

Second, the characterization of VANGL1, S100A2 and TBX3 has provided very exciting information about the roles of these genes in early breast cancer progression. However, there are still areas for each gene that need further development. Additionally, now that the functional effects of these candidate genes have been carefully characterized *in vitro*, the more time consuming and expensive confirmatory nude mouse assays can be done in a more selective fashion. Since 21T series cells require one year to develop lesions in mammary fat pads of nude mice, selective injection of cells that are up- or down-regulated for the well characterized gene targets will save much time and money. Injection of VANGL1 overexpressing 21PT cells into nude mice can be compared to 21PT+EV, 21NT and 21MT-1 cells to determine if VANGL1 results in progression to DCIS or even IMC. S100A2 knockdown 21NT cells can be injected into nude mice and compared to 21NT+EV and 21MT-1 cells to determine if loss of S100A2 drives 21NT cells to an IMC phenotype. Finally, injection of TBX3 overexpressing 21NT cells (both isoforms) into nude mice can be compared to

21NT+EV and 21MT-1 cells to determine if TBX3 promotes development of IMC. It will also be interesting to see if manipulation of any of these genes will result in a reduced latency in lesion development in nude mice.

Given the interplay between VANGL1 and Wnt5A in the planar cell polarity (PCP) pathway, it would be of interest to further explore the relationship between these two genes in PCP signalling. To examine the interplay between VANGL1 and Wnt5a, Wnt5a could be upregulated in 21NT cells, which have low Wnt5a (compared to 21PT cells), but elevated VANGL1 (compared to 21PT cells). Functional assays could then be used to analyze the effects on the transitions through early breast cancer progression. This manipulation would also aid in our understanding of the biphasic role of the PCP pathway in breast cancer. Additionally, it would be interesting to determine whether VANGL1 affects the Wnt/Fzd/Dvl interaction and this could be easily viewed by comparing the downstream PCP signals after up- and down-regulating VANGL1. Finally, since VANGL1 can potentially complex with and regulate KAI1, further study into the levels of KAI1 in the 21T series cells, as well as examination for direct interaction of VANGL1 with KAI1 and potential effects on activation of downstream targets of KAI1 (growth factor receptors and integrins) may elucidate if the promotion of malignancy and invasion observed here is due in part to VANGL1 regulation of KAI1.

Much of the literature points to the down-regulation of Cox-2 gene expression by S100A2 as a means by which S100A2 exerts its tumour suppressing ability. We did not see an alteration in Cox-2 expression with the microarray data, with the level of change that we had set for our initial screen.

However given that S100A2 has been shown to repress Cox-2, resulting in reduced tumourigenesis, it would be of interest to perform a qRT-PCR experiment to more accurately determine if Cox-2 is altered in the 21T series cells as well as the S100A2 knockdown cells. Also, it would be worth examining the regulation of S100A2 on both NFkB2 and RUNX3 and their respective signalling pathways, given that both the literature and our microarray data have elucidated a possible role for S100A2 signalling through these genes. qRT-PCR experiments could be conducted to determine if the levels of NFkB2 and/or RUNX3 are altered in the S100A2 knockdown cells compared to the 21NT+EV control cells. Additionally, levels of downstream effectors in the respective pathways of each of these genes can be viewed to determine if loss of S100A2 affects signalling.

Since TBX3 is a transcription factor, its effects on cells are numerous. Two pathways identified by the literature and partly corroborated by this thesis involve a role with p14 (ARF) and in EMT. Given that levels of p14 (ARF) are marginally decreased in 21MT-1 cells compared to 21NT cells, it would be of interest to determine if there is an alteration in expression of p14 (ARF) in the TBX3 (both isoforms) overexpressing 21NT cells. This thesis also used decreased E-cadherin and increased vimentin as indicators that TBX3 may play a role in promoting EMT. To further analyze this theory, other markers of EMT, including increased fibronectin, snail1, snail2 (slug) and accumulation of β -catenin in the nucleus, could be investigated.

Collectively these studies indicate that the 21T 3D model system is an influential tool that not only is able to identify targets with potential significance in

breast cancer progression, but also provides a rapid and manipulatable system to test the functional characteristics of the targets. Continued research in the areas described above should elucidate more targets in early breast cancer progression and further our understanding of the targets already identified, which will aid in the development of novel detection, treatment and preventative strategies for progression.

5.4. REFERENCES

1. Arpino G, Laucirica R, Elledge RM: **Premalignant and in situ breast disease: biology and clinical implications.** Ann Intern Med 2005, **143**(6):446-457.
2. Bodian CA, Perzin KH, Lattes R, Hoffmann P: **Reproducibility and validity of pathologic classifications of benign breast disease and implications for clinical applications.** Cancer 1993, **71**(12):3908-3913.
3. Carter CL, Corle DK, Micozzi MS, Schatzkin A, Taylor PR: **A prospective study of the development of breast cancer in 16,692 women with benign breast disease.** Am J Epidemiol 1988, **128**(3):467-477.
4. Allred DC, Wu Y, Mao S, Nagtegaal ID, Lee S, Perou CM, Mohsin SK, O'Connell P, Tsimelzon A, Medina D: **Ductal carcinoma in situ and the emergence of diversity during breast cancer evolution.** Clin Cancer Res 2008, **14**(2):370-378.
5. Allred DC, Mohsin SK, Fuqua SA: **Histological and biological evolution of human premalignant breast disease.** Endocr Relat Cancer 2001, **8**(1):47-61.
6. Band V, Zajchowski D, Swisshelm K, Trask D, Kulesa V, Cohen C, Connolly J, Sager R: **Tumor progression in four mammary epithelial cell lines derived from the same patient.** Cancer Res 1990, **50**(22):7351-7357.
7. Souter LH, Andrews JD, Zhang G, Cook AC, Postenka CO, Al-Katib W, Leong HS, Rodenhiser DI, Chambers AF, Tuck AB: **Human 21T breast epithelial cell lines mimic breast cancer progression in vivo and in vitro and show stage-specific gene expression patterns.** Lab Invest 2010, **90**(8):1247-1258.

8. Ma XJ, Salunga R, Tuggle JT, Gaudet J, Enright E, McQuary P, Payette T, Pistone M, Stecker K, Zhang BM, Zhou YX, Varnholt H, Smith B, Gadd M, Chatfield E, Kessler J, Baer TM, Erlander MG, Sgroi DC: **Gene expression profiles of human breast cancer progression.** Proc Natl Acad Sci U S A 2003, **100**(10):5974-5979.
9. Abba MC, Drake JA, Hawkins KA, Hu Y, Sun H, Notcovich C, Gaddis S, Sahin A, Baggerly K, Aldaz CM: **Transcriptomic changes in human breast cancer progression as determined by serial analysis of gene expression.** Breast Cancer Res 2004, **6**(5):R499-513.
10. Schuetz CS, Bonin M, Clare SE, Nieselt K, Sotlar K, Walter M, Fehm T, Solomayer E, Riess O, Wallwiener D, Kurek R, Neubauer HJ: **Progression-specific genes identified by expression profiling of matched ductal carcinomas in situ and invasive breast tumors, combining laser capture microdissection and oligonucleotide microarray analysis.** Cancer Res 2006, **66**(10):5278-5286.
11. Nishidate T, Katagiri T, Lin ML, Mano Y, Miki Y, Kasumi F, Yoshimoto M, Tsunoda T, Hirata K, Nakamura Y: **Genome-wide gene-expression profiles of breast-cancer cells purified with laser microbeam microdissection: identification of genes associated with progression and metastasis.** Int J Oncol 2004, **25**(4):797-819.
12. Milovanovic T, Planutis K, Nguyen A, Marsh JL, Lin F, Hope C, Holcombe RF: **Expression of Wnt genes and frizzled 1 and 2 receptors in normal breast epithelium and infiltrating breast carcinoma.** Int J Oncol 2004, **25**(5):1337-1342.
13. Minn AJ, Kang Y, Serganova I, Gupta GP, Giri DD, Doubrovin M, Ponomarev V, Gerald WL, Blasberg R, Massague J: **Distinct organ-specific metastatic potential of individual breast cancer cells and primary tumors.** J Clin Invest 2005, **115**(1):44-55.
14. Kang Y, Siegel PM, Shu W, Drobnjak M, Kakonen SM, Cordon-Cardo C, Guise TA, Massague J: **A multigenic program mediating breast cancer metastasis to bone.** Cancer Cell 2003, **3**(6):537-549.
15. Wang Y, Klijn JG, Zhang Y, Sieuwerts AM, Look MP, Yang F, Talantov D, Timmermans M, Meijer-van Gelder ME, Yu J, Jatkoe T, Berns EM, Atkins D, Foekens JA: **Gene-expression profiles to predict distant metastasis of lymph-node-negative primary breast cancer.** Lancet 2005, **365**(9460):671-679.

16. Asaka S, Fujimoto T, Akaishi J, Ogawa K, Onda M: **Genetic prognostic index influences patient outcome for node-positive breast cancer.** Surg Today 2006, **36**(9):793-801.
17. O'Brien N, O'Donovan N, Foley D, Hill AD, McDermott E, O'Higgins N, Duffy MJ: **Use of a Panel of Novel Genes for Differentiating Breast Cancer from Non-Breast Tissues.** Tumour Biol 2008, **28**(6):312-317.
18. Shen R, Ghosh D, Chinnaiyan AM: **Prognostic meta-signature of breast cancer developed by two-stage mixture modeling of microarray data.** BMC Genomics 2004, **5**(1):94.
19. van 't Veer LJ, Dai H, van de Vijver MJ, He YD, Hart AA, Mao M, Peterse HL, van der Kooy K, Marton MJ, Witteveen AT, Schreiber GJ, Kerkhoven RM, Roberts C, Linsley PS, Bernards R, Friend SH: **Gene expression profiling predicts clinical outcome of breast cancer.** Nature 2002, **415**(6871):530-536.
20. Briand P, Lykkesfeldt AE: **An in vitro model of human breast carcinogenesis: epigenetic aspects.** Breast Cancer Res Treat 2001, **65**(2):179-187.
21. Weaver VM, Howlett AR, Langton-Webster B, Petersen OW, Bissell MJ: **The development of a functionally relevant cell culture model of progressive human breast cancer.** Semin Cancer Biol 1995, **6**(3):175-184.
22. Santner SJ, Dawson PJ, Tait L, Soule HD, Eliason J, Mohamed AN, Wolman SR, Heppner GH, Miller FR: **Malignant MCF10CA1 cell lines derived from premalignant human breast epithelial MCF10AT cells.** Breast Cancer Res Treat 2001, **65**(2):101-110.
23. Miller FR: **Xenograft models of premalignant breast disease.** J Mammary Gland Biol Neoplasia 2000, **5**(4):379-391.
24. Miller FR, Santner SJ, Tait L, Dawson PJ: **MCF10DCIS.com xenograft model of human comedo ductal carcinoma in situ.** J Natl Cancer Inst 2000, **92**(14):1185-1186.
25. Lee JH, Park SR, Chay KO, Seo YW, Kook H, Ahn KY, Kim YJ, Kim KK: **KAI1 COOH-terminal interacting tetraspanin (KITENIN), a member of the tetraspanin family, interacts with KAI1, a tumor metastasis suppressor, and enhances metastasis of cancer.** Cancer Res 2004, **64**(12):4235-4243.
26. Lee JK, Bae JA, Sun EG, Kim HD, Yoon TM, Kim K, Lee JH, Lim SC, Kim KK: **KITENIN increases invasion and migration of mouse squamous cancer cells and promotes pulmonary metastasis in a mouse squamous tumor model.** FEBS Lett 2009, **583**(4):711-717.

27. Lee JK, Yoon TM, Seo DJ, Sun EG, Bae JA, Lim SC, Choi YD, Lee JH, Joo YE, Kim KK: **KAI1 COOH-terminal interacting tetraspanin (KITENIN) expression in early and advanced laryngeal cancer.** Laryngoscope 2010, **120**(5):953-958.
28. Kho DH, Bae JA, Lee JH, Cho HJ, Cho SH, Lee JH, Seo YW, Ahn KY, Chung IJ, Kim KK: **KITENIN recruits Dishevelled/PKC delta to form a functional complex and controls the migration and invasiveness of colorectal cancer cells.** Gut 2009, **58**(4):509-519.
29. Ryu HS, Park YL, Park SJ, Lee JH, Cho SB, Lee WS, Chung IJ, Kim KK, Lee KH, Kweon SS, Joo YE: **KITENIN is associated with tumor progression in human gastric cancer.** Anticancer Res 2010, **30**(9):3479-3486.
30. Lee JH, Cho ES, Kim MY, Seo YW, Kho DH, Chung IJ, Kook H, Kim NS, Ahn KY, Kim KK: **Suppression of progression and metastasis of established colon tumors in mice by intravenous delivery of short interfering RNA targeting KITENIN, a metastasis-enhancing protein.** Cancer Res 2005, **65**(19):8993-9003.
31. Salama I, Malone PS, Mihaimed F, Jones JL: **A review of the S100 proteins in cancer.** Eur J Surg Oncol 2008, **34**(4):357-364.
32. Tsai WC, Tsai ST, Jin YT, Wu LW: **Cyclooxygenase-2 is involved in S100A2-mediated tumor suppression in squamous cell carcinoma.** Mol Cancer Res 2006, **4**(8):539-547.
33. van Dieck J, Teufel DP, Jaulent AM, Fernandez-Fernandez MR, Rutherford TJ, Wyslouch-Cieszyńska A, Fersht AR: **Posttranslational modifications affect the interaction of S100 proteins with tumor suppressor p53.** J Mol Biol 2009, **394**(5):922-930.
34. Matsubara D, Niki T, Ishikawa S, Goto A, Ohara E, Yokomizo T, Heizmann CW, Aburatani H, Moriyama S, Moriyama H, Nishimura Y, Funata N, Fukayama M: **Differential expression of S100A2 and S100A4 in lung adenocarcinomas: clinicopathological significance, relationship to p53 and identification of their target genes.** Cancer Sci 2005, **96**(12):844-857.
35. Brummelkamp TR, Kortlever RM, Lingbeek M, Trettel F, MacDonald ME, van Lohuizen M, Bernards R: **TBX-3, the gene mutated in Ulnar-Mammary Syndrome, is a negative regulator of p19ARF and inhibits senescence.** J Biol Chem 2002, **277**(8):6567-6572.
36. Brummelkamp TR, Kortlever RM, Lingbeek M, Trettel F, MacDonald ME, van Lohuizen M, Bernards R: **TBX-3, the gene mutated in Ulnar-Mammary**

- Syndrome, is a negative regulator of p19ARF and inhibits senescence.** J Biol Chem 2002, **277**(8):6567-6572.
37. Carlson H, Ota S, Song Y, Chen Y, Hurlin PJ: **Tbx3 impinges on the p53 pathway to suppress apoptosis, facilitate cell transformation and block myogenic differentiation.** Oncogene 2002, **21**(24):3827-3835.
38. Bamshad M, Le T, Watkins WS, Dixon ME, Kramer BE, Roeder AD, Carey JC, Root S, Schinzel A, Van Maldergem L, Gardner RJ, Lin RC, Seidman CE, Seidman JG, Wallerstein R, Moran E, Sutphen R, Campbell CE, Jorde LB: **The spectrum of mutations in TBX3: Genotype/Phenotype relationship in ulnar-mammary syndrome.** Am J Hum Genet 1999, **64**(6):1550-1562.
39. Fan W, Huang X, Chen C, Gray J, Huang T: **TBX3 and its isoform TBX3+2a are functionally distinctive in inhibition of senescence and are overexpressed in a subset of breast cancer cell lines.** Cancer Res 2004, **64**(15):5132-5139.
40. Hoogaars WM, Barnett P, Rodriguez M, Clout DE, Moorman AF, Goding CR, Christoffels VM: **TBX3 and its splice variant TBX3 + exon 2a are functionally similar.** Pigment Cell Melanoma Res 2008, **21**(3):379-387.
41. Rodriguez M, Aladowicz E, Lanfrancone L, Goding CR: **Tbx3 represses E-cadherin expression and enhances melanoma invasiveness.** Cancer Res 2008, **68**(19):7872-7881.

Appendix A

**Copyright agreement for previously published work
and animal protocol approval**



Permission requests

On this page

Nature Publishing Group grants permission for authors, readers and third parties to reproduce material from its journals and online products as part of another publication or entity. This includes, for example, the use of a figure in a presentation, the posting of an abstract on a web site, or the reproduction of a full article within another journal. Certain permissions can be granted free of charge; others incur a fee.

For answers to frequently asked questions [click here](#)

- [Type of permission request](#)
- [Permission request options](#)

Types of permission request

Permission can be obtained for re-use of portions of material - ranging from a single figure to a whole paper - in books, journals/magazines, newsletters, theses/dissertations, classroom materials/academic course packs, academic conference materials, training materials (including continuing medical education), promotional materials, and web sites. Some permission requests can be granted free of charge, others carry a fee.

Nature Publishing Group rarely grants free permission for PDFs of full papers to be reproduced online, however e-print PDFs can be [purchased as commercial reprints](#). If you wish to purchase multiple stand-alone copies of a Nature Publishing Group paper, which is then printed and shipped to you, please go to [commercial reprints](#).

Permission request options

Permission requests from authors

The authors of articles published by Nature Publishing Group, or the authors' designated agents, do not usually need to seek permission for re-use of their material as long as the journal is credited with initial publication. For further information about the terms of re-use for authors please see below.

Author Requests

If you are the author of this content (or his/her designated agent) please read the following. Since 2003, ownership of copyright in in original research articles remains with the Authors*, and provided that, when reproducing the Contribution or extracts from it, the Authors acknowledge first and reference publication in the Journal, the Authors retain the following non-exclusive rights:

1. To reproduce the Contribution in whole or in part in any printed volume (book or thesis) of which they are the author(s).
2. They and any academic institution where they work at the time may reproduce the Contribution for the purpose of course teaching.
3. To reuse figures or tables created by them and contained in the Contribution in other works created by them.
4. To post a copy of the Contribution as accepted for publication after peer review (in Word or Tex format) on the Author's own web site, or the Author's institutional repository, or the Author's funding body's archive, six months after publication of the printed or online edition of the Journal, provided that they also link to the Journal article on NPG's web site (eg through the DOI).

NPG encourages the self-archiving of the accepted version of your manuscript in your funding agency's or institution's repository, six months after publication. This policy complements the recently announced policies of the US National Institutes of Health, Wellcome Trust and other research funding bodies around the world. NPG recognizes the efforts of funding bodies to increase access to the research they fund, and we strongly encourage authors to participate in such efforts.

Authors wishing to use the published version of their article for promotional use or on a web site must request in the normal way.

If you require further assistance please read NPG's online author reuse guidelines.

Note: British Journal of Cancer and Clinical Pharmacology & Therapeutics maintain copyright policies of their own that are different from the general NPG policies. Please consult these journals to learn more.

* Commissioned material is still subject to copyright transfer conditions

Ordering permissions online

Most permission requests can be granted online through the Rightslink® service. To use this system, locate the article for which you wish to request a permission by using the [advanced search](#).

Beneath the listing for the paper (when found through the search), you will find a clickable option 'Rights and Permissions', which will take you to the order entry page from which you can request your permission.

To request a permission through the Rightslink® service you will be required to create an account by filling out a simple online form. Most customers can order and, where necessary, make payment - by credit card or invoice - through the Rightslink® service. Rightslink then issues a printable licence, which is the official confirmation that permission has been granted.

For questions about Rightslink® accounts, please telephone Copyright Clearance Center customer support on 877 622 5543 (toll free inside the USA) or e-mail customer@copyright.com. Note that once you have created a Rightslink® account you can use this in the future to request and pay for permissions from other participating publishers.

If the abstract or article does not contain a 'Rights and permissions' link, or the article that you wish to request permission to re-use has not yet been published, or pre-dates our online archive, please e-mail [the appropriate permissions manager for the journal](#).



The UNIVERSITY of WESTERN ONTARIO

University of Council on Animal Care
Animal Use Subcommittee

November 22, 2000

This is the 2nd renewal of this protocol
A Full protocol submission will be required in 2002

Dear Dr. Chambers and Dr. Tuck:

Your "Application to Use Animals for Research or Teaching" entitled:

" Osteopontin and Breast Cancer: Functional Contribution to Malignancy and Potential as a Plasma and Tumor Marker of Progression "
Funding Agency- CBCRI

has been approved by the University Council on Animal Care. This approval expires in one year on the last day of the month. The number for this project is 00236-12 and replaces 99238-12

1. This number must be indicated when ordering animals for this project.
2. Animals for other projects may not be ordered under this number.
3. If no number appears please contact this office when grant approval is received.
If the application for funding is not successful and you wish to proceed with the project, request that an internal scientific peer review be performed by the Animal Use Subcommittee office.
4. Purchases of animals other than through this system must be cleared through the ACVS office. Health certificates will be required.

ANIMALS APPROVED

Mice - nude, Ncr and Balb/ C, 4-8 weeks, F - 100

STANDARD OPERATING PROCEDURES

Procedures in this protocol should be carried out according to the following SOPs. Please contact the Animal Use Subcommittee office (661-2111 ext. 6770) in case of difficulties or if you require copies. SOP's are also available at <http://www.uwo.ca/animal/acvs>

- # 310 Holding Period Post Admission
- # 320 Euthanasia
- # 100 Monitoring/Tumour Growth/Rodents
- # 321 Criteria for Early Euthanasia-Rodent
- # 330 Postoperative Care - Rodent
- # 343 Surgical Prep/Rodent/Recovery Surgery
- # 360 Blood Collection/Volumes/Multiple Species

REQUIREMENTS/COMMENTS

Please ensure that individual(s) performing procedures on live animals, as described in this protocol, are familiar with the contents of this document.

CHANGES New incision method added; new anaesthetic and analgesic regimes added; new staff added.

After hours emergency contact is: C. Hota - 433-0854 K. Furger - 649-2312

c.c. Approved Protocol
Approval Letter

✓ A. Chambers, A. Tuck, S. Vantigham, P. Coakwell
- A. Tuck, S. Vantigham, P. Coakwell

Appendix B

Supplementary data for Chapter 2

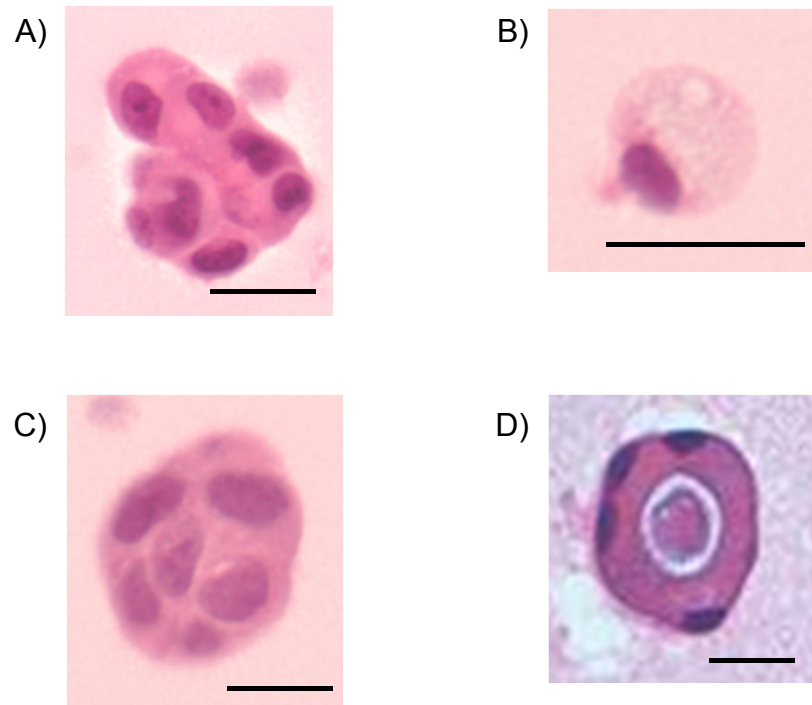


Figure 1. Examples of each type of cell colony examined in the 3D colony morphology assay. A) represents a cell group/colony, while B) represents a single cell. C) is representative of a spherical colony, while A) would not be considered spherical. The cell colony in D) is able to form an extracellular lumen, while a lumen is not present in the cell colony displayed in C). Finally, the cells within the colony in D) are polarized, as the nuclei are basally oriented, while the cells found within the cell colony in C) are not polarized. Scale bar represents 10 μm .

Table 1. Genes that are significantly different among the 21T series cell lines (Supplemental Table 1 and 2) and also present on clinically relevant databases from the literature (Supplemental Table 3).

A) 21PTci to 21NTci

Probe Set ID	Gene Symbol	21NTci (ratio to 21PTci)
216620_s_at	ARHGEF10	0.59
211022_s_at	ATRX	1.97
208478_s_at	BAX	0.57
211813_x_at	DCN	0.60
242605_at	DCN	7.52
220668_s_at	DNMT3B	1.39
217497_at	ECGF1	1.60
208180_s_at	HIST1H4H	1.56
209984_at	JMJD2C	1.66
210662_at	KYNU	4.98
208403_x_at	MAX	0.65
242479_s_at	MCM4	0.62
230848_s_at	MGA	3.23
204475_at	MMP1	0.24
221805_at	NEFL	0.31
209997_x_at	PCM1	0.65
212240_s_at	PIK3R1	1.75
206509_at	PIP	3.95
204051_s_at	SFRP4	0.65
219103_at	UPLC1	9.31
229997_at	VANGL1	2.19
229802_at	WISP1	2.18
213425_at	WNT5A	0.53

B) 21NTci to 21MT-1

Probe ID	Gene Symbol	21MT-1 (ratio to 21NTci)
208161_s_at	ABCC3	0.05
202850_at	ABCD3	0.61
206513_at	AIM2	7.16
224655_at	AK3L1	0.47
224151_s_at	AK3L1	0.30
205623_at	ALDH3A1	0.01
223333_s_at	ANGPTL4	0.28

222608_s_at	ANLN	0.38
1552619_a_at	ANLN	0.37
208702_x_at	APLP2	0.58
204205_at	APOBEC3G	3.37
201288_at	ARHGDIB	0.03
209394_at	ASMTL	1.96
218782_s_at	ATAD2	0.43
222740_at	ATAD2	0.40
213106_at	ATP8A1	0.10
202391_at	BASP1	4.23
204908_s_at	BCL3	1.84
209373_at	BENE	0.06
210538_s_at	BIRC3	2.49
230499_at	BIRC3	2.23
207655_s_at	BLNK	0.04
203571_s_at	C10orf116	0.01
211368_s_at	CASP1	3.62
205476_at	CCL20	19.98
205099_s_at	CCR1	7.85
201131_s_at	CDH1	0.02
207173_x_at	CDH11	0.24
204252_at	CDK2	0.26
213618_at	CENTD1	0.07
209395_at	CHI3L1	0.13
209396_s_at	CHI3L1	0.09
201428_at	CLDN4	0.02
208792_s_at	CLU	3.43
225438_at	CML66	0.50
204740_at	CNKSR1	0.29
222073_at	COL4A3	1.64
212489_at	COL5A1	0.15
203325_s_at	COL5A1	0.11
207442_at	CSF3	11.23
210140_at	CST7	18.14
823_at	CX3CL1	2.04
204470_at	CXCL2	0.04
211919_s_at	CXCR4	0.20
209201_x_at	CXCR4	0.07
217028_at	CXCR4	0.04
202435_s_at	CYP1B1	0.18
202436_s_at	CYP1B1	0.15

202437_s_at	CYP1B1	0.10
211896_s_at	DCN	33.95
209335_at	DCN	21.17
211813_x_at	DCN	20.03
201893_x_at	DCN	15.35
242605_at	DCN	1.77
210749_x_at	DDR1	0.18
1007_s_at	DDR1	0.13
208779_x_at	DDR1	0.06
207169_x_at	DDR1	0.04
211272_s_at	DGKA	0.23
222621_at	DNAJC1	1.93
201843_s_at	EFEMP1	0.07
201842_s_at	EFEMP1	0.04
201325_s_at	EMP1	0.28
214782_at	EMS1	1.85
201313_at	ENO2	10.08
217061_s_at	ETV1	2.05
211742_s_at	EVI2B	3.64
221565_s_at	FAM26B	0.21
202995_s_at	FBLN1	0.46
202994_s_at	FBLN1	0.13
201540_at	FHL1	7.54
218035_s_at	FLJ20273	0.07
214915_at	FLJ25476	0.62
214211_at	FTH1	2.84
206002_at	GPR64	0.30
219327_s_at	GPRC5C	0.08
212873_at	HA-1	2.63
216693_x_at	HDGFRP3	0.40
213537_at	HLA-DPA1	11.27
212143_s_at	IGFBP3	0.02
210095_s_at	IGFBP3	0.01
206172_at	IL13RA2	13.55
205992_s_at	IL15	6.56
206295_at	IL18	0.06
226218_at	IL7R	14.04
205798_at	IL7R	3.87
208436_s_at	IRF7	3.73
228462_at	IRX2	0.25
204990_s_at	ITGB4	0.04

1566465_at	KCNK1	0.11
204678_s_at	KCNK1	0.02
204679_at	KCNK1	0.02
212314_at	KIAA0746	0.16
206785_s_at	KLRC1	3.77
212236_x_at	KRT17	2.16
213680_at	KRT6B	0.26
209016_s_at	KRT7	0.11
213711_at	KRTHB1	0.09
241305_at	KYNU	2.98
210663_s_at	KYNU	2.32
204385_at	KYNU	2.04
211651_s_at	LAMB1	1.84
202728_s_at	LTBP1	15.51
205668_at	LY75	0.16
213489_at	MAPRE2	0.09
202350_s_at	MATN2	0.19
211340_s_at	MCAM	3.28
242479_s_at	MCM4	1.69
203417_at	MFAP2	0.54
203434_s_at	MME	2.16
204475_at	MMP1	20.75
201069_at	MMP2	0.48
205828_at	MMP3	7.41
204259_at	MMP7	0.24
219959_at	MOCOS	2.35
37408_at	MRC2	0.16
201521_s_at	NCBP2	1.64
209949_at	NCF2	0.16
206022_at	NDP	0.62
202237_at	NNMT	5.23
202238_s_at	NNMT	5.05
219773_at	NOX4	1.91
205552_s_at	OAS1	0.36
213075_at	OLFML2A	0.09
205041_s_at	ORM1	46.41
210448_s_at	P2RX5	2.15
202465_at	PCOLCE	3.31
214582_at	PDE3B	0.27
222719_s_at	PDGFC	0.07
218718_at	PDGFC	0.02

205226_at	PDGFRL	7.30
205960_at	PDK4	0.04
225207_at	PDK4	0.02
221816_s_at	PHF11	0.08
225136_at	PLEKHA2	0.48
205479_s_at	PLAU	0.59
236297_at	PLXDC2	1.62
201578_at	PODXL	0.10
210910_s_at	POMZP3	0.52
203407_at	PPL	0.05
201602_s_at	PPP1R12A	1.66
201858_s_at	PRG1	5.89
209606_at	PSCDBP	18.29
202006_at	PTPN12	1.67
203029_s_at	PTPRN2	20.15
210127_at	RAB6B	0.48
218723_s_at	RGC32	0.02
200962_at	RPL31	0.50
204268_at	S100A2	0.25
206027_at	S100A3	3.67
203453_at	SCNN1A	0.19
201286_at	SDC1	0.19
204855_at	SERPINB5	0.03
209044_x_at	SF3B4	1.81
209980_s_at	SHMT1	0.04
213355_at	SIAT10	0.44
206510_at	SIX2	0.23
202800_at	SLC1A3	6.78
1569054_at	SLC1A3	5.98
206097_at	SLC22A1LS	2.03
202498_s_at	SLC2A14	3.60
202499_s_at	SLC2A3	4.06
206628_at	SLC5A1	0.56
209830_s_at	SLC9A3R2	0.06
213139_at	SNAI2	2.93
220987_s_at	SNARK	0.67
227697_at	SOCS3	7.01
212560_at	SORL1	0.12
220922_s_at	SPANXB1	18.34
220217_x_at	SPANXC	5.36
218638_s_at	SPON2	0.21

233555_s_at	SULF2	0.05
224724_at	SULF2	0.02
202168_at	TAF9	2.00
225973_at	TAP2	2.07
225544_at	TBX3	2.84
203919_at	TCEA2	0.65
214476_at	TFF2	9.71
201506_at	TGFBI	3.65
201147_s_at	TIMP3	15.63
219580_s_at	TMC5	0.03
222450_at	TMEPAI	0.02
202644_s_at	TNFAIP3	3.94
206025_s_at	TNFAIP6	1.50
202688_at	TNFSF10	0.06
210314_x_at	TNFSF13	0.46
209500_x_at	TNFSF13	0.44
221601_s_at	TOSO	5.07
201746_at	TP53	1.62
209863_s_at	TP73L	0.36
209227_at	TUSC3	0.50
201009_s_at	TXNIP	0.31
201010_s_at	TXNIP	0.23
226681_at	UBE2H	1.90
208998_at	UCP2	0.51
225242_s_at	URB	0.33
210513_s_at	VEGF	3.09
212171_x_at	VEGF	2.48
210512_s_at	VEGF	2.15
202664_at	WASPIP	8.87
213425_at	WNT5A	9.30
203585_at	ZNF185	0.37
213196_at	ZNF629	0.44
211796_s_at		30.26
213193_x_at		2.60
243020_at		0.63
244579_at		0.57
210136_at		0.23

Appendix C

Supplementary data for Chapter 3

Table 1. S100A2 shRNA sequence.

Mature Product (22 mer) Sequence	Hairpin Sequence
CCAGACCGACCC TGAAGCA	TGCTGTTGACAGTGAGCGACCCAGACCGACCCTGAAG CAGTAGTGAAGCCACAGATGTACTGCTTCAGGGTCGG TCTGGGCTGCCTACTGCCTCGGA

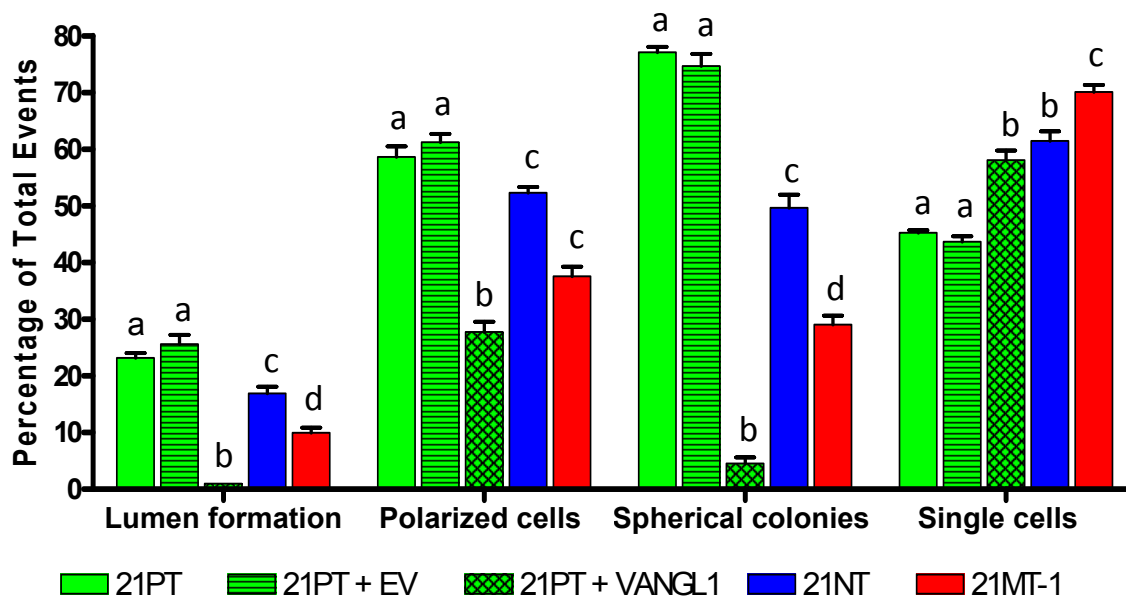


Figure 1. Quantification of characteristics of 21T and VANGL1 overexpressing cells after 9 days growth in 3D Matrigel. 21PT+VANGL1 cells show no lumen formation and fewer polarized cells than 21PT+empty vector (EV) cells, indicating that the VANGL1 cells are more disorganized. In addition, VANGL1 transfected cells also formed far fewer spherical colonies, with the percentage being lower than even 21MT-1 cells. The percentage of single cells seen in Matrigel plugs for 21PT+VANGL1 cells was at the same level as 21NT cells. 21PT+EV cells show no differences from 21PT cells. For ‘single cells’, an event is either a single cell or a cell group, whereas for the ‘lumen formation’, ‘polarized cells’ and ‘spherical colonies’ comparisons, an ‘event’ was defined as a cell group only. Bars labeled with letters that are not the same indicate significant difference between the bars at a p-value of at least <0.05 . Statistics for each comparison were calculated separately from the other comparisons.

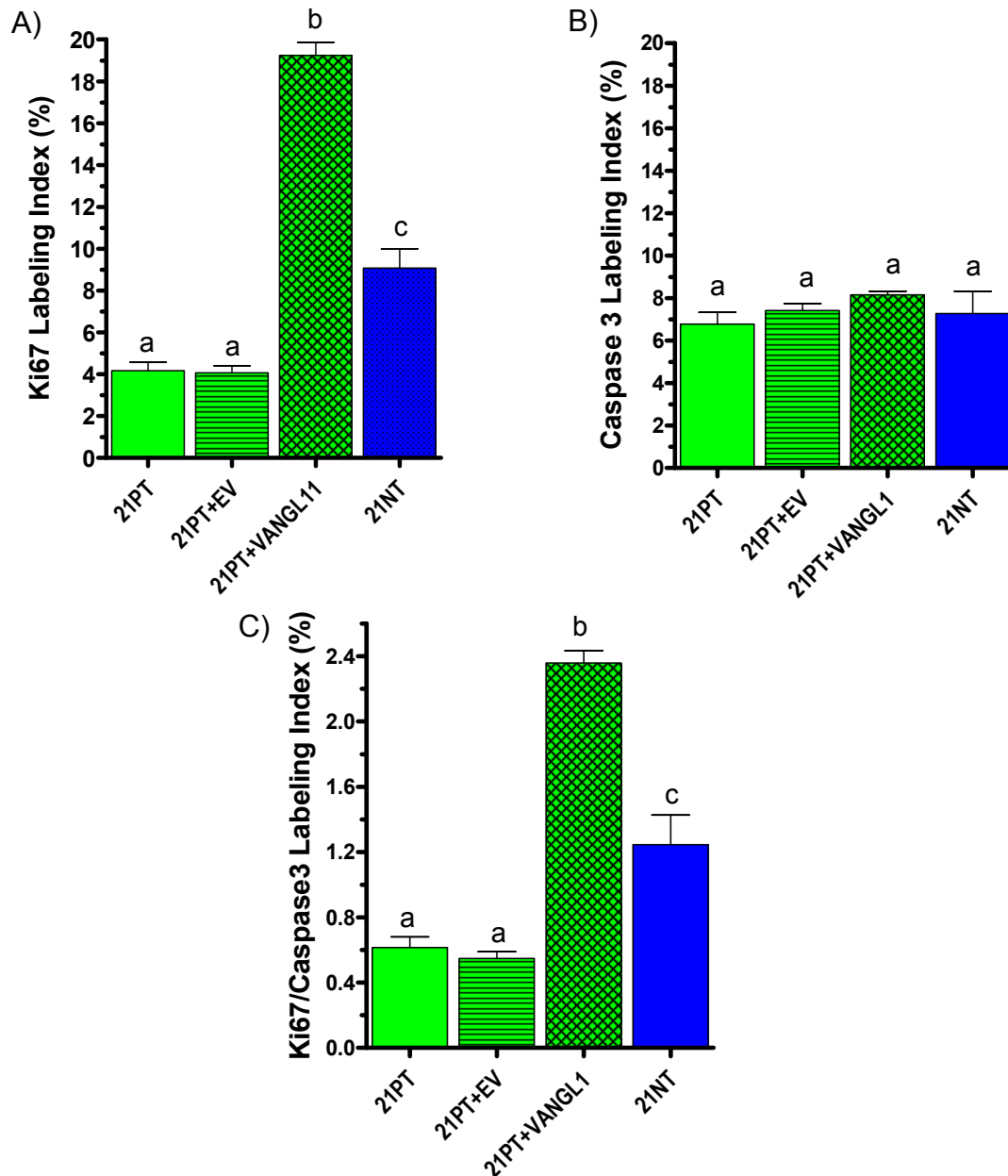


Figure 2. Proliferative and apoptotic activity of 21T and VANGL1 overexpressing cell lines after 9 days growth in 3D Matrigel. Proliferation (A) was quantified by Ki67 immunohistochemical staining of Matrigel plugs, while apoptosis (B) was quantified by caspase 3 immunohistochemistry. 21PT+VANGL1 cells showed a large increase in proliferation (A) over 21PT+EV cells, while apoptosis levels (B) were unaltered from 21PT+EV cells. When the ratio of proliferation/apoptosis was calculated (C), VANGL1 overexpressing cells showed a much higher ratio than the 21PT+EV and even the 21NT cells. 21PT+EV cells showed no differences from the 21PT cells. Bars labeled with letters that are not the same indicate significant difference between the bars at a p-value of at least <math><0.05</math>.

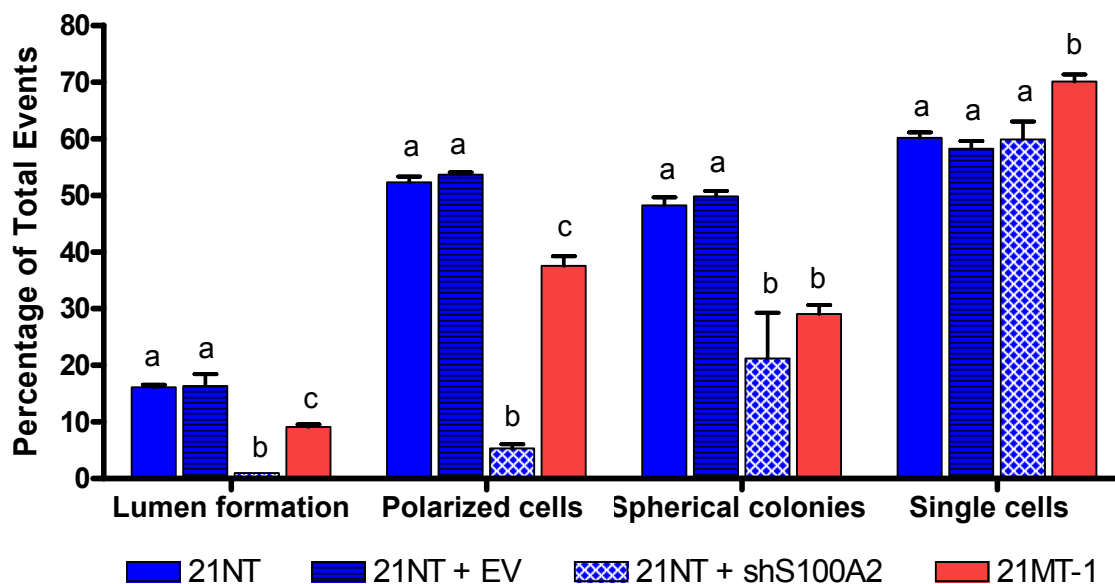


Figure 3. Quantification of characteristics of 21T and S100A2 knockdown cells after 9 days growth in 3D Matrigel. 21NT+shS100A2 cells show complete loss of lumen forming ability and fewer polarized cells than 21NT+EV or 21MT-1 cells, indicating that the S100A2 knockdown cells are less organized. In addition, S100A2 shRNA cells also formed fewer spherical colonies than 21NT+EV cells and in line with 21MT-1 cells. The percentage of single cells seen in Matrigel plugs for 21NT+shS100A2 cells was unaltered from 21NT+EV (or 21NT) cells. 21NT+EV cells show no differences from 21NT cells. For 'single cells', an event is either a single cell or a cell group, whereas for the 'lumen formation', 'polarized cells' and 'spherical colonies' comparisons, an 'event' was defined as a cell group only. Bars labeled with letters that are not the same indicate significant difference between the bars at a p-value of at least <math><0.05</math>. Statistics for each comparison were calculated separately from the other comparisons.

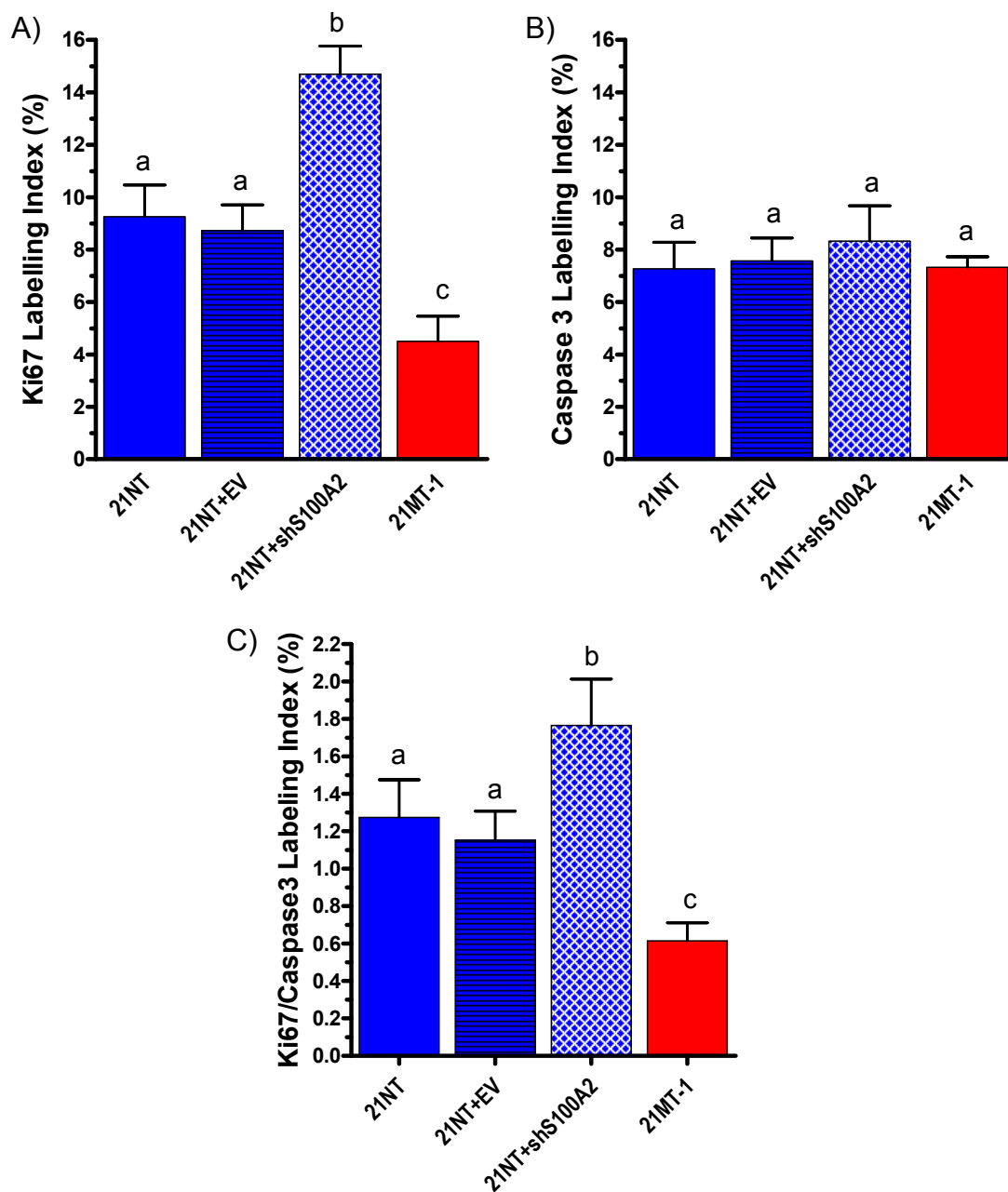


Figure 4. Proliferative and apoptotic activity of 21T and S100A2 knockdown cell lines after 9 days growth in 3D Matrigel. Proliferation (A) was quantified by Ki67 immunohistochemical staining of Matrigel plugs, while apoptosis (B) was quantified by caspase 3 immunohistochemistry. 21NT+shS100A2 cells showed an increase in proliferation (A) over 21NT+shEV and 21MT-1 cells, while apoptosis levels (B) of S100A2 shRNA cells were not different from 21NT cells. When the ratio of proliferation/apoptosis was calculated (C), S100A2 knockdown 21NT cells showed a higher ratio than 21NT+EV cells. 21NT+shEV cells showed no differences from the 21NT cells. Bars labeled with letters that are not the same indicate significant difference between the bars at a p-value of at least <0.05.

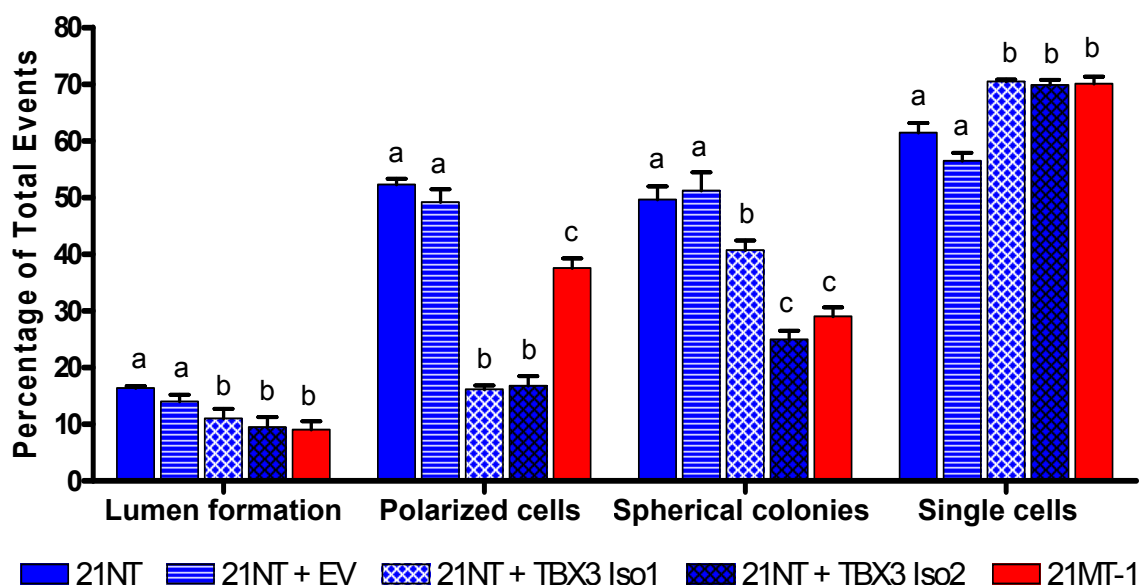


Figure 5. Quantification of characteristics of 21T and TBX3 transfected cells after 9 days growth in 3D Matrigel. 21NT +TBX3 Iso1 and Iso2 cells form fewer lumens and polarized cells than 21NT+EV cells, indicating that the TBX3 cells are less organized. In addition, TBX3 transfected cells also formed less spherical colonies than 21NT+EV cells and more single cells, similarly to 21MT-1 cells. 21NT+EV cells show no differences from 21NT cells. For 'single cells', an event is either a single cell or a cell group, whereas for the 'lumen formation', 'polarized cells' and 'spherical colonies' comparisons, an 'event' was defined as a cell group only. Bars labeled with letters that are not the same indicate significant difference between the bars at a p-value of at least <0.05 . Statistics for each comparison were calculated separately from the other comparisons.

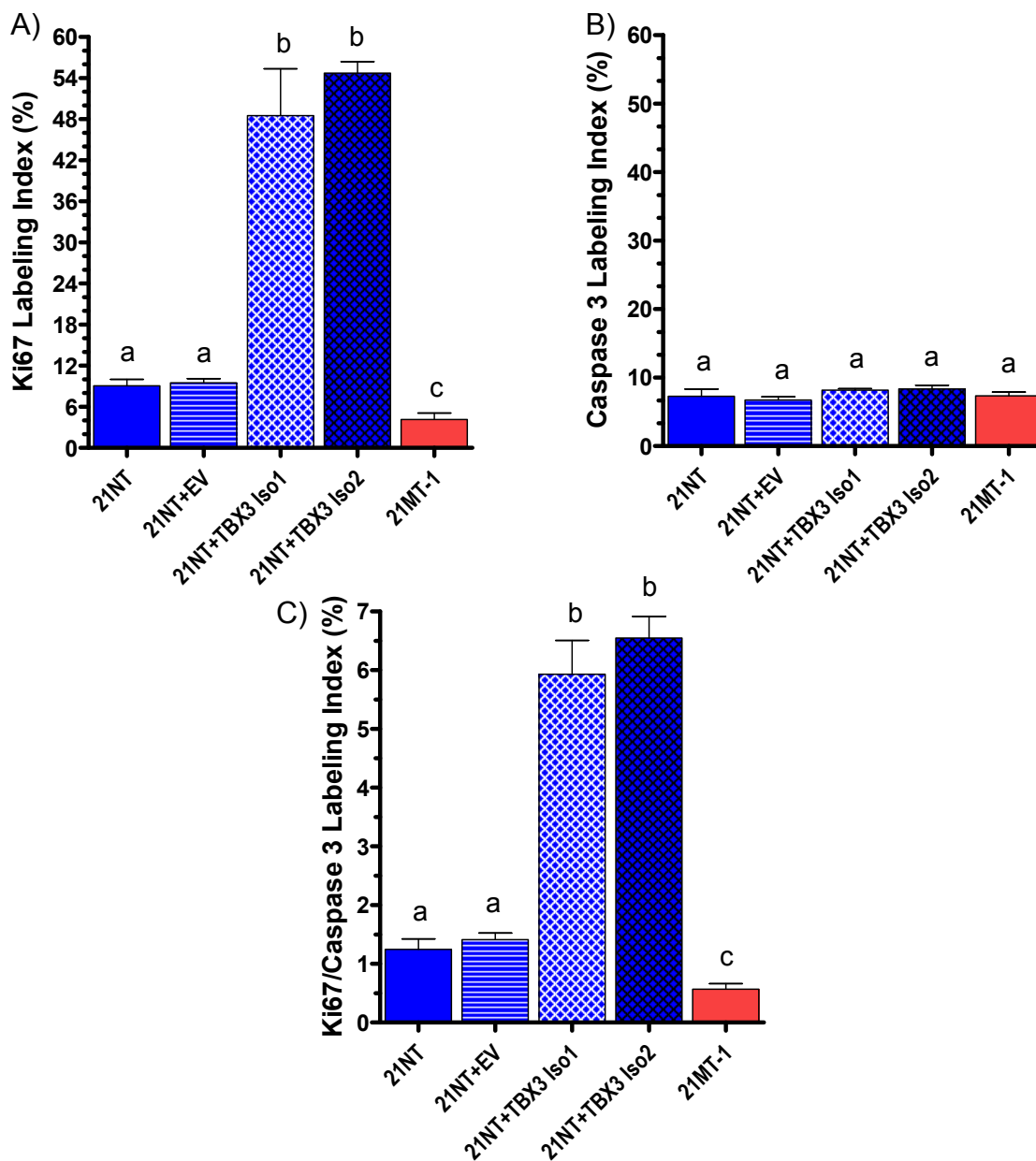


Figure 6. Proliferative and apoptotic activity of 21T and TBX3 transfected cell lines after 9 days growth in 3D Matrigel. Proliferation (A) was quantified by Ki67 immunohistochemical staining of Matrigel plugs, while proliferation (B) was quantified by caspase 3 immunohistochemistry. 21NT+TBX3 Iso1 and Iso2 cells showed a large increase in proliferation (A) over 21NT+EV cells, while apoptosis levels (B) remained similar to the 21T cells. When the ratio of proliferation/apoptosis was calculated (C), TBX3 transfected cells showed a much higher ratio than the 21NT+EV and the 21MT-1 cells. 21NT+EV cells showed no differences from the 21NT cells. Bars labeled with letters that are not the same indicate significant difference between the bars at a p-value of at least <math><0.05</math>.

LESLEY SOUTER

POST-SECONDARY EDUCATION

DOCTOR OF PHILOSOPHY, PATHOLOGY • 2006 – 2011

University of Western Ontario, London, ON, N6A 5B7

Thesis Title: A Model System for Rapid Identification and Functional Testing of Genes Involved in Early Breast Cancer Progression

Supervisors: Dr. Ann Chambers and Dr. Alan Tuck

MASTER OF SCIENCE, BIOLOGY • 2004 – 2006

University of Western Ontario, London, ON, N6A 5B7

Thesis Title: Regulation of Expression and Activity of the Progesterone Metabolizing Enzymes in Human Breast Cancer Cell Lines

Supervisor: Dr. John Wiebe

BACHELOR OF SCIENCE, HONORS BIOLOGY • 2000 – 2004

University of Western Ontario, London, ON, N6A 5B7

EMPLOYMENT EXPERIENCE

RESEARCH ASSISTANT • Summer 2002, 2003, 2004

Hormonal Regulatory Mechanisms Laboratory, Department of Biology, University of Western Ontario, London, ON

Supervisor: Dr. John Wiebe

TEACHING ASSISTANT • 2004 – 2007

Courses: Vertebrate Biology, Comparative Animal Physiology

AWARDS AND SCHOLARSHIPS

Translational Breast Cancer Research Unit Traineeship Program Scholarship recipient, funded by the Southwestern Ontario Women's Cashspiel Fundraiser • Fall 2006 - 2011

Schulich Research Scholarship • 2006 – 2011

Dutkevich Memorial Foundation Travel Award, Department of Pathology • 2010

UWO Division of Experimental Oncology Graduate Student Travel Award • 2010

Poster Presentation Award for a Graduate Student of the Department of Pathology Research Day • 2007

Western Graduate Research Scholarship • 2005 - 2006

Nominated for a Teaching Assistant Award • 2005 – 2007

University of Western Ontario Entrance Scholarship • 2000

VOLUNTEER AND ORGANIZATION EXPERIENCE

- Co-organized evenings with breast cancer researchers and breast cancer survivors
- Co-organized a breast cancer research graduate student dragon boat team for the 2010 London Dragon Boat Festival
- Volunteered with the London Health Science Foundation doing lab tours and lay talks as a Translational Breast Cancer Research Unit representative
- Conducted lay talks for Southwestern Ontario Women's Charity
- Served as an organizing committee member on Put It Into Practice, a one day conference for graduate work at the University of Western Ontario
- Volunteer with One Run to raise funds for breast cancer research

PUBLICATIONS

1. Souter, L.H., Andrews, J.D., Zhang, G., Cook, A.C., Postenka, C.O., Al-Katib, W., Leong, H.S., Rodenhiser, D.I., Chambers, A.F. and Tuck, A.B. Human 21T breast epithelial cell lines mimic breast cancer progression in vivo and in vitro and show stage-specific gene expression patterns. *Laboratory Investigation*, 90:1247-1258, 2010
2. Xu, J., Souter, L.H., Chambers, A.F., Rodenhiser, D.I. and Tuck, A.B. Distinct karyotypes in three breast cancer cell lines 21PTCi, 21NTCi and 21MT-1 derived from the same patient and representing different stages of tumor progression. *Cancer Genetics and Cytogenetics*, 186:33-40, 2009.
3. Wiebe, J.P., Souter, L., and Zhang, G. Dutasteride affects progesterone metabolizing enzyme activity/expression in human breast cell lines, resulting in suppression of cell proliferation and detachment. *Journal of Steroid Biochemistry and Molecular Biology*, 100:129-140, 2006.

ABSTRACTS

1. Souter, L.H., Postenka, C.O., Andrews, J.D., Rodenhiser, D.I., Chambers, A.F. and Tuck, A.B. The role of S100A2 in the transition to the invasive phenotype as identified and characterized by the human 21T series 3D model of breast cancer progression. Metastasis Research Society-American Association for Cancer Research Special Conference on Metastasis and the Tumor Microenvironment, Philadelphia, PA. September 12-15, 2010.
2. Souter, L.H., Leong, H.S., Andrews, H.S., Zhang, G., Cook, A.C., Rodenhiser, D.I., Chambers, A.F. and Tuck, A.B. Genes identified by the human 21T series 3D model system are potentially involved in controlling the transitions between stages of early breast cancer progression. UWO Moffat Graduate Student Research Day, 2010. (Also UWO Pathology Research Day, 2010 and CIHR – Strategic Training Program in Cancer Research Technology Transfer and the Department of Oncology – Research and Education Day, UWO, 2010)

3. Souter, L.H., Goulet, B., Andrews, J.D., Zhang, G., Cook, A.C., Rodenhiser, D.I., Chambers, A.F. and Tuck, A.B. Stage-specific changes in gene expression during early breast cancer progression as modeled by the 21T series cell lines. Metastasis Research Society-American Association for Cancer Research Special Conference on 'Metastasis', Vancouver, BC. August 3-7, 2008. (Also UWO Pathology Research Day, 2008 and CIHR – Strategic Training Program in Cancer Research Technology Transfer and the Department of Oncology – Research and Education Day, UWO, 2008).
4. Souter, L.H., Rodenhiser, D.I., Zhang, G., Andrews, J.D., Cook, A.C., Vantyghem, S.A., Postenka, C.O., Chamber, A.F. and Tuck, A.B. A 3D culture model to examine critical steps in mammary tumor progression. Canadian Breast Cancer Research Alliance 'Reasons for Hope' Conference, Vancouver, BC. April 25-17, 2008.
5. Souter, L.H., Rodenhiser, D.I., Zhang, G., Andrews, J.D., Cook, A.C., Vantyghem, S.A., Postenka, C.O., Chamber, A.F. and Tuck, A.B. Modeling critical steps in mammary tumour progression in 3D culture. AACR Special Conference, Advances in Breast Cancer Research, San Diego, CA. Oct 17-20, 2007. (Also UWO Moffat Graduate Student Research Day, 2007).
6. Souter, L., and Wiebe, J.P. Prolactin affects progesterone metabolizing enzyme activity and expression in MCF-7 human breast cancer cells. The Endocrine Society's 88th Annual Meeting, June 2006.
7. Wiebe, J.P., Souter, L., and Zhang, G. Dutasteride affects progesterone metabolizing enzyme activity/expression in human breast cell lines resulting in suppression of cell proliferation and detachment. The Endocrine Society's 88th Annual Meeting, June 2006.